Title
Intercellular signaling in the developing nervous system

Author
Ng, Norman

Publication Date
2004

Peer reviewed|Thesis/dissertation

Intercellular Signaling in the Developing Nervous System - Analyses of Drosophila Creb Binding Protein and the Drosophila *flexins* in Coordinated Neural Development

by

Norman Ng

DISSERTATION

Submitted in partial satisfaction of the requirements for the degree of

DOCTOR OF PHILOSOPHY

in

Pharmaceutical Chemistry

in the

GRADUATE DIVISION

of the

UNIVERSITY OF CALIFORNIA, SAN FRANCISCO

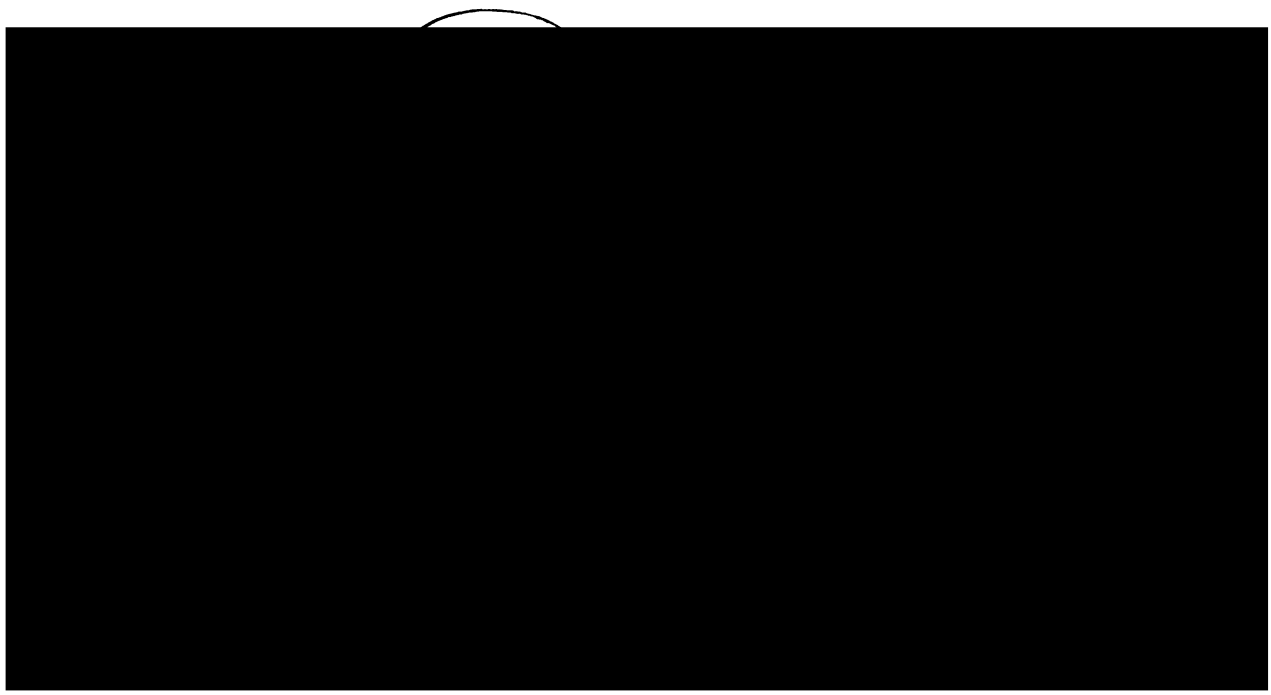

ACKNOWLEDGMENTS

The text of Chapter II of this thesis is a reprint of the material as it appears in Neuron, "A Genetic Analysis of Synaptic Development: Pre- and Postsynaptic dCBP Control Transmitter Release at the Drosophila NMJ," Volume 25(3), pp. 537-547, for which I conducted the molecular analyses, and is reprinted with the permission of Elsevier.

The text of Appendix I of this thesis is a reprint of the material as it appears in Neuron, "Drosophila Futsch Regulates Synaptic Microtubule Organization and is Necessary for Synaptic Growth," Volume 26(2), pp. 371-382, including my contribution towards *flexin1*, is reprinted with the permission of Elsevier.

Date: Mon, 6 Sep 2004 17:24:18 -0700 (PDT)
From: Norman Ng <normg@itsa.ucsf.edu>
To: permissions@elsevier.co.uk
Subject: Reprint Permission for Thesis

To Whom It May Concern,

I am writing to obtain permission to reproduce the following articles on which I am an author, published in Neuron for my doctoral dissertation at the University of California, San Francisco :

(1) "A Genetic Analysis of Synaptic Development: Pre- and Postsynaptic dCBP Control Transmitter Release at the Drosophila NMJ"
(Neuron 2000 25: 537-547)

(2) "Drosophila Futsch Regulates Synaptic Microtubule Organization and is Necessary for Synaptic Growth"
(Neuron 2000 26: 371-382)

Please let me know what form of acknowledgment to the source you prefer. Your correspondence can be emailed to normg@itsa.ucsf.edu or faxed to (415) 502-5145. Thank you for your time.

Norman Ng
normg@itsa.ucsf.edu
Department of Biochemistry and Biophysics
UCSF Box 2822
1550 4th St. GD 447
San Francisco, CA 94143-2822

phone: 415-502-4840
fax : 415-502-5145

ELSEVIER

20 September 2004 Our ref: HG/mm/sept 04.J075

Norman Ng
UCSF
normg@itsa.ucsf.edu

Dear Mr Ng

NEURON, Vol 25, 2000, pp 537-547, Marek et al, "A genetic analysis..."

As per your letter dated 9 September 2004, we hereby grant you permission to reprint the aforementioned material at no charge **in your thesis** subject to the following conditions:

1. If any part of the material to be used (for example, figures) has appeared in our publication with credit or acknowledgement to another source, permission must also be sought from that source. If such permission is not obtained then that material may not be included in your publication/copies.

2. Suitable acknowledgment to the source must be made, either as a footnote or in a reference list at the end of your publication, as follows:

   "Reprinted from Publication title, Vol number, Author(s), Title of article, Pages No., Copyright (Year), with permission from Elsevier".

3. Reproduction of this material is confined to the purpose for which permission is hereby given.

4. This permission is granted for non-exclusive world **English** rights only. For other languages please reapply separately for each one required. Permission excludes use in an electronic form. Should you have a specific electronic project in mind please reapply for permission.

5. This includes permission for UMI to supply single copies, on demand, of the complete thesis. Should your thesis be published commercially, please reapply for permission.

Yours sincerely

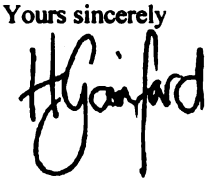

Helen Gainford
Rights Manager

Your future requests will be handled more quickly if you complete the online form at www.elsevier.com/locate/permissions

ELSEVIER

28 September 2004

Our Ref: HG/jj/Sept04/J494
Your Ref:

Norman Ng
UCSF
1550 4th St. GD 447
San Francisco 94143-2822
USA

Dear Norman Ng

NEURON, Vol 26, No 2, 2000, pp 371-382, Roos et al: "Drosophila Futsch regulates ..."

As per your letter dated 27 September 2004, we hereby grant you permission to reprint the aforementioned material at no charge **in your thesis** subject to the following conditions:

1. If any part of the material to be used (for example, figures) has appeared in our publication with credit or acknowledgement to another source, permission must also be sought from that source. If such permission is not obtained then that material may not be included in your publication/copies.

2. Suitable acknowledgment to the source must be made, either as a footnote or in a reference list at the end of your publication, as follows:

   "Reprinted from Publication title, Vol number, Author(s), Title of article, Pages No., Copyright (Year), with permission from Elsevier".

3. Reproduction of this material is confined to the purpose for which permission is hereby given.

4. This permission is granted for non-exclusive world **English** rights only. For other languages please reapply separately for each one required. Permission excludes use in an electronic form. Should you have a specific electronic project in mind please reapply for permission.

5. This includes permission for UMI to supply single copies, on demand, of the complete thesis. Should your thesis be published commercially, please reapply for permission.

Yours sincerely

Helen Gainford
Rights Manager

Your future requests will be handled more quickly if you complete the online form at www.elsevier.com/wps/find/obtainpermissionform.cws_home/obtainpermissionform

I'd like to thank all those who made grad school the interesting experience that it was. I acknowledge various members of the department in shepherding my progress through the program as well as the members of the committee for their contributions and for getting things done in the nick of time.

I am grateful to my folks for their support for all the long years they so patiently endured. Ngoh jun hai ho doh je ney dey. I know they would have wanted things to move a little faster. Well, Life is funny that way. Graduate school has certainly not been easy. In my class of nine, four bowed out. Were someone to ask me when I was a bright-eyed, bushy-tailed young pup whether I had any inkling of what I was getting myself into, most certainly the answer would have been a sardonic "You're kidding me, right?"

The journey was long, the road fraught with potholes, and the destination shrouded in fog. Somehow I hung in there. (Ah, the familiar thesis acknowledgment refrain.) I certainly learned a lot - knowledge that allowed me to avail myself of the perfect storm of events that could not have happened any other way. Maybe things do happen for a reason. Maybe chance does favor the prepared mind. Whatever the case, it works for me. Strike while the iron's hot.

I owe an immense debt of gratitude also to shaochuan. Xie xie ni ah so much for being a pillar of strength, inspiration, and encouragement all these years. When things were dark, you were the light. When disappointment reigned, you radiated hope. Through it all, I am grateful for your steadfast and unwavering support.

I also want to thank my friends, you know who you are, there's too many of you people to list! - especially my local campus buds, and of course, mah bros - you guys R the best.

And now, I can stop hitting the snooze bar on Life, the Universe, and broccoli?...

Norman Ng

Intercellular Signaling in the Developing Nervous System – Analyses of Drosophila Creb Binding Protein and the Drosophila *flexins* in Coordinated Neural Development

by

Norman Ng

ABSTRACT

Neural development is a precisely regulated process. Continual remodeling of the nervous system refines its ability to effect an appropriate response. Numerous cues temporally and spatially coordinate developmental and activity-dependent plasticity. To uncover intercellular signals underlying this process, we conducted forward genetic gain-of-function screens in the Drosophila neuromuscular junction, a system exquisitely dedicated for communication. We isolated novel neurodevelopmental functions and molecules. This dissertation describes our analyses of three molecules implicated by our screens.

Drosophila Creb Binding Protein (dCBP) was identified as a crucial component of synaptic signaling. Postsynaptic dCBP is required for presynaptic functional development and participates in a postsynaptic homeostatic control of synaptic function.

Our morphological screen identified a novel gene family in Drosophila named *flexins*. *flexins* bear a putative nucleic acid binding domain homologous to the

evolutionarily conserved CENP-B proteins. *flexin1* is expressed in bodywall muscle and the Flexin1 protein traffics to both the muscle cytoplasm and nucleus. Postsynaptic muscle over-expression increases presynaptic nerve-terminal branching without altering bouton number. In imaginal tissues, *flexin1* gain-of-function exhibit opposing phenotypes to that produced by the loss-of-function of the neurally expressed homolog, *flexin2*.

We find *flexin2* transcript ubiqitous in the central and peripheral nervous system. It is essential in neurogenic tissue throughout development. Silencing of *flexin2* in imaginal tissues evokes classic hallmarks of perturbed Notch signaling. We demonstrate *flexin2* synergistically enhances Notch mutations, suggesting that it participates in the Notch pathway.

The study of Notch signaling has involved intense characterization of its component members. Numerous modulators have been described to act in a limited context to influence specific Notch responses. We have now identified a previously unknown role of the ancient metazoan family of CENP-B containing proteins to function in the evolutionarily conserved Notch signaling. Novel molecules that impinge upon Notch signaling offer additional avenues to uncover the complex interplay mediated by multiple developmental signaling systems that converge to coordinate neural development.

TABLE OF CONTENTS

LIST OF FIGURES

Chapter II: A Genetic Analysis of Synaptic Development: Pre- and Postsynaptic dCBP Control Transmitter Release at the Drosophila NMJ

Chapter III: *flexin1*, a Member of Novel Gene Family in Drosophila, Participates in Trans-Synaptic and Imaginal Tissue Development

CHAPTER I: INTRODUCTION

Neural development generates the remarkable diversity elaborated in cellular form and function. The robustness of the nervous system depends upon intercellular signals that serve precise and appropriate roles. The nervous system must continually adapt to intrinsic and extrinsic signals and elicit the proper response. Its development does not occur in isolation but through a panoply of communicated cues that mediate survival, growth, differentiation, death, and migration. Coordinated neural remodeling is temporally and spatially regulated by a complex interplay of multiple signaling systems that induce, eliminate, and refine neuron-target connections. These mechanisms are deployed to ensure proper formation and function within physiologically relevant parameters. The process by which orderly developmental and activity dependent plasticity occur to produce the stereotypical cell types and functional target innervations are being elucidated (Krubitzer and Kahn, 2003).

Numerous signals modulate neural development whether cell-autonomous or target derived. Ligands and their respective pathways impinge upon the receiving cell to effect specific developmental programs in the appropriate time and place (Huang and Reichardt 2001; Lu and Je, 2003; English, 2003). What underlies this critical process of coordinated development? Characterizing the molecules involved is necessary to understand the phenomenon. Many participants have been remarkably conserved in metazoans, and paralleled in particular in Drosophila, which is readily amenable to a host of manipulations. Traditional approaches enroll forward genetic screens to elucidate a process of interest. These phenotype driven loss- and gain-of-function screens underpin functional genetic analysis.

Loss-of-function screens are incredibly useful in deciphering gene function. It is the removal of endogenous gene activity that illuminates its native role (reviewed by St Johnson, 2002). The ease of analysis bestowed by loss-of-function mutations has provided tremendous value in determining essential genes. Indeed, only seven genes are vital in early Drosophila embryogenesis (Wieschaus, 1996). Loss-of-function screens have been indispensable in the study of genes that participate during early developmental processes such as embryonic patterning (Nüsslein-Volhard and Wieschaus, 1980; St Johnson, 2002). The power inherent to the loss-of-function approach has been recognized by the Nobel Prize committee.

While valuable for functional analysis, loss-of-function screens have a well demonstrated drawback dependent upon developmental context. Ectopic substitution of another pathway due to the lack of a gene can create non-native interactions (Madhani and Fink, 1998). Phenotypes thus derived may be secondary effects to a gene's primary role, fomenting spurious over-interpretation. Conversely, a gene's pleiotropic requirement also renders isolating its specific function difficult. Loss-of-function screens can unknowingly be biased to certain classes of mutations. Behavioral mutants identified in such fashion are typically hypomorphs because most genes that affect behavior are essential, thus null mutants are inherently eliminated (Sokolowski, 2001). One must resort to sufficiently sensitized backgrounds or homozygous mutant clones engendered via FRT/FLP to score a signal (McGuire et al., 2004; Branda and Dymecki, 2004). Even so, loss-of-function screens require readily mutable elements as illustrated by the plethora of microRNAs that have long eluded detection until recently (Pasquinelli and Ruvkun, 2002; He and Hannon, 2004). Furthermore, not all genes can be identified due to

developmental compensation or overlapping activity. Except for rare haploinsufficiency, most genes are recessive such that the loss of one copy frequently has no phenotype (St Johnston, 2002).

The logical alternative to loss-of-function screens, the gain-of-function approach utilizes dominant gene function. The quality of this approach is replete with its own caveats however; its output being only as good as its input. Both methods for example, overlook genes that when mutated cause sterility. By its nature, improper expression raises the red flag of biological relevance. Defects caused by ectopic or mis- expression can produce specious artifacts adulterated by neomorphic phenotypes completely unrelated to endogenous gene function such as lethality, requiring vigilant sorting of signal from noise (Guichard et al., 2002). Generally considered the loss-of-function's poor cousin, it does have its own strengths if used appropriately as its emerging popularity attests (Lai and Rubin, 2003). Under what conditions might one pursue a gain-of-function screen? Obviously, when loss-of-function screens have saturated a pathway, more of the same would not attract additional funding. And for genes that do not have a loss-of-function, a gain-of-function screen is the logical and powerful alternative to discern gene function obscured by functional redundancy.

Gain-of-function crosstalk is critical in the study of novel pathways that occur during disease states. Positive selection for the desired traits can marshal adaptive or non-canonical mechanisms particularly useful in dissecting the unpredictable responses of infectious organisms and neoplasms (Hide and Isokpehi, 2004; Hoek et al., 2004). The burgeoning field of neurodegenerative disease exhibits a Who's Who list of mis-

expressed housekeeping genes gone wild that can only be identified by this approach (Sipione and Cattaneo, 2001).

Gain-of-function studies are exquisitely positioned for investigating native versus activated or aberrant signaling pathways. The level of gene activation has been shown to switch the mode of response with above basal amounts eliciting a different set of interactions. Immune surveillance of the complement system hinges upon just such a bimodal output. At endogenous levels, complement participates in distinct cellular activities whereas exogenous amounts initiate lytic events by co-opting alternative signaling pathways (Bohana-Kashtan et al., 2004). A similar advantage of upregulation is the identification of genes such as transcription factors that normally lie dormant until activated. These genes may have no loss-of-function.

Many genes that have more than one function are difficult to tease out as loss-of-function mutations. Thus, it is the increased expression of gene function with phenotypic consequences that allows the selection of these elusive mutations. Similarly, mis-expression sidesteps tissue-specific lethality. The search for modulators of signal transduction pathways has been heavily dependent upon modifier screens genetically sensitized for the process of interest (St Johnston, 2002). Genes participating in these transcriptional regulatory signaling complexes frequently display opposing loss- and gain-of-function (Lai and Rubin, 2001). Hypermorphs found in this fashion conveniently facilitate and anticipate hypomorphic analysis.

Mis- or over-expressed genes in whole or in part, have served as workhorses to divine and finely tune gene activity. Screens for dominant mutations have been especially useful for identifying genes of unknown function (Guichard et al., 2002). In

particular, the allelic variations divulged are unavailable elsewhere (St Johnston, 2002). Forced activation has identified previously unknown crucial classes of molecules in well characterized pathways (Schulz et al., 2004). Large numbers of genes involved in synapse formation and peripheral neurogenesis have been identified in this manner (Abdelilah-Seyfried et al., 2000; Kraut et al., 2001 ; St Johnson 2002). In Drosophila neurobiology, the UAS-Gal4 system has been indispensable for targeted Gal4 mis- or over-expression of random transposable P-element insertions (Rorth 1998; St Johnston 2002). While the UAS-Gal4 system is limited by the diversity of insertions available and unanticipated expression of genes far downstream of the UAS element, it has nonetheless well rewarded its demanding taskmasters. The tissue and stage specific control conferred by its versatility avoids the lethality associated with either embryonic requirement or ubiquitous over-expression. Post-embryonic phenotypes are spatio-temporally refined for ease of analysis (Suster et al., 2004). The UAS-Gal4 over-expression approach has incriminated the tiny novel genetic elements, microRNAs, as the culprits for phenotypic consequences of P-element over-expression where the usual coding suspects have not been found. Indeed, Drosophila Bantam was identified in this manner (Hipfner et al., 2002; Brennecke et al., 2003; He and Hannon, 2004).

To characterize components involved in neural development and function, we conducted a forward genetic UAS-Gal4 gain-of-function screen by perturbing intercellular communication over the course of Drosophila larval development. We undertook our screens in the system dedicated to signaling, the neuromuscular junction (NMJ). Random UAS bearing P-element insertions were mated to muscle expressing Gal4 and the progeny assayed for defects at the synapse. A similar screen was performed

in a sensitized background of activated PKA. We isolated novel synaptic functions for these mutations (Sweeney and Davis, 2002; Marek et al., 2000; Clyne, P pers. comm.).

Chapter 2 describes our published work on Drosophila Creb Binding Protein (dCBP), a gene required for normal synaptic efficacy (Marek et al., 2000). Subsequent chapters pertain to *flexin1* and *flexin2*, members of a novel family of genes homologous to vertebrate CENP-B proteins implicated by our screen to participate in intercellular signaling (Roos et al., 2001). *flexin1*, discussed in Chapter 3, is sufficient to perturb synaptic morphology non-cell autonomously. In imaginal tissue, its gain-of-function phenocopies the loss-of-function of its neuronal counterpart, *flexin2*. *flexin2*, the subject of Chapter 4, is required for Notch-mediated neurogenic signaling.

The evolutionarily conserved Notch pathway is necessary throughout metazoan development (Artavanis-Tsakonas et al., 1999). An intensive effort has been underway in a large number of labs to identify novel components that modulate Notch (Portin, 2002). While heavily scrutinized, no Notch-based screens to date have fingered the CENP-B containing proteins, validating the power of the screen we employed in ferreting out novel functions and molecules overlooked by conventional methods (Hall et al., 2004).

References

Abdelilah-Seyfried S, Chan YM, Zeng C, Justice NJ, Younger-Shepherd S, Sharp LE, Barbel S, Meadows SA, Jan LY, Jan YN. A gain-of-function screen for genes that affect the development of the *Drosophila* adult external sensory organ. *Genetics* 155, 733-752 (2000).

Artavanis-Tsakonas S, Rand MD, Lake RJ. Notch signaling: cell fate control and signal integration in development. Science. 1999 Apr 30;284(5415):770-6. Review.

Branda CS, Dymecki SM. Talking about a revolution: The impact of site-specific recombinases on genetic analyses in mice. Dev Cell. 2004 Jan;6(1):7-28. Review.

Brennecke J, Hipfner DR, Stark A, Russell RB, Cohen SM. bantam encodes a developmentally regulated microRNA that controls cell proliferation and regulates the proapoptotic gene hid in Drosophila. Cell. 2003 Apr 4;113(1):25-36.

Bohana-Kashtan O, Ziporen L, Donin N, Kraus S, Fishelson Z. Cell signals transduced by complement. Mol Immunol. 2004 Jul;41(6-7):583-97.

English AW. Cytokines, growth factors and sprouting at the neuromuscular junction. J Neurocytol. 2003 Jun-Sep;32(5-8):943-60. Review.

Guichard A, Srinivasan S, Zimm G, Bier E. A screen for dominant mutations applied to components in the Drosophila EGF-R pathway. Proc Natl Acad Sci U S A. 2002 Mar 19;99(6):3752-7.

Hall LE, Alexander SJ, Chang M, Woodling NS, Yedvobnick B. An EP overexpression screen for genetic modifiers of Notch pathway function in Drosophila melanogaster. Genet Res. 2004 Apr;83(2):71-82.

He L, Hannon GJ. MicroRNAs: small RNAs with a big role in gene regulation. Nat Rev Genet. 2004 Jul;5(7):522-31. Review.

Hide WA, Isokpehi RD. Positive selection scanning of parasite DNA sequences. Methods Mol Biol. 2004;270:127-50.

Hipfner DR, Weigmann K, Cohen SM. The bantam gene regulates Drosophila growth. Genetics. 2002 Aug;161(4):1527-37.

Hoek K, Rimm DL, Williams KR, Zhao H, Ariyan S, Lin A, Kluger HM, Berger AJ, Cheng E, Trombetta ES, Wu T, Niinobe M, Yoshikawa K, Hannigan GE, Halaban R. Expression profiling reveals novel pathways in the transformation of melanocytes to melanomas. Cancer Res. 2004 Aug 1;64(15):5270-82.

Huang EJ, Reichardt LF. Neurotrophins: roles in neuronal development and function. Annu Rev Neurosci. 2001;24:677-736. Review.

Kraut, R., Menon, K. & Zinn, K. A gain-of-function screen for genes controlling motor axon guidance and synaptogenesis in *Drosophila*. *Curr. Biol.* 11, 417-430 (2001).

Krubitzer L, Kahn DM. Nature versus nurture revisited: an old idea with a new twist. Prog Neurobiol. 2003 May;70(1):33-52. Review.

Lai EC, Rubin GM. The psychology and sociology of fly geneticists: de facto discrimination against dominant mutants. Drosophila Research Conference 2003. Program Nr: 727A. http://www.drosophila-conf.org/genetics/gsa/dros/dros2003/abstract/f0727a.htm

Lai EC, Rubin GM. neuralized functions cell-autonomously to regulate a subset of notch-dependent processes during adult Drosophila development. Dev Biol. 2001 Mar 1;231(1):217-33.

Lu B, Je HS. Neurotrophic regulation of the development and function of the neuromuscular synapses. J Neurocytol. 2003 Jun-Sep;32(5-8):931-41. Review.

Madhani HD, Fink GR. The riddle of MAP kinase signaling specificity. Trends Genet. 1998 Apr;14(4):151-5. Review.

Marek KW, Ng N, Fetter R, Smolik S, Goodman CS, Davis GW. A genetic analysis of synaptic development: pre- and postsynaptic dCBP control transmitter release at the Drosophila NMJ. Neuron. 2000 Mar;25(3):537-47.

McGuire SE, Roman G, Davis RL. Gene expression systems in Drosophila: a synthesis of time and space. Trends Genet. 2004 Aug;20(8):384-91.

Nüsslein-Volhard, C. & Wieschaus, E. Mutations affecting segment number and polarity in *Drosophila*. *Nature* 287, 795-801 (1980).

Pasquinelli, A. E. & Ruvkun, G. Control of developmental timing by micrornas and their targets. *Annu. Rev. Cell Dev. Biol.* 18, 495–513 (2002).

Portin P. General outlines of the molecular genetics of the Notch signalling pathway in Drosophila melanogaster: a review. Hereditas. 2002;136(2):89-96. Review.

Rørth, P. A modular misexpression screen in *Drosophila* detecting tissue-specific phenotypes. *Proc. Natl Acad. Sci. USA* 93, 12418-12422 (1996).

Rørth, P. *et al.* Systematic gain-of-function genetics in *Drosophila*. *Development* 125, 1049-1057 (1998).

Schulz C, Kiger AA, Tazuke SI, Yamashita YM, Pantalena-Filho LC, Jones DL, Wood CG, Fuller MT. A misexpression screen reveals effects of bag-of-marbles and TGF beta class signaling on the Drosophila male germ-line stem cell lineage. Genetics. 2004 Jun;167(2):707-23.

Sipione S, Cattaneo E. Modeling Huntington's disease in cells, flies, and mice. Mol Neurobiol. 2001 Feb;23(1):21-51.

Sokolowski MB. Drosophila: genetics meets behaviour. Nat Rev Genet. 2001 Nov;2(11):879-90. Review.

St Johnston D. The art and design of genetic screens: Drosophila melanogaster. Nat Rev Genet. 2002 Mar;3(3):176-88.

Sweeney ST, Davis GW. Unrestricted synaptic growth in spinster-a late endosomal protein implicated in TGF-beta-mediated synaptic growth regulation. Neuron. 2002 Oct 24;36(3):403-16.

Suster ML, Seugnet L, Bate M, Sokolowski MB. Refining GAL4-driven transgene expression in Drosophila with a GAL80 enhancer-trap. Genesis. 2004 Aug;39(4):240-245.

Wieschaus E. Embryonic transcription and the control of developmental pathways. Genetics. 1996 Jan;142(1):5-10. Review.

CHAPTER II

A Genetic Analysis of Synaptic Development: Pre- and Postsynaptic dCBP Control Transmitter Release at the Drosophila NMJ

Reprinted from Neuron, Volume 25(3), Marek KW, Ng N, Fetter R, Smolik S, Goodman CS, Davis GW, "A Genetic Analysis of Synaptic Development: Pre- and Postsynaptic dCBP Control Transmitter Release at the Drosophila NMJ", pp. 537-547, Copyright (2000), with permission from Elsevier.

Neuron, Vol. 25, 537–547, March, 2000, Copyright ©2000 by Cell Press

A Genetic Analysis of Synaptic Development: Pre- and Postsynaptic dCBP Control Transmitter Release at the *Drosophila* NMJ

Kurt W. Marek,* Norman Ng,* Richard Fetter,†
Sarah Smolik,‡ Corey S. Goodman,†
and Graeme W. Davis*§
*Department of Biochemistry and Biophysics
Programs in Cell Biology and Neuroscience
University of California Medical School
San Francisco, California 94143
†Howard Hughes Medical Institute
Department of Molecular and Cell Biology
University of California, Berkeley
Berkeley, California 94720
‡Department of Cell and Developmental Biology
Oregon Health Science University
Portland, Oregon 97201

Summary

Postsynaptic dCBP (*Drosophila* homolog of the CREB binding protein) is required for presynaptic functional development. Viable, hypomorphic dCBP mutations have a ~50% reduction in presynaptic transmitter release without altering the Ca^{2+} cooperativity of release or synaptic ultrastructure (total bouton number is increased by 25%–30%). Exogenous expression of dCBP in muscle rescues impaired presynaptic release in the dCBP mutant background, while presynaptic dCBP expression does not. In addition, overexpression experiments indicate that elevated dCBP can also inhibit presynaptic functional development in a manner distinct from the effects of dCBP loss of function. Pre- or postsynaptic overexpression of dCBP (in wild type) reduces presynaptic release. However, we do not observe an increase in bouton number, and presynaptic overexpression impairs short-term facilitation. These data suggest that dCBP participates in a postsynaptic regulatory system that controls functional synaptic development.

Introduction

The regulation of synaptic growth and plasticity must include mechanisms that constrain synaptic change within reasonable physiological limits. During development, there is a dramatic proliferation and remodeling of new synaptic connections (Buchs and Muller, 1996; Katz and Shatz, 1996; Engert and Bonhoeffer, 1999). In each system, it is essential that increased synaptic function is moderate and in register with the normal physiological range of the target neuron (Davis and Goodman, 1998a, 1998b). A fundamental question concerns how a neuron is able to generate a modest, yet physiologically relevant, change in synaptic function in response to a developmental or activity-dependent cue.

One hypothesis for regulated control of synaptic strengthening is the activity-dependent release of a highly localized and limited amount of trophic factor or signaling molecule (Arancio et al., 1996; Shieh and Ghosh, 1997). A second possibility is that regulation of synaptic function is achieved locally at the synapse by a biochemical tag that specifies those select synapses that will sustain long-term changes in synaptic function (Frey and Morris, 1997; Martin et al., 1997; Casadio et al., 1999). A third form of regulation is negative feedback within the system that generates increased synaptic function. Such negative feedback could allow for homeostatic control of synaptic strength, thereby preventing excessive synaptic strengthening.

Transcription via the cAMP response element binding protein (CREB) has been implicated in many forms of long-term synaptic plasticity (Bourtchuladze et al., 1994; Bito et al., 1996; Davis et al., 1996; Deisseroth et al., 1996; Silva et al., 1998). Indeed, CREB has been shown to participate in signaling via neurotrophins and may be an essential component of the biochemical tag hypothesis (Casadio et al., 1999). Here, we demonstrate a role for the *Drosophila* homolog of the CREB binding protein (dCBP), a transcriptional coactivator of CREB, in the homeostatic regulation of synaptic functional development.

CBP was identified as a coactivator of CREB-mediated transcription (Chrivia et al., 1993). However, a role for CBP during synaptic development and plasticity has not been thoroughly investigated. CBP function is complex and is not restricted to an interaction with CREB. CBP can act as a transcriptional coactivator with other transcriptional partners (Akimaru et al., 1997; Giordano and Avantaggiati, 1999; Johnston et al., 1999; Waltzer and Bienz, 1999). In addition, CBP has been implicated as a histone acetylase potentially involved in basal transcriptional regulation (Waltzer and Bienz, 1998, 1999; Giordano and Avantaggiati, 1999). The acetylase activity of dCBP has also been implicated in the regulation of Wingless signaling through acetylation of *Drosophila* T cell factor (Waltzer and Bienz, 1998). Thus, CBP has numerous functions, acting as a transcriptional regulator and as an intracellular signaling molecule in the cell nucleus.

Very little is known about the role of CBP at the synapse despite increasing evidence that CREB is an essential element of long-term synaptic plasticity (Davis et al., 1996; Casadio et al., 1999). Experiments in vitro using a GAL4-GFP reporter system indicate that CREB/CBP-mediated transcription is responsive to differential Ca^{2+} entry through voltage-gated Ca^{2+} channels and ligand-gated ion channels (Hardingham et al., 1999; Hu et al., 1999). Rubenstein-Taybi syndrome, a disorder characterized by severe mental retardation and limb malformation, is associated with a truncation of the CBP gene (Tenaka et al., 1997; Taine et al., 1998). Mice heterozygous for mutations in the CBP locus show dominant deficits in learning and memory (Tanaka et al., 1997; Oike et al., 1999). These data implicate CBP as being essential for normal neural development and activity-dependent synaptic plasticity.

§To whom correspondence should be addressed (e-mail: gdavis@biochem.ucsf.edu).

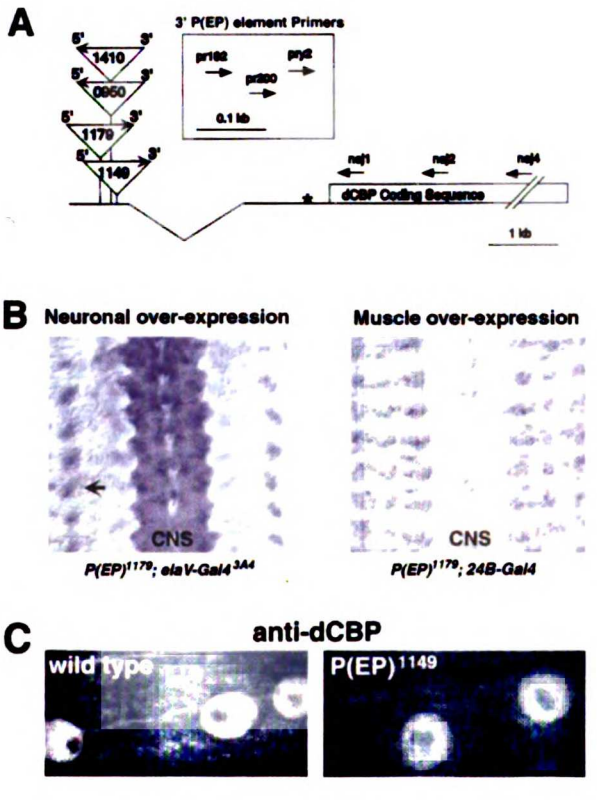

Figure 1. Molecular Characterization of the dCBP P(EP) Insertions

(A) Schematic diagram of the dCBP genomic region showing the P(EP) insertion sites upstream of the published dCBP sequence. The published coding sequence (open box) and position of the 5′ end of the published dCBP sequence (asterisk) are shown. P(EP)^{1179} and P(EP)^{1149} are oriented to overexpress dCBP, while P(EP)^{1410} and P(EP)^{0950} are oppositely oriented. The precise insertion sites for P(EP) elements 1179, 1410, 0950, and 1149, relative to the published dCBP sequence, are 2981 base pairs, 2781 base pairs, 2780 base pairs, and 2747 base pairs upstream of the dCBP start site, respectively. The approximate position and orientation of PCR primers used for PCR amplification are indicated.

(B) P(EP)^{1179} drives specific overexpression of the endogenous dCBP transcript in the embryonic nervous system using the *elaV-GAL4* driver ("Neuronal over-expression") or in embryonic muscle using the *24B-GAL4* driver ("Muscle over-expression").

(C) Expression of dCBP in postsynaptic muscle, as detected by anti-dCBP. Expression in muscle is reduced by ~75%–80% in the hypomorphic loss-of-function mutant background [P(EP)^{1149}] based on reduced fluorescence intensity.

Here, we present a complete genetic and electrophysiological analysis of dCBP function during synaptic development at the *Drosophila* neuromuscular junction (NMJ). We present evidence that postsynaptic dCBP is necessary for normal presynaptic functional development. In addition, we demonstrate that overexpression of dCBP can act to inhibit presynaptic functional development. We propose that dCBP participates in a postsynaptic homeostatic regulatory system that controls presynaptic function through both positive and negative regulation. This model provides a mechanism that can allow for the precise control of new synapse formation during development.

Results

Molecular and Genetic Identification of dCBP P(EP) Element Mutations

dCBP is expressed both pre- and postsynaptically at the developing larval NMJ. dCBP is ubiquitously expressed based on in situ experiments and protein expression (data not shown). More specifically, an antibody raised against dCBP shows that the protein is present in larval muscle nuclei (Figure 1) and throughout the CNS (data not shown).

We have identified four P(EP) elements that are located in a region ~3 kb upstream of the dCBP open reading frame. Two of these elements—P(EP)^{1179} and P(EP)^{1149}—are oriented to overexpress dCBP, and two are in the opposite orientation. P(EP) elements are mobile genetic elements (P elements) containing upstream transcription activation sequences (UAS sequence) that exploit the tendency for P elements to insert in 5′ regulatory regions of a gene. Insertion of such an element in the proper 5′-3′ orientation places random genes under the control of the UAS element, allowing them to be expressed in specific tissues under the control of an appropriate GAL4 driver.

P(EP)^{1179} and P(EP)^{1149} can initiate overexpression of dCBP. Crossing P(EP)^{1179} or P(EP)^{1149} to GAL4 drivers that promote expression in nerve or muscle causes tissue-specific overexpression of dCBP, as detected by in situ hybridization using probes specific to the dCBP gene (Figure 1). Overexpression of dCBP was also demonstrated by RT-PCR using primers from the P(EP) elements and primers within the dCBP open reading frame. Each PCR product isolated by RT-PCR was sequenced to ensure that the correct open reading frame was driven by the P(EP) element.

To ensure that we are not driving overexpression of an additional message located between our P(EP) elements and the start of the dCBP open reading frame, we subcloned and sequenced the entire 3 kb genomic region between P(EP)^{1179} (the furthest insertion upstream of dCBP) and the start of dCBP. This region did not contain an additional transcript. Furthermore, our overexpression phenotype is phenocopied by overexpression of the *dCBP* cDNA under UAS control (see below). Based

on this sequence data and data obtained from RT-PCR from the P(EP)^{1179} and P(EP)^{1148} elements, we present a more complete characterization of the 5′ untranslated region of dCBP that extends to, and most likely beyond, these P(EP) elements. These results also predict that these P(EP) elements will generate a hypomorphic loss of dCBP function.

Genetic, histological, and electrophysiological evidence demonstrate that the P(EP) elements P(EP)^{1148} and P(EP)^{1179} are hypomorphic mutations in dCBP. dCBP expression in muscle nuclei, as detected by an anti-dCBP antibody, is significantly reduced in the P(EP)^{1148} hypomorphic mutant (expression being decreased by ~75%–80%, based on reduced fluorescence intensity; Figure 1). Genetic experiments demonstrate that null or strong hypomorphic mutations in dCBP die as late embryos or first instar larvae (Florence and McGinnis, 1998; Waltzer and Bienz, 1998). Patterning defects are associated with these null mutations (Akimaru et al., 1997; Florence and McGinnis, 1998; Waltzer and Bienz, 1998). Here, we demonstrate that P(EP)^{1179} and P(EP)^{1148} fail to complement previously characterized hypomorphic alleles of dCBP, including *dCBP*$^{\Delta A57}$ and *dCBP*$^{\Delta 342}$, for synaptic transmission defects. P(EP)^{1179} or P(EP)^{1148} trans-heterozygous with *dCBP*$^{\Delta A57}$ or *dCBP*$^{\Delta 342}$ are semi-viable as third instar larvae. These trans-heterozygous larvae are developmentally delayed by ~1 day and emerge as sluggish third instar larvae. We were therefore able to proceed with anatomical and electrophysiological characterization of these dCBP loss-of-function mutations at the third instar larval synapse.

dCBP Is Necessary for Functional Synaptic Development

Hypomorphic dCBP loss-of-function alleles (reduced function) cause a specific ~50% decrease in presynaptic transmitter release at the NMJ. The homozygous viable P(EP)^{1149} insertion shows a significant decrease in presynaptic transmitter release (quantal content; see Experimental Procedures) without any change in the average quantal size compared with wild-type and heterozygous P(EP)^{1148} element controls (Figure 2). P(EP)^{1179} homozygous viable larvae do not show any change in synaptic structure or function. However, when P(EP)^{1179} is placed in *trans* to known hypomorphic alleles of dCBP, including *dCBP*$^{\Delta A57}$ and *dCBP*$^{\Delta 342}$, we observe a decrease in presynaptic quantal content that is identical to that observed in P(EP)^{1148} homozygous larvae; there is a ~50% decrease in quantal content without any change in quantal size compared with wild-type and heterozygous controls, including P(EP)^{1179}/+, *dCBP*$^{\Delta 342}$/+, and *dCBP*$^{\Delta A57}$/+ (Figure 2). We never observed a change in the average muscle resting potential or in the average muscle input resistance in any genotype demonstrating the specificity of these phenotypes to changes in presynaptic release.

Previously identified homozygous dCBP mutations are all lethal during early development. We therefore used a previously identified dominant-negative allele of dCBP to further demonstrate the specificity of this dCBP physiological phenotype. The *dCBP*^{D7} allele has been characterized as an antimorphic allele with a presumed dominant-negative function (Florence and McGinnis, 1998). Consistent with these previously published data,

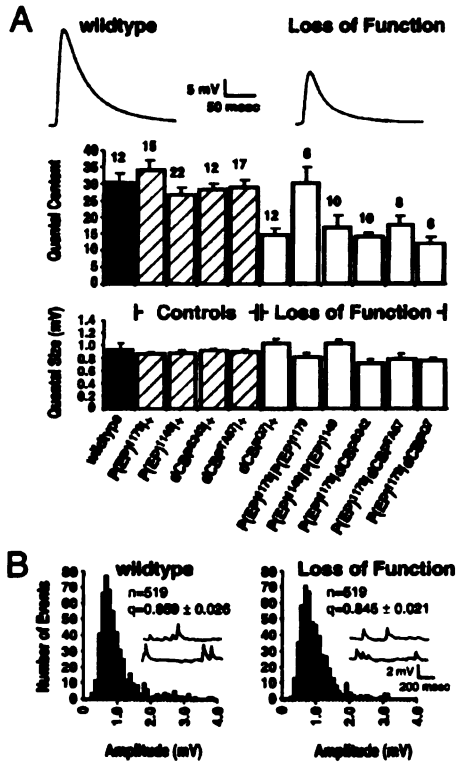

Figure 2. dCBP Loss of Function Decreases Quantal Content without Affecting Quantal Size

(A) Quantification of quantal content, as estimated by dividing the average EPSP by the average mEPSP. Average quantal content is significantly reduced in strong hypomorphic mutations (open bars), including *dCBP*^{D7}/+ (dominant-negative allele), *P(EP)*^{1148}/*P(EP)*^{1148}, *P(EP)*^{1179}/*dCBP*$^{\Delta 342}$, *P(EP)*^{1179}/*dCBP*$^{\Delta A57}$, and *P(EP)*^{1179}/*dCBP*^{D7} ($p < 0.01$ for all genotypes compared with wild type [closed bar]). Quantal content was not significantly altered in the heterozygous controls (hatched bars), including *P(EP)*^{1179}/+, *P(EP)*^{1148}/+, *dCBP*$^{\Delta 342}$/+, and *dCBP*$^{\Delta A57}$/+. Quantal size is not significantly altered in any genotype compared with wild type. The number of recordings for each genotype is shown above the bar. Representative EPSPs from wild type and a strong hypomorphic mutation are shown above the graphs. Coding of genotypes in this and subsequent figures are is follows: wild type, closed bars; heterozygous controls, hatched bars; and experimental genotypes, open bars.

(B) Distribution of mEPSPs for recordings of wild type and *P(EP)*^{1179}/*dCBP*$^{\Delta A57}$ (abbreviations: n, number of events; q, mean quantal size). Inset, sample traces for each genotype. The distribution of mEPSPs is unaltered in strong dCBP hypomorphs.

dCBP^{D7} shows a dominant reduction in presynaptic transmitter release without any change in quantal size (Figure 2). The anatomical and electrophysiological phenotypes of the *dCBP*^{D7} allele are identical to the phenotypes of the *P(EP)*^{1148} homozygous larvae and to P(EP)^{1179} in *trans* with *dCBP*$^{\Delta A57}$ and *dCBP*$^{\Delta 342}$. Consistent with *dCBP*^{D7} having a dominant-negative (antimorphic) activity, the electophysiological phenotype is not significantly enhanced in *trans* to the P(EP)^{1179} loss-of-function insertion (Figure 2). Thus, our recently identified hypomorphic

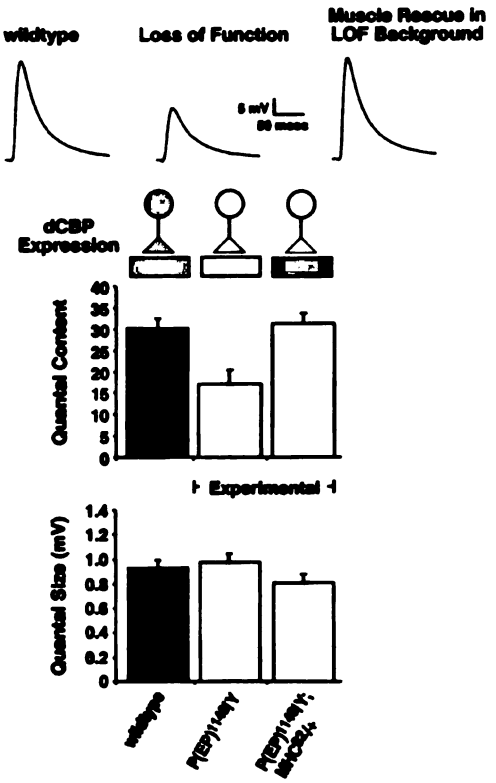

Figure 3. Postsynaptic dCBP Expression Rescues Presynaptic Transmitter Release in the dCBP Mutant Background

Quantal content and quantal size are quantified for dCBP loss of function ("Loss of Function") and when dCBP is expressed in postsynaptic muscle in this loss-of-function genetic background ("Muscle Rescue in LOF Background"). Sample traces are shown at the top for each genetic background (traces are signal averages of 10–20 individual EPSPs). dCBP expression is shown schematically above each bar of the graph.

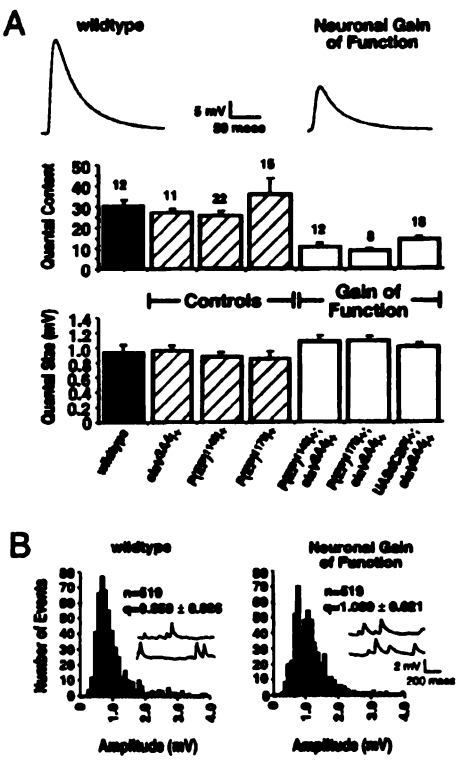

Figure 4. Presynaptic dCBP Overexpression Decreases Quantal Content without Affecting Quantal Size

(A) Quantification of quantal content, as estimated by dividing the average EPSP by the average mEPSP. Average quantal content is significantly reduced in genotypes that overexpress dCBP presynaptically, including *P(EP)^{1148}/+;elaV3A4/+*, *P(EP)^{1179}/+;elaV^{3A1}/+*, and *UAS-dCBP1+;elaV^{3A1}/+*. Quantal size is not significantly altered in any genotype compared with wild type. The number of recordings for each genotype is shown above the bar. Representative EPSPs from wild type and presynaptic overexpressing genotypes are shown above the graphs.

(B) Distribution of mEPSPs for recordings of wild type and *P(EP)^{1179}/elaV^{3A1}dCBP^{A51}* (abbreviations: n, number of events; q, mean quantal size). Inset, sample traces for each genotype. Presynaptic overexpression of dCBP does not alter the distribution of mEPSPs compared with wild type.

P(EP) element insertions in the 5′ UTR of dCBP show an electrophysiological phenotype that is identical to a dCBP dominant-negative allele and fail to complement previously identified hypomorphic alleles of dCBP, indicating that these P(EP) elements disrupt dCBP activity. These data demonstrate that dCBP is necessary for functional synaptic development at the NMJ.

Postsynaptic dCBP Rescues Presynaptic Release in the Loss-of-Function Mutant

To address whether dCBP is necessary in the pre- or postsynaptic cell for normal synaptic development, we have rescued dCBP expression on either side of the synapse in the hypomorphic mutant background. P(EP)^{1148} males show a ~50% reduction in presynaptic transmitter release that is identical to homozygous females and other loss-of-function allelic combinations (Figure 3). We therefore used P(EP)^{1148} males as a hypomorphic mutant background and expressed dCBP with either *MHC-GAL4* (all muscle) or *elaV-GAL4* (all neurons). Expression of dCBP in muscle in the hypomorphic mutant background rescues presynaptic quantal content to wild-type levels (Figure 3). However, expression of dCBP in nerve in the same hypomorphic mutant background resulted in early larval lethality (0.5% survival). Thus, postsynaptic dCBP can rescue presynaptic functional development in the hypomorphic mutant background.

dCBP Overexpression Inhibits Functional Presynaptic Development

Overexpression of dCBP in either the pre- or postsynaptic cell causes a reduction in presynaptic transmitter release (Figures 4 and 5). dCBP was overexpressed in

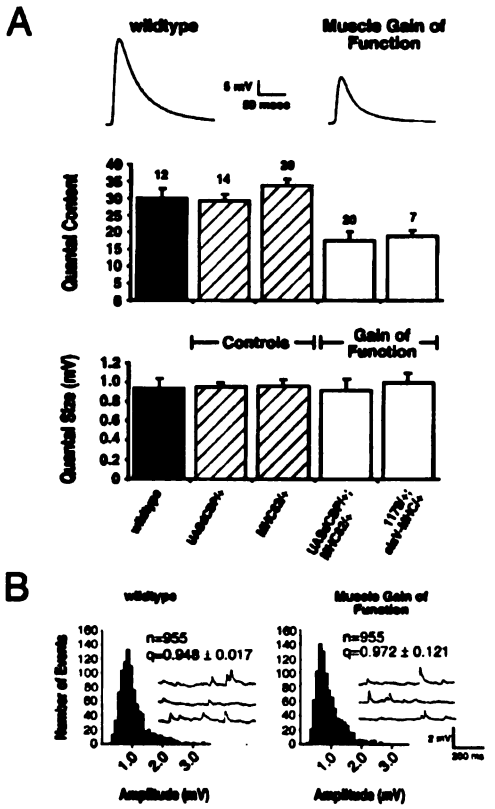

Figure 5. Postsynaptic dCBP Overexpression Decreases Quantal Content without Affecting Quantal Size

(A) Quantal content and quantal size are quantified for two genetic controls and when dCBP is overexpressed in muscle using *MHC-GAL4* and *UAS-dCBP*. A significant difference is observed for quantal content at the *UAS-dCBP/MHC-GAL4*$^{\#2}$ synapse (expression postsynaptically) and at the *P(EP)*^{1179}/+;*elaV-GAL4*/+;*MHC-GAL4*$^{\#2}$/+ synapse (expression both pre- and postsynaptically) compared with all other genotypes ($p < 0.001$, student's t test). Sample traces are shown at top (averages of 10–20 individual EPSPs).

(B) There is no change in the distribution of spontaneous miniature release events when dCBP is overexpressed in muscle. The number of events analyzed (n), the average quantal size (q), and the standard deviation (±) are indicated for each histogram. Inset, sample traces showing spontaneous miniature release events from the distribution quantified in each histogram.

the wild-type background using the *dCBP* cDNA under UAS control (*UAS-dCBP*). Presynaptic overexpression was driven by *elaV-GAL4*. We observe a decrease in presynaptic transmitter release (~70%) without a change in the average size or distribution of the spontaneous miniature release events and without any change in the average resting potential or average input resistance of the postsynaptic muscle (Figure 4). We also overexpressed dCBP from either P(EP)^{1148}/+ or P(EP)^{1179}/+. These heterozygous P(EP) elements are electrophysiologically wild type in the absence of GAL4 (Figure 4). When dCBP is overexpressed from the P(EP) elements using *elaV-GAL4*, we observe a reduction in presynaptic release identical to the overexpression of *UAS-dCBP*. Overexpression of dCBP in muscle, or in both muscle and nerve, also inhibits presynaptic transmitter release (Figure 5). Again, we do not observe any change in quantal size or muscle physiological parameters. We conclude that overexpression of dCBP either pre- or postsynaptically inhibits presynaptic functional development.

Ultrastructural Analysis

We examined the synaptic ultrastructure to determine whether the observed impairment of presynaptic release is due to gross ultrastructural abnormalities. Synaptic ultrastructure appears normal at neuromuscular boutons in both gain- and loss-of-function genetic backgrounds despite reduced presynaptic transmitter release at these synapses. There does not appear to be any alteration in the extent of subsynaptic reticulum or in the integrity of individual active zones (Figure 6). Indeed, there is an increase in the number of presynaptic T bars per active zone in the dCBP loss-of-function synapse (n = 183 active zones in P(EP)^{1148}, and n = 219 active zones in wild type, $p < 0.001$). It has been hypothesized that T bars may facilitate transmitter release; however, their precise function in synaptic transmission remains unclear. We therefore conclude that gross ultrastructural abnormalities are not the cause of decreased presynaptic release.

Synapse Morphology at dCBP Gain- and Loss-of-Function Mutant Synapses

A morphological analysis demonstrates that reduced transmitter release in the dCBP gain- and loss-of-function backgrounds is not due to a disruption of morphological synaptic development. Synaptic structure and function were both calculated for each individual preparation by fixing and staining each electrophysiological preparation with anti-Synaptotagmin to reveal the nerve terminal boutons. Thus, we can precisely correlate changes in synaptic function with a change in the synapse morphology. Strong loss-of-function allelic combinations and the dominant-negative *dCBP*$^{\Delta 7}$ allele all cause an increase in bouton number (255; 35% increase) at the NMJ of muscles 6 and 7 (Figure 7) and muscle 4 (data not shown). There is only a modest change in the number of synaptic boutons, and, therefore, we suspect that this is a compensatory response due to the observed decrease in synaptic function in these dCBP mutants. These data indicate that the health of the pre- and postsynaptic cells has not been compromised.

In contrast, overexpression of dCBP either pre- or postsynaptically does not alter bouton number despite a reduction in transmitter release that is comparable to that observed at dCBP loss-of-function synapses (Figure 7). Thus, dCBP overexpression inhibits presynaptic release without any morphological compensation.

We have also performed experiments to control for any potential dCBP-dependant alteration in axon guidance, target selection, or alteration in neuronal and glial cell fate at dCBP gain- or loss-of-function backgrounds. Synaptic connectivity in the larval neuromuscular system appears normal based on visual inspection of type

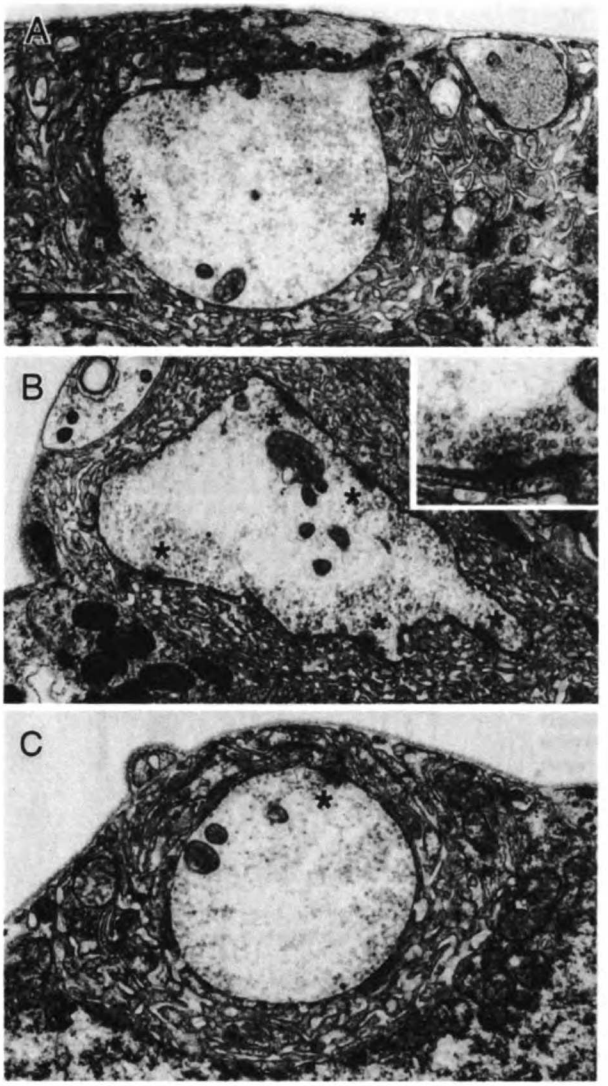

Figure 6. Synaptic Ultrastructure Is Normal in dCBP Mutants and When dCBP Is Overexpressed

Single sections from EM serial reconstruction of third instar synapses on muscle 6 in abdominal segment 3.

(A) Cross-section of a wild-type bouton. Active zones with T bars are indicated (asterisk).

(B) Cross-section of a synaptic bouton from dCBP loss of function, $P(EP)^{1149}/P(EP)^{1149}$. Inset, higher magnification of an active zone with a presynaptic T bar.

(C) Cross-section of a synaptic bouton from a synapse overexpressing dCBP both pre- and postsynaptically [$P(EP)^{1178}$;*elaV-GAL4*; *MHC-GAL4*].

Ia, type Ib, and type II synapses at muscle 6, 7, 13, 12, 4, 3, 2, and 1. These synapses were inspected during the quantitation of bouton number in each genotype (over 400 segments analyzed). We do not observe any alteration in axon guidance in the embryonic CNS, indicating that cell fate and guidance are normal in the CNS (data not shown). In the embryo, we do observe weakly penetrant axon guidance defects in the neuromuscular system (data not shown). In the experiments presented here, we controlled for any defect in target selection by quantitating synapse morphology and bouton number for each electrophysiological preparation. We did not observe any alteration in target selection or innervation at the muscles from which we recorded electrophysiologically. Finally, we have examined the distribution of glial cell bodies in the embryo and larva, visualized with the anti-REPO antibody. We did not observe any change in the number or distribution of glia within the embryonic or larval CNS or PNS (data not shown).

Ca^{2+} Cooperativity and Synaptic Facilitation

We performed additional experiments to determine whether decreased transmitter release in the dCBP gain-of-function and dCBP loss-of-function mutations can be further distinguished. We examined the Ca^{2+} dependence of transmitter release at synapses with either increased or decreased dCBP. At both dCBP gain- and loss-of-function synapses, the Ca^{2+} cooperativity of transmitter release remains in the range of what is considered to be wild type (slope, ~4) despite a shift

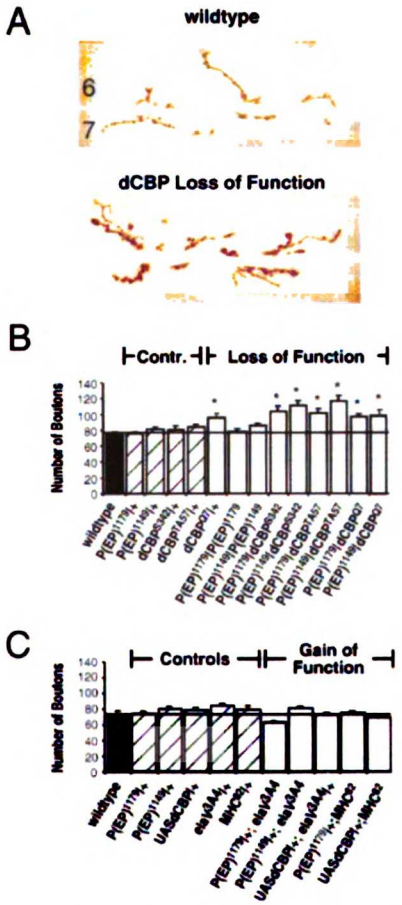

Figure 7. Hypomorphic Mutations in dCBP Cause a Moderate Increase in Synapse Size

(A) Representative light micrographs of muscles 6 and 7 in segment A3 of wild type and dCBP loss-of-function ($P(EP)^{1179}/dCBP^{7A57}$) third instar larvae stained with anti-Fasciclin II and anti-Synaptotagmin. dCBP loss of function causes a moderate (~25%) increase in bouton number.

(B and C) Quantification of synapse size in dCBP loss-of-function (B) and overexpression (C) genotypes. Synapse size was quantified by staining with anti-Fasciclin II and anti-Synaptotagmin and counting boutons at muscles 6 and 7 of segment A3 in third instar larvae. Strong dCBP loss-of-function mutations show a significant increase in synapse size, including $P(EP)^{1179}/dCBP^{5342}$, $P(EP)^{1149}/dCBP^{5342}$, $P(EP)^{1179}/dCBP^{7A57}$, $P(EP)^{1149}/dCBP^{7A57}$, $dCBP^{07}/+$ (dominant-negative), $P(EP)^{1179}/dCBP^{07}$, and $P(EP)^{1149}/dCBP^{07}$ ($p < 0.01$). One presynaptic overexpression genotype ($P(EP)^{1179}/+;elaV^{3A4}/+$) showed a significant decrease in synapse size ($p = 0.013$).

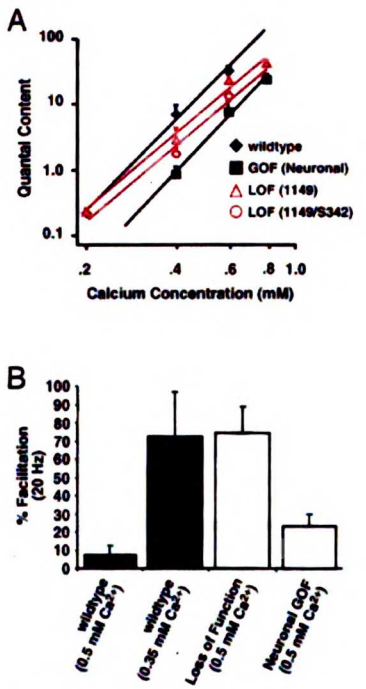

Figure 8. Ca^{2+} Cooperativity and Facilitation in dCBP Gain and Loss of Function

(A) Ca^{2+} cooperativity data are shown for both dCBP loss of function [$P(EP)^{1149}/P(EP)^{1149}$ ($R^2 = 0.9894$) and $P(EP)^{1149}/dCBP^{5342}$ ($R^2 = 0.9626$)] and presynaptic overexpression [*UAS-dCBP/+;elaV*^{3A4}*/+* ($R^2 = 0.9925$)] compared with wild type ($R^2 = 0.9951$). Cooperativity is maintained within a normal range (slope, ~4) despite a consistent reduction in cooperativity in the two loss-of-function genetic backgrounds.

(B) Short-term facilitation is examined at wild-type synapses (closed bars) at two different Ca^{2+} concentrations (0.5 mM and 0.35 mM). Facilitation is also examined at 0.5 mM Ca^{2+} in both dCBP loss of function [$P(EP)^{1149}/P(EP)^{1149}$] and when dCBP is overexpressed presynaptically in the wild-type genetic background [*UAS-dCBP/+; elaV-GAL4/+*].

toward smaller quantal contents at all but the lowest Ca^{2+} concentrations used (Figure 8). There is a consistent reduction in the cooperativity of release in the loss-of-function background compared with wild-type and dCBP overexpression. However, this change in cooperativity is relatively minor. These data demonstrate that the decrease in presynaptic release in the dCBP gain- and loss-of-function backgrounds is not due to a substantial alteration in the Ca^{2+}-dependent transmitter release mechanism (Figure 8).

We also analyzed short-term facilitation in these dCBP gain- and loss-of-function backgrounds. Short-term facilitation was induced with five stimuli delivered with an interpulse interval of 50 ms (20 Hz). Facilitation was calculated by the percent change in excitatory postsynaptic potential (EPSP) amplitude from the first to the fifth EPSP (Davis et al., 1996). In the dCBP mutant background, there is 74% facilitation compared with 9% facilitation in wild type at 0.5 mM extracellular Ca^{2+}. However, the initial EPSP in the dCBP mutant background is 50% of that of wild type. When we reduced the first EPSP in wild-type larvae to a similar level (10.0 ± 1.2 mV) by recording in 0.35 mM extracellular Ca^{2+}, we observed 73% facilitation. These data indicate that altered facilitation in the dCBP mutant background is due to a reduction in the initial EPSP amplitude. These data further

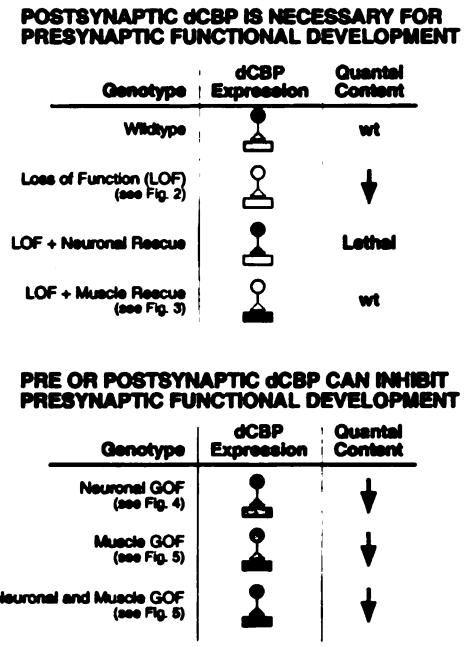

Figure 9. dCBP Both Positively and Negatively Regulates Presynaptic Functional Development

(A) Summary of results from loss-of-function and rescue experiments.

(B) Summary of experiments overexpressing dCBP either pre- or postsynaptically in the wild-type genetic background. A reference to primary data is indicated below each experiment. Levels of dCBP expression are indicated schematically, with darker shading indicating higher levels of expression.

suggest that reduced transmitter release in the dCBP loss-of-function background may be due to a reduction in the probability of presynaptic release.

Facilitation at synapses with presynaptic dCBP overexpression is not increased despite a ~50% reduction in the initial EPSP amplitude. At 0.5 mM extracellular Ca^{2+}, we observe 23% facilitation. This is significantly less facilitation than observed at dCBP loss-of-function synapses and at wild-type synapses in 0.35 mM Ca^{2+}, which have a comparable initial EPSP amplitude. Thus, the reduced initial EPSP amplitude in dCBP neuronal gain of function does not correlate with increased facilitation, suggesting that decreased transmitter release may be due to a reduction in the number of functional active zones. However, we do not observe a change in the frequency of spontaneous vesicle fusion events (mEPSPs) in dCBP neuronal gain of function compared with wild type (data not shown). In conclusion, reduced transmitter release in dCBP gain- and loss-of-function is likely due to different mechanisms.

Discussion

Our data demonstrate that postsynaptic dCBP is necessary and may also be sufficient for the development of normal presynaptic transmitter release at the NMJ. This indicates that dCBP participates in a retrograde signaling pathway that controls presynaptic development. We further demonstrate that dCBP can inhibit the development of presynaptic transmitter release when overexpressed either pre- or postsynaptically. This indicates that dCBP-dependent mechanisms can act as both positive and negative regulators of presynaptic development. We hypothesize that postsynaptic dCBP participates in the homeostatic control of presynaptic function.

dCBP Is Necessary for Presynaptic Functional Development

We have analyzed five different loss-of-function alleles of dCBP. In each viable genetic combination in which dCBP activity is reduced, there is a 45%–50% decrease in presynaptic transmitter release. The observed decrease in presynaptic release is severe, being comparable to phenotypes observed in Synaptotagmin mutant larvae (Littleton et al., 1993; DiAntonio and Schwarz, 1994). The loss of dCBP does not alter the health of the synapse, as assayed by light microscopy and ultrastructural analysis, and is not due to altered muscle innervation or altered glial or neuronal cell fate. Thus, dCBP loss of function dramatically and specifically impairs functional synaptic development.

Genetic rescue experiments indicate that the developmental requirement for dCBP is postsynaptic. Exogenous expression of dCBP in muscle in the loss-of-function genetic background rescues presynaptic functional development to wild type. Since transmitter release is wild type despite reduced presynaptic dCBP, we conclude that postsynaptic dCBP expression is necessary for normal functional synaptic development. These postsynaptic rescue data also suggest that postsynaptic dCBP may be sufficient for presynaptic functional development. However, these rescues are conducted in hypomorphic loss-of-function backgrounds, and, as such, there remains a residual level of dCBP presynaptically (Figures 2, 3, and 9).

Expression of dCBP presynaptically in the loss-of-function background causes lethality. We hypothesize that this lethality is due to an additive effect of dCBP loss of function postsynaptically and an inhibitory effect of presynaptic dCBP overexpression. Overexpression presynaptically in the wild-type background (normal muscle dCBP) inhibits transmitter release. Additional data indicate that the inhibitory effect of dCBP overexpression may act via a mechanism different from dCBP loss of function (see next section). Therefore, the effects of presynaptic overexpression and postsynaptic loss of function are likely to be additive. However, these data also raise the possibility that the ratio of dCBP expression in the presynaptic neuron, relative to the postsynaptic target, may also be an important parameter. We are unable to assay expression levels accurately enough to address this issue.

dCBP Overexpression Inhibits Presynaptic Functional Synaptic Development

Overexpression of dCBP in the postsynaptic muscle or the presynaptic nerve inhibits presynaptic transmitter

release (Figures 4, 5, and 9b). Anatomical, ultrastructural, and electrophysiological data indicate that dCBP overexpression does not poison the synapse. One possibility is that overexpression of wild-type dCBP in the wild-type genetic background can somehow act as a dominant-negative and therefore mimics the loss-of-function phenotype. However, postsynaptic dCBP expression can rescue the loss-of-function phenotype, indicating that exogenous dCBP can function correctly during synaptic development. In addition, the gain- and loss-of-function phenotypes can be distinguished by differential changes in synapse morphology and short-term facilitation. Therefore, we interpret our overexpression data as indicating that dCBP can function normally to inhibit presynaptic functional development by a mechanism that is distinct from dCBP loss of function.

We observe increased synapse morphology in the loss-of-function background, while there is no change in bouton number when dCBP is overexpressed either pre- or postsynaptically. Since the increased morphology in the dCBP mutant background is moderate, we hypothesize that this is a compensatory response due to reduced presynaptic release. This implies that dCBP overexpression blocks this form of compensation. However, it is unclear whether this is a direct or indirect effect of dCBP overexpression.

dCBP gain- and loss-of-function phenotypes can also be distinguished by analysis of short-term facilitation. There is a reduction in the initial EPSP amplitude in both dCBP gain and loss of function. At 0.5 mM extracellular Ca^{2+}, the reduced initial EPSP is correlated with increased facilitation at the dCBP loss-of-function synapse, whereas facilitation is normal in the dCBP gain-of-function synapse (despite a reduced initial EPSP). When the initial EPSP amplitude at a wild-type synapse is experimentally reduced by reducing extracellular Ca^{2+} (to 0.35 mM Ca^{2+}), we observe facilitation that is similar to that observed at a dCBP loss-of-function synapse recorded at 0.5 mM Ca^{2+}. These data indicate that the EPSP amplitude is reduced by different mechanisms in the dCBP gain- and loss-of-function genetic backgrounds. We suspect that dCBP overexpression inhibits some aspect of presynaptic release that is independent of the probability of presynaptic release.

dCBP and the Homeostatic Regulation of Synaptic Function

At the larval NMJ, an experimental decrease in postsynaptic excitation causes a compensatory enhancement of presynaptic release (Petersen et al., 1997; Davis et al., 1998). These previous experiments define a homeostatic regulatory system that maintains postsynaptic excitation through a retrograde signal(s) from muscle to nerve. A homeostatic regulatory system will likely include mechanisms that can monitor postsynaptic excitation and transduce this information through a retrograde signal to modulate presynaptic transmitter release. In principle, homeostatic regulation will require both positive and negative regulation of synaptic function.

We hypothesize that dCBP is centrally involved in the mechanisms that monitor postsynaptic activity. We identified the dCBP P(EP) element mutations described here in a screen for mutations in genes that participate in the homeostatic regulation of presynaptic transmitter release (G. W. Davis et al., submitted). We demonstrate here that perturbations in postsynaptic dCBP can affect presynaptic transmitter release. Furthermore, postsynaptic dCBP can act as both a positive and negative regulator of synaptic function. Finally, CBP in *Drosophila* and other systems is well suited to participate in a system that monitors postsynaptic activity. CBP function can be regulated by Ca^{2+} influx through voltage-gated channels and ionotropic receptors (Hardingham et al., 1999; Hu et al., 1999). Furthermore, CBP can act as a transcriptional coactivator with CREB and other transcription factors, as well as function as an intracellular signaling molecule via acetylase activity (Waltzer and Bienz, 1998). In conclusion, we propose that dCBP is an essential component of the postsynaptic homeostatic mechanism that monitors activity and regulates presynaptic transmitter release.

We have previously proposed that the homeostatic retrograde increase in presynaptic release is due to a signal that can enhance presynaptic transmission, similar to that proposed for the presynaptic expression of long-term potentiation (Bliss and Collingridge, 1993). Our current data suggest an additional model, that a homeostatic increase in presynaptic transmission could also be achieved by relieving an inhibitory signal derived from postsynaptic dCBP function.

Homeostatic control of presynaptic function at the *Drosophila* NMJ ensures that presynaptic release is precisely coupled to the growth of the postsynaptic muscle throughout development. To achieve constant muscle depolarization during development, homeostatic signaling must achieve a progressive and gradual increase in synaptic function. A progressive and gradual increase in synaptic function could be achieved through dCBP-dependent mechanisms since it can both promote and inhibit synaptic development. Activation of dCBP could promote synaptic strengthening, while sustained dCBP activation could inhibit further synaptic development, preventing runaway excitation. This is consistent with our demonstration that postsynaptic dCBP is necessary for normal synaptic development but that sustained overexpression of dCBP can inhibit presynaptic functional development.

CBP/CREB Function during Synaptic Development and Activity-Dependent Plasticity

Our results are consistent with previous data examining CREB activity in *Drosophila*. Neither CREB nor dCBP directly alters synaptic morphology (Davis et al., 1996). Here, we demonstrate a role for dCBP in regulated functional synaptic development. However, we have previously demonstrated that CREB is unlikely to be involved in synaptic development based on heat shock overexpression of dCREB2b (Davis et al., 1996). Thus, dCBP may regulate synaptic development though non CREB-dependent mechanisms.

In vertebrates, CBP has been broadly implicated as being necessary for normal brain development, as well as learning. CBP mutant mice show dominant defects in neuronal development, as well as learning and memory. In humans, CBP mutations are associated with Rubenstein-Taybi syndrome, a disorder that is characterized by developmental limb defects and severe mental

retardation (Tenaka et al., 1997). Our data implicate dCBP as having a specific role at the synapse. A similar role for CBP in vertebrate systems could contribute to our understanding of the observed phenotypes.

CBP is a transcriptional coactivator for CREB. CREB has been investigated in detail for a role in activity-dependent synaptic plasticity (Bartsch et al., 1995, 1998; Deisseroth et al., 1996; Yin and Tully, 1996; Casadio et al., 1999). CREB has also been implicated in the mechanisms of learning in the mouse (Silva et al., 1998). In Aplysia, presynaptic CREB is considered necessary for seratonin- and protein synthesis–dependent long-term synaptic facilitation (Bartch et al., 1995, 1998; Casadio et al., 1999). Experiments on vertebrate neurons in cell culture implicate a role for postsynaptic CREB in activity-dependent plasticity and neurotrophin-dependent neuronal survival (Deisseroth et al., 1996; Finkbeiner et al., 1997). CBP has also been implicated in the neurotrophin-dependent survival mechanisms (Liu et al., 1998). However, the precise relationship between CREB and CBP in the control of these processes remains unclear. For example, CREB and CBP may be differentially phosphorylated in response to different sources of postsynaptic Ca^{2+} influx (Hardingham et al., 1999; Hu et al., 1999). In addition, CBP is known to act as a coactivator with other transcription factors and as a signaling molecule via acetylase activity (Johnston et al., 1999; Waltzer and Bienz 1998, 1999). *Drosophila* now opens the possibility for a forward genetic analysis of CBP function at the synapse.

Experimental Procedures

Electron Microscopy

Wild-type and mutant larvae were prepared for electron microscropy (EM) according to procedures previously described (Schuster et al., 1996). Serial sections were taken at 0.1 μm, as described previously. EM for dCBP loss-of-function analysis was done on homozygous $P(EP)^{1148}$ third instar larvae.

Genetics

$P(EP)^{1148}$ and $P(EP)^{1178}$ were obtained from the Berkeley *Drosophila* Genome Project. $dCBP^{e543}$/*Fm7c*, $dCBP^{e543}$/*Fm7c*, and $dCBP^{07}$/*FM7c* were obtained from the laboratory of William McGinnis. Homozygous lethal dCBP alleles were maintained over an *Fm7c-kruppel*-GFP balancer (provided by Tom Kornberg). dCBP mutant chromosomes were identified in the larvae based on malpigian tubule and mouth hook color (Schuster et al., 1996) and based on the absence of the *FM7c*-GFP balancer. Muscle overexpression of dCBP was achieved using the *MHC-GAL4*[17] line (Winberg and C. S. G., unpublished data). Presynaptic overexpression of dCBP was achieved using the *elaV-GAL4*[3A4] line. *UAS-dCBP* is a complete dCBP open reading frame cloned into the P-UAS transformation vector and inserted on the X chromosome.

Histology

Following dissection and electrophysiological recording, each larval fillet was fixed in 3.7% formaldehyde in HL3 saline (Stewart et al., 1994). The NMJ was visualized with anti-Synaptotagmin and anti-Fasciclin II double staining, as described previously (Davis et al., 1997). Bouton numbers were quantified at muscles 6 and 7 in larval segment A3, as described previously (Davis et al., 1997), allowing direct correlation between the electrophysiology and anatomy for each neuromuscular synapse. All bouton counts were done blind. Glia were stained using the anti-Repo antibody, provided by C. S. Goodman. Axon guidance was assayed in the embryonic nervous system using anti-Fasciclin II (Goodman) and the monoclonal antibody BP102 (Goodman). dCBP expression was assayed using a dCBP antibody (chicken). dCBP imaging was done on a DeltaVision deconvolution confocal microscope (Applied Precision). Relative fluorescence intensity was measured using the line profile tool of DeltaVision software, allowing comparison of pixel intensity between the muscle and nuclear dCBP fluorescence. Averages were take from 30–40 muscle nuclei from 24–30 separate synapses in wild-type and $P(EP)^{1148}$ homozygous mutant larvae.

Molecular Reagents

Genomic sequences flanking the P element insertion were amplified by PCR from *P(EP)*[1178] genomic DNA using a primer from the 3′ end of the P element (pry2) and primers from dCBP (nej1, nej2, and nej4). PCR products were cloned into pGEM-T (Promega) and sequenced. For analysis of the P element–driven transcript, $P(EP)^{1178}$ females were crossed to heat shock GAL4 males. Embryos were heat shocked at 37°C for 2 hr, and the RNA isolated (Qiagen). RT-PCR was performed (GIBCO) using the following primer pairs: first round, pr192 and nej2; second round, pr200 and nej1. In situ hybridizations were performed on embryos derived from two GAL4 enhancer lines, *24B-GAL4* and *elaV-GAL4*[3A4], crossed to $P(EP)^{1178}$ females. Embryos were probed with a dCBP probe. The dCBP probe was generated from bases 766 to 1279 of the known dCBP sequence and subcloned into pGEM-T, and the digoxigenin-labeled RNA probe was synthesized accordingly (Roche Molecular Biochemicals). The sequences for the PCR primers designated in Figure 1 are as follows: pry2, CTTGCCGACGGGACCACCTTATGTTATT; pr192, GAGTTAATTCAA ACCCCACGGACATGC; pr200, CTCTAGACAAGCATACGTTAAGTG GATGTC; nej1, CGAGGACACCAGCTCATC; nej2, GGATTCCCGCT TACCAG; and nej4, GTGGTGCTGGAATGTTGC.

Electrophysiology

All recordings were made from muscle fiber 6 in abdominal segment A3 in 0.5 mM Ca^{2+} HL3 saline, as previously described, except where indicated (Davis et al., 1996). For each recording, the resting membrane potential and input resistance were recorded. Only recordings with resting potentials of at least −60 and input resistances of at least 8 MΩ were included in our analysis. Quantal content was calculated by dividing the average maximal EPSP amplitude by the average amplitude of the spontaneous miniature release events (mEPSP). Quantal size was determined by the average amplitude of the spontaneous release events recorded in the absence of stimulation. To compare the distribution of spontaneous release events between different mutant lines, mEPSPs were pooled for at least five recordings from at least five preparations in which the muscle input resistance and resting membrane potentials were closely matched (RMP, between −65 and −72; R_{in} between 8 and 9 MΩ). Frequency-dependent facilitation experiments were performed and quantified as described previously (Davis et al., 1996). Measurements of maximal EPSP amplitude were done by hand, as described previously. Measurements of spontaneous miniature release events were semiautomated using MiniAnalysis software (Jaejin) and edited by hand.

Acknowledgments

We thank James Spiess and Jennie Brotman for technical support throughout these projects, Peter Clyne and Suzanne Paradis for discussion and critical evaluation of the manuscript, and Tom Komberg for GFP balancer stocks. We thank the Sandler Foundation and the Howard Hughes Medical Institute for start-up funding for the laboratory of G. W. D. This work was supported by Burroughs Wellcome, a Klingenstein award, a Merck Scholar award, and a National Institutes of Health grant (444908-32374) to G. W. D. and by a Howard Hughes Medical Institute predoctoral fellowship to K. M. C. S. G. is an investigator, and R. F. a research scientist, with the Howard Hughes Medical Institute.

Received December 6, 1999; revised February 18, 2000.

References

Akimaru, H., Chen, Y., Dai, P., Hou, D.X., Nonaka, M., Smolik, S.M., Armstrong, S., Goodman, R.H., and Ishiim, S. (1997). Drosophila

CBP is a co-activator of cubitus interruptus in hedgehog signalling. Nature *386*, 735–738.

Arancio, O., Kiebler, M., Lee, C.J., Lev-Ram, V., Tsien, R.Y., Kandel, E.R., and Hawkins, R.D. (1996). Nitric oxide acts directly in the presynaptic neuron to produce long-term potentiation in cultured hippocampal neurons. Cell *87*, 1025–1035.

Bartsch, D., Ghirardi, M., Skehel, P.A., Karl, K.A., Herder, S.P., Chen, M., Bailey, C.H., and Kandel, E.R. (1995). Aplysia CREB2 represses long-term facilitation: relief of repression converts transient facilitation into long-term functional and structural change. Cell *83*, 979–992.

Bartsch, D., Casadio, A., Karl, K.A., Serodio, P., and Kandel, E.R. (1998). CREB1 encodes a nuclear activator, a repressor, and a cytoplasmic modulator that form a regulatory unit critical for long-term facilitation. Cell *95*, 211–223.

Bito, H., Deisseroth, K., and Tsien, R.W. (1996). CREB phosphorylation and dephosphorylation: a Ca(2+)- and stimulus duration-dependent switch for hippocampal gene expression. Cell *87*, 1203–1214.

Bliss, T.V., and Collingridge, G.L. (1993). A synaptic model of memory: long-term potentiation in the hippocampus. Nature *361*, 31–39.

Bourtchuladze, R., Frenguelli, B., Blendy, J., Cioffi, D., Schutz, G., and Silva, A.J. (1994). Deficient long-term memory in mice with a targeted mutation of the cAMP-responsive element-binding protein. Cell *79*, 59–68.

Buchs, P.A., and Muller, D. (1996). Induction of long-term potentiation is associated with major ultrastructural changes of activated synapses. Proc. Natl. Acad. Sci. USA *93*, 8040–8045.

Casadio, A., Martin, K.C., Giustetto, M., Zhu, H., Chen, M., Bartsch, D., Bailey, C.H., and Kandel, E.R. (1999). A transient, neuron-wide form of CREB-mediated long-term facilitation can be stabilized at specific synapses by local protein synthesis. Cell *99*, 221–237.

Chrivia, J.C., Kwok, R.P., Lamb, N., Hagiwara, M., Montminy, M.R., and Goodman, R.H. (1993). Phosphorylated CREB binds specifically to the nuclear protein CBP. Nature *365*, 855–859.

Davis, G.W., and Goodman, C.S. (1998a). Genetic analysis of synaptic development and plasticity: homeostatic regulation of synaptic efficacy. Curr. Opin. Neurobiol. *8*, 149–156.

Davis, G.W., and Goodman, C.S. (1998b). Synapse-specific control of synaptic efficacy at the terminals of a single neuron. Nature *392*, 82–86.

Davis, G.W., Schuster, C.M., and Goodman, C.S. (1996). Genetic dissection of structural and functional components of synaptic plasticity. III. CREB is necessary for presynaptic functional plasticity. Neuron *17*, 669–679.

Davis, G.W., Schuster, C.M., and Goodman, C.S. (1997). Genetic analysis of the mechanisms controlling target selection: target-derived Fasciclin II regulates the pattern of synapse formation. Neuron *19*, 561–573.

Davis, G.W., DiAntonio, A., Petersen, S.A., and Goodman, C.S. (1998). Postsynaptic PKA controls quantal size and reveals a retrograde signal that regulates presynaptic transmitter release in *Drosophila*. Neuron *20*, 305–315.

Deisseroth, K., Bito, H., and Tsien, R.W. (1996). Signaling from synapse to nucleus: postsynaptic CREB phosphorylation during multiple forms of hippocampal synaptic plasticity. Neuron *16*, 89–101.

DiAntonio, A., and Schwarz, T.L. (1994). The effect on synaptic physiology of synaptotagmin mutations in Drosophila. Neuron *12*, 909–920.

Engert, F., and Bonhoeffer, T. (1999). Dendritic spine changes associated with hippocampal long-term synaptic plasticity. Nature *399*, 66–70.

Finkbeiner, S., Tavazoie, S.F., Maloratsky, A., Jacobs, K.M., Harris, K.M., and Greenberg, M.E. (1997). CREB: a major mediator of neuronal neurotrophin responses. Neuron *19*, 1031–1047.

Florence, B., and McGinnis, W. (1998). A genetic screen of the Drosophila X chromosome for mutations that modify Deformed function. Genetics *150*, 1497–1511.

Frey, U., and Morris, R.G. (1997). Synaptic tagging and long-term potentiation. Nature *385*, 533–536.

Giordano, A., and Avantaggiati, M.L. (1999). p300 and CBP: partners for life and death. J. Cell. Physiol. *181*, 218–230.

Hardingham, G.E., Chawla, S., Cruzalegui, F.H., and Bading, H. (1999). Control of recruitment and transcription-activating function of CBP determines gene regulation by NMDA receptors and L-type calcium channels. Neuron *22*, 789–798.

Hu, S.C., Chrivia, J., and Ghosh, A. (1999). Regulation of CBP-mediated transcription by neuronal calcium signaling. Neuron *22*, 799–808.

Johnston, H., Kneer, J., Chackalaparampil, I., Yaciuk, P., and Chrivia, J. (1999). Identification of a novel SNF2/SWI2 protein family member, SRCAP, which interacts with CREB-binding protein. J. Biol. Chem. *274*, 16370–16376.

Katz, L.C., and Shatz, C.J. (1996). Synaptic activity and the construction of cortical circuits. Science *274*, 1133–1138.

Littleton, J.T., Stern, M., Schulze, K., Perin, M., and Bellen, H.J. (1993). Mutational analysis of Drosophila synaptotagmin demonstrates its essential role in Ca(2+)-activated neurotransmitter release. Cell *74*, 1125–1134.

Liu, Y.Z., Chrivia, J.C., and Latchman, D.S. (1998). Nerve growth factor up-regulates the transcriptional activity of CBP through activation of the p42/p44(MAPK) cascade. J. Biol. Chem. *273*, 32400–32407.

Martin, K.C., Casadio, A., Zhu, H., Yaping, E., Rose, J.C., Chen, M., Bailey, C.H., and Kandel, E.R. (1997). Synapse-specific, long-term facilitation of aplysia sensory to motor synapses: a function for local protein synthesis in memory storage. Cell *91*, 927–938.

Oike, Y., Hata, A., Mamiya, T., Kaname, T., Noda, Y., Suzuki, M., Yasue, H., Nabeshima, T., Araki, K., and Yamamura, K. (1999). Truncated CBP protein leads to classical Rubinstein-Taybi syndrome phenotypes in mice: implications for a dominant-negative mechanism. Hum. Mol. Genet. *8*, 387–396.

Petersen, S.A., Fetter, R.D., Noordermeer, J.N., Goodman, C.S., and DiAntonio, A. (1997). Genetic analysis of glutamate receptors in Drosophila reveals a retrograde signal regulating presynaptic transmitter release. Neuron *19*, 1237–1248.

Schuster, C.M., Davis, G.W., Fetter, R.D., and Goodman, C.S. (1996). Genetic dissection of structural and functional components of synaptic plasticity. I. Fasciclin II controls synaptic stabilization and growth. Neuron *17*, 641–654.

Shieh, P.B., and Ghosh, A. (1997). Neurotrophins: new roles for a seasoned cast. Curr. Biol. *7*, 627–630.

Silva, A.J., Kogan, J.H., Frankland, P.W., and Kida, S. (1998). CREB and memory. Annu. Rev. Neurosci. *21*, 127–148.

Stewart, B.A., Atwood, H.L., Renger, J.J., Wang, J., and Wu, C.F. (1994). Improved stability of Drosophila larval neuromuscular preparations in haemolymph-like physiological solutions. J. Comp. Physiol. *175*, 179–191.

Taine, L., Goizet, C., Wen, Z.Q., Petrij, F., Breuning, M.H., Ayme, S., Saura, R., Arveiler, B., and Lacombe, D. (1998). Submicroscopic deletion of chromosome 16p13.3 in patients with Rubinstein-Taybi syndrome. Am. J. Med. Genet. *78*, 267–270.

Tanaka, Y., Naruse, I., Maekawa, T., Masuya, H., Shiroishi, T., and Ishii, S. (1997). Abnormal skeletal patterning in embryos lacking a single CBP allele: a partial similarity with Rubinstein-Taybi syndrome. Proc. Natl. Acad. Sci. USA *94*, 10215–10220.

Waltzer, L., and Bienz, M. (1998). Drosophila CBP represses the transcription factor TCF to antagonize Wingless signalling. Nature *395*, 521–525.

Waltzer, L., and Bienz, M. (1999). A function of CBP as a transcriptional co-activator during Dpp signalling. EMBO J. *18*, 1630–1641.

Yin, J.C., and Tully, T. (1996). CREB and the formation of long-term memory. Curr. Opin. Neurobiol. *6*, 264–268.

CHAPTER III

flexin1, a Member of Novel Gene Family in Drosophila, Participates in Trans-Synaptic and Imaginal Tissue Development

ABSTRACT

We have identified a novel gene family in Drosophila named *flexins*. *flexin1* is expressed in bodywall muscle and imaginal tissues. The Flexin1 protein traffics to both the muscle cytoplasm and nucleus. Over-expression studies in muscle using full-length and truncated *flexin1* transgenes indicate that cytoplasmic Flexin1 is sufficient to cause increased presynaptic nerve-terminal branching without altering bouton number. A reorganization of the presynaptic microtubule cytoskeleton accompanies the observed increase in synaptic branching. Exogenous levels of *flexin1* in imaginal tissues phenocopy *flexin2* and Notch loss-of-function mutations. Sequence analysis indicates that the *flexins* are the Drosophila CENP-B homologues of the *jerky* gene implicated in epilepsy and motor control in vertebrates.

INTRODUCTION

In both the central and peripheral nervous systems, synaptic growth is precisely regulated. A particularly important aspect of synaptic growth regulation is the coordination of synaptic growth with the developmental increase (or decrease) in the size of the target cell. As a neuron or muscle cell increases in size, for example, it requires increased synaptic input to continue functioning appropriately (Davis and Goodman, 1998). This phenomenon, the matching of synaptic input to the size of the postsynaptic target, was central to the initial neurotrophic hypothesis. According to this hypothesis, targets of innervation were thought to release limiting amounts of a trophic molecule, in proportion to their size, that ensured a balance between target size and synaptic input (Purves, 1988). Despite a wealth of research, the molecular mechanisms that precisely control the complex and inter-related processes of synaptic sprouting, branching, retraction and elimination during development remain generally obscure (Huang and Reichardt, 2001; Sanes and Lichtman, 1999; Cantallops et al., 2000; Wan et al., 2000).

There are very few candidate molecules identified in any system implicated as part of a trans-synaptic signaling system capable of coordinating bouton addition (synaptic growth) with the changing developmental properties (size and function) of the pre- and postsynaptic partners. Cell adhesion molecules are implicated in the modulation of synaptic bouton addition/retraction in many systems, but the means by which altered adhesion on one side of the synapse is translated into altered bouton addition/retraction remains unclear (Schuster et al., 1996a; Schuster et al., 1996b; Mayford et al., 1992; Rohrbough et al., 2000). Furthermore, it is unknown how the modulation of cell adhesion might be achieved in response to increased target size as a means to couple

target size to the extent of innervation. Similarly, scaffold molecules such as PSD-95 and *discs-large* are implicated in synapse formation, being sufficient to drive the process of bouton formation, but these molecules have not been demonstrated to be necessary for bouton addition (El-Husseini et al., 2000, Budnik et al., 1996). Several secreted molecules including neurotrophins as well as CPG-15 and a novel glial-derived factor have been implicated in synapse formation and synaptic growth (Huang and Reichardt, 2001; Ullian et al., 2001; Nedivi et al., 1998; Cantallops et al., 2000). Again, however, it is unclear whether they are necessary for the process of coordinated pre- and postsynaptic growth and development.

We would like to understand the logic of how synaptic growth and cellular growth are coordinated, and would like to elucidate the signaling mechanisms that achieve this type of regulation. To identify the relevant synaptic signaling mechanisms we have taken a forward genetic approach using the glutamatergic Drosophila neuromuscular junction as a genetic system to isolate mutations in these synaptic signaling molecules. The Drosophila neuromuscular synapse grows continuously throughout four days of larval development through a process of synaptic sprouting and active zone insertion (Schuster et al., 1996a; Zito et al., 1999). During this four day period the muscle size increases nearly 50-fold and the synapse increases from approximately 20 synaptic boutons (early first instar at muscles 6/7) to approximately 100 synaptic boutons (late third instar muscles 6/7) (Schuster et al., 1996a). Not only is there elaboration of new synaptic boutons, but active zones are continuously incorporated into both new and pre-existing synaptic boutons (Schuster et al., 1996a). Remarkably, at any time point during this four-day developmental period, the correct number of synaptic

boutons and active-zones are added to this synapse, thereby keeping pace with the growing muscle fiber to assure appropriate muscle contraction. It is thought that this precisely coordinated growth of the synapse and muscle is controlled by a homeostatic regulatory system that monitors muscle excitation and then signals to modulate synaptic growth and function (Davis and Goodman, 1998; Davis and Bezprozvanny, 2000). Our genetic screens are directed toward understanding the molecular mechanisms that can achieve this type of precisely regulated structural and functional synaptic growth.

We have identified a novel gene that participates in structural and synaptic growth at the Drosophila NMJ. *flexin1* has a role in the regulation of synaptic nerve-terminal branching. Over-expression experiments demonstrate that *flexin1* can influence synapse morphology. *flexin1* may participate in the signaling systems that normally coordinate structural synaptic growth. We also observe endogenous *flexin1* expression in the imaginal tissue of the wing disc. *flexin1* gain-of-function in wing tissue reduces wing size and increases the number of scutellar bristles. The adult *flexin1* hypermorphic phenotypes recapitulate *flexin2* loss-of-function, which in turn are identical to Notch hypomorphs. In Chapter 3, we show that *flexin2* participates in Notch signaling. Our data suggests *flexin1* may play a role in Notch signaling.

RESULTS

The *flexin1* gene was identified in a genetic screen for synaptic signaling molecules at the Drosophila NMJ. In this screen a muscle-specific GAL4 driver drove expression of random genes downstream of a collection of EP-elements. The EP element allows for systematic screening of gain-of-function phenotypes in Drosophila (Rorth, 1996). In our genetic screen we identified EP(3)3666 [referred to as *P(flexin1)^{1}*] which caused a dramatic alteration in nerve-terminal morphology when over-expressed in muscle (Figure 1A,B).

Over-expression of the transcript downstream of *P(flexin1)^{1}* with either of two different muscle GAL4 drivers (*24B-GAL4* or *BG57-GAL4*) causes a striking increase in nerve-terminal branching, observed at the third instar neuromuscular synapse (Figure 1). *flexin1* muscle over-expression causes the nerve-terminal to branch extensively forming clusters of synaptic boutons rather than extending long chains of synaptic boutons as normally observed in wild type. This increased branching phenotype was observed at several different muscles including muscles 6/7, 12, 13 and 4. Importantly, we do not observe any evidence of ectopic muscle innervation and the nerve appears to innervate each muscle target at the correct location indicating that axon guidance and synapse specificity are not perturbed by *flexin1* over-expression. Finally, *flexin1* is normally expressed in muscle (see below) which means that these data are due to over-expression of *flexin1* at the time and place it is normally expressed.

We quantified increased branching by counting the number of branch points at each synapse, and we quantified synapse size by counting the number of synaptic boutons at each synapse. The developmental growth of the Drosophila NMJ, like many

neuromuscular synapses, is coordinated such that the increase in bouton number is coupled to the increase in muscle size during development (Lnenicka and Mellon, 1983; Schuster et al., 1996a). Therefore, we have normalized bouton numbers to the estimated rectangular surface area of each muscle to account for any differences in muscle size (Davis and Goodman, 1998; Schuster et al., 1996a,b; Roos et al., 2000; Wan et al., 2000; Paradis et al., 2001). We have also calculated the ratio of branch points to bouton number to get an estimate of the rate of branch point addition during development. This was necessary to separate the process of nerve-terminal branching from bouton addition since the absolute number of branch points will scale with synapse size (bouton number) during normal development. For example, synapses in the *highwire* mutant have nearly twice as many boutons as wild type and have twice as many branches indicating that bouton addition and branching are increased in parallel in the *highwire* mutation (Wan et al., 2000).

Over-expression of the transcript downstream of *P(flexin1)^1* in muscle by *24B-GAL4* (Davis et al., 1997) caused as much as a 70% increase in nerve-terminal branching (Figure 1F). Quantitatively similar results were obtained at muscle 6/7 using the muscle driver *BG57-GAL4* to drive expression of *P(flexin1)^1* (branching is increased by 136% compared to wild type; $p<0.001$; no change in bouton number $p=0.11$). Presynaptic over-expression, however, using the pan-neuronal driver *elaV-GAL4* did not alter nerve-terminal branching (Figure 1F). Thus, postsynaptic over-expression of *flexin1* is sufficient to induce presynaptic nerve-terminal branching and this effect is specific to muscle over-expression of *flexin1*.

In most examples of synaptic development and plasticity, synapse size and branching are altered in parallel by activity-dependent and activity-independent mechanisms (Budnik et al., 1990; Schuster et al., 1996b, Wan et al., 2000, Cantallops et al., 2000). At synapses over-expressing *flexin1*, however, the large increase in nerve-terminal branching is not accompanied by an increase in bouton number (Figure 1E). These data demonstrate that the mechanisms of synaptic bouton addition and nerve-terminal branching are genetically separable. Furthermore, it suggests that *flexin1* is not a growth factor but rather a signaling molecule that is able to modulate a specific aspect of nerve-terminal morphology, branching, from the postsynaptic side of the synapse.

The consequence of increased branching without increased synaptic growth appears to be the fragmentation of the nerve terminal into a population of abnormally small boutons. We imaged *P(flexin1)^{1}/ 24B-GAL4* synapses that also over-express the muscle-specific myc-tagged Drosophila glutamate receptor (*DGluR2Amyc*) to visualize postsynaptic GluR hotspots (Petersen et al., 1997). In these experiments we identified synaptic boutons based on presynaptic synapsin staining that was juxtaposed to postsynaptic GluR hot-spots (Figure 1C, D). We quantified bouton numbers in this manner and measured synaptic bouton sizes based on the dimensions of the presynaptic synapsin staining that outlines the dimensions of individual boutons. Synaptic boutons are significantly smaller when EP3666is expressed postsynaptically (Figure 1G). Furthermore, we observe that a large fraction of boutons contain only a single GluR hot-spot at these synapses. This type of small bouton is only rarely observed at wild type synapses (Figure 1C, D inset).

It is important to note that the very small puncta of synaptic staining were not quantified as synaptic boutons in the HRP stained synapses that were used to quantify bouton number and synaptic branching in figure 1E and 1F. Based on quantification of bouton numbers by fluorescent microscopy these minute boutons accounted for ~15% of the total population of boutons at any given *P(flexin1)^{1}/24B-GAL4* synapse, but only 2-3% of boutons at a wild type synapse. Thus, the quantitative data presented in figure 1 under-estimate the increase in branching and also underestimate bouton numbers by ~12%.

Postsynaptic *flexin1* expression modulates the presynaptic microtubule cytoskeleton

The increase in presynaptic nerve-terminal branching observed when *P(flexin1)^{1}* is over-expressed in muscle is associated with a dramatic rearrangement of the presynaptic microtubule cytoskeleton (Figure 2A). The ability of *P(flexin1)^{1}* to induce this type of microtubule rearrangement (inducing microtubule flexion) is the source of the gene name –*flexin* (Roos et al,. 2000, Appendix B). We observe a high frequency of microtubule loop-like structures at synapses that over-express *flexin1* postsynaptically. The arrangement of presynaptic microtubules into loop conformations is observed at most nerve-terminal branch points and has been implicated in the process of regulated nerve-terminal growth and branching (Roos et al., 2000). We therefore quantified these structures at wild type and *flexin1* over-expressing synapses. In wild type, microtubule loops are present at 22% (muscle 6/7 segment A3) of all boutons where as at *P(flexin1)^{1}/24B-GAL4* synapses this is increased to 51% (muscle 6/7 segment A3). This increase in loop formation, thus, mirrors the increase in branching at this synapse.

Interestingly, microtubule loops in wild type generally form in the plane of the muscle fiber, while those at *flexin1* over-expressing synapses do not have a predictable orientation. In the most extreme examples of *flexin1* over-expression the nerve-terminal not only branches along the surface plane of the muscle fiber, as in wild type, but also branches into the volume of the muscle, creating synapses that have multiple layers of synaptic boutons (Figure 2 C, D). This suggests that normal branching involves a signaling component that specifies the plane of synaptic growth and that this type of polarized growth is perturbed when *flexin1* is over-expressed in muscle. Furthermore, the orientation of microtubule loops reflects the planar growth of the synapse and may be involved in this process.

Identification and characterization of the *flexin1* locus

Multiple methods were employed to determine the location, orientation, nearby loci, and expressed transcripts. *P(flexin1)^{1}* sits in the first small exon of the *flexin1* gene and is able to drive over-expression of this gene in the presence of a source of GAL4. The full extent of the *flexin1* gene was subsequently determined by 5' and 3' RACE. RT-PCR and sequence analysis indicates that the transcript driven from *P(flexin1)^{1}* lacks only the first seven amino acids due to the position of the P-element just downstream of the translation start site. Three exons comprise the final transcript. The first seven amino acids of the *flexin1* ORF are spliced from the intervening 267bp intron onto third exon. Further molecular analysis of *flexin1* indicates that splicing occurs exactly as predicted using the donor GTRAGT and acceptor A(C/G). *flexin1* transcript encodes two intervening introns bearing the consensus Drosophila splice sites AG/GTRAGT (R =

purine) (Mount et al., 1992). 3' RACE by heat-shock induced expression revealed a terminal exon encoding 492 residues. The complete transcript is 1908bp containing an ORF of 1497bp encoding a 499 amino acid protein.

Kyte-Doolittle (DNA Strider 1.0) hydropathy analysis reveals N-terminal hydrophobic and a central proline, glutamate and aspartate rich hydrophilic region. Structural predictions from NN-predict indicate a large percentage of alpha-helical content. There is one predicted PKA phosphorylation site. A dozen Casein Kinase 1 and 2 sites including tyrosine and serine residues saturate the gene indicating a phosphoprotein possibly involved in signaling and regulated cellular distribution (EMBL, BDGP). BDGP also predicts a nucleic acid binding function involved in cell communication and signal transduction.

Most of the ORF is present in the last exon and there are multiple methionine residues that can serve as additional or cryptic translation initiators, *P(flexin1)^{1}* may not be a null. We demonstrated using intron-spanning primers that splicing from the 3' end of the *P(flexin1)^{1}* to the beginning of the third exon occurs autonomously in vivo in the absence of a Gal4 driver. Likewise, EP(3)3465, another *flexin1* locus insertion, does not eliminate transcription. Because mRNA continues to be produced from both EP insertions, their level of transcriptional expression relative to wild-type as well as translational expression is unknown. We conclude therefore that neither strains are transcriptional nulls and likely not to be protein nulls.

The *flexin* gene family in Drosophila

The *flexin* gene family is a group of six genes, five of which are present at 61D of the third chromosome. There are no predicted genes between the five *flexin* genes located at 61D suggesting that this family arose from an early gene duplication event (Figure 3A). Family members were identified based on a common C-terminal motif (which we have called the Flexin domain) present in all family members (Figure 3C and 3D). In addition, 4 of the 6 *flexin* family members include a CENP-B-like DNA binding domain in their N-terminus (22% identity and 41% homology between the *Flexin1* and human CENP-B DNA binding domains; Figure 3E). *flexin6* is a divergent member of the family and is present at 78D. It has a CENP-B motif and a divergent Flexin domain.

Alignment of the *flexin1* sequence performed by Peter Clyne using SeqVu shows that *flexin1* bears significant homology to CENP-B in the N terminal region. Further analysis of this region by 3cnd structural blast-p prediction supports the identification of *flexin1* as a CENP-B homolog (discussed further below). BLAST analysis shows two CENP-B domains in a tandem repeat suggesting an internal duplication event with conserved key residues (Ponting et al., 1998; Tawaramoto et al., 2003). Consesus bipartite nuclear localization sequences also flank the putative nucleic acid binding motifs such as that found in THAP and occupy domains typical for transcription factors (Hashemolhosseini et al. 2003). Adjacent NLS and phosphorylation sites have been shown to modulate the efficacy of transcription factors and nucleocytoplasmic shuttling proteins (Komeili and O'Shea, 1999; Hubner et al., 1997; Briggs et al., 1998). Taken together, the nucleic acid binding motifs, nuclear localization, and central polynucleotide

repeat domain bear similar structural organization to transcriptional modulators in known signaling pathways, such as Notch (Si et al., 2003, Iso et al., 2003; Verzi et al., 2002).

Sequence analysis indicates that the *flexins* may represent the Drosophila homologues of the mouse *jerky* gene. The mouse *jerky* gene was identified based on an insertional mutation that causes epilepsy and motor dysfunction (Toth et al., 1995). The *jerky* gene is characterized by N-terminal CENP-B DNA binding domains similar to that observed in the *flexins* (24% amino acid identity and 46% amino acid homology between the CENP-B domains of *jerky* and *flexin1*). Both *jerky* and *flexin1* contain N-terminal tandem domains also found in CENP-B. This duplicated motif in *jerky* has been shown to be necessary and sufficient to bind mRNA and DNA (Liu et al., 2003). The *jerky* gene in mouse is nearly identical in amino acid number to *flexin1-3* and, like the majority of the *flexins*, is encoded in a single large open reading frame (*flexin1* has a single additional small exon at the extreme 5' ORF). The central portion of the *flexin* family members is highly divergent, and is lacking in *flexin4*. Since this portion of the *flexin* genes is so divergent, the lack of sequence homology in this region to the *jerky* gene may not be informative.

In addition to the *jerky* gene, the *flexins* also share homology with the CENP-B gene based on the N-terminal DNA binding domain. However, the CENP-B genes are conserved throughout the majority of the protein from yeast to human (22% sequence identity and 37% sequence homology between yeast *abp1* and human *CENP-B*). There is no gene in Drosophila with high homology to CENP-B throughout the protein, although the Drosophila *cag* gene may represent a homologue of *CENP-B*. Thus, based on sequence analysis and the possible presence of a distinct *CENP-B* homologue in

Drosophila, we propose that the *flexins* are the Drosophila homologues of the mouse *jerky* gene.

Flexin family members have diverse expression patterns

Embryonic in situ hybridization with a probe unique to *flexin1* demonstrates that *flexin1* is expressed in mesoderm (myoblasts and gut) beginning in the mid-stage embryo with no detectable staining in the central nervous system (Figure 4 A, B). *flexin1* is expressed at low levels in the muscle during early development and expression drops off by the end of larval development. Embryonic expression in vivo was also independently confirmed by RT-PCR with intron spanning primers from cDNA synthesized from wild-type *yellow-white 67* embryos. At larval stages *flexin1* is also expressed in the optic lobes and central brain (Figure 4C), but is absent from the ventral ganglion where the motoneurons reside (data not shown). Expression in the optic lobes is concentrated within the optic anlage, a site of retinal axon innervation. 3rd instar larval wing and eye discs show imaginal tissue expression. These tissues undergo gross developmental changes during pupation suggesting a role for *flexin1* in peripheral neurogenesis. Thus, the phenotype of increased branching caused by over-expression of *flexin1* in muscle is due to over-expression of this protein in a tissue where *flexin1* is normally expressed. We are also able to detect over-expressed *flexin1* mRNA by *in situ* hybridization when *P(flexin1)^{1}* is paired with either neural or muscle specific GAL4 drivers (Figure 4).

Embryonic in situ hybridizations with probes unique to three of the other four *flexin* family members demonstrate that members of the Flexin gene family are expressed in distinct but over-lapping tissues (see Chapter 3). *flexin2* is expressed in the embryonic

and larval central nervous systems but not in the peripheral nervous system. *flexin3* is expressed ubiquitously at low levels. Expression of *flexin4* is detectable by RT-PCR from larval tissue. No expression data is available for *flexin5* or *flexin6*.

***flexin1* traffics to both the nucleus and the muscle plasma membrane**

Over-expression of a myc-epitope tagged full-length *flexin1* transgene in muscle reveals that Flexin1 is present at high concentrations in the cell nucleus, but also appears to be present cytoplasmically (Figure 5). Within the nucleus, Flexin1-myc concentrates into large inclusions that vary in size and number, and are observed throughout the nuclear volume (Figure 5B). The presence of cytoplasmic Flexin1-myc staining at or near the muscle membrane is based on confocal sectioning and comparison with wild type muscle fibers stained simultaneously with the myc antibody (Figure 5 A-C)

In order to distinguish between the presumed cytoplasmic versus nuclear function of *flexin1* we generated a C-terminal myc-tagged Flexin1 transgene consisting of the C-terminal 185 amino acids that lack a nuclear localization motif as well as the CENP-B-like DNA binding domain (see Figure 3B). When the *UAS-flexin1-Cterm* transgene is over-expressed in muscle we observe staining in the peri-nuclear space (Figure 5). *UAS-flexin1-Cterm* is also observed at or near the muscle membrane (Figure 5E, F). Neither full-length nor *UAS-flexin1-Cterm* concentrate to the postsynaptic membrane folds as is observed for molecules such as *discs-large* (*dlg*) which show characteristic intense halos of staining surrounding presynaptic markers such as synapsin (Zito et al., 1998). It therefore appears that Flexin1 is trafficked throughout the entire muscle rather than being concentrating to the synaptic membrane.

The over-expression of C-terminal *flexin1*, which is largely excluded from the nucleus, is also sufficient to induce increased synaptic branching. As with over-expression of full-length *flexin1*, there is an increase in nerve-terminal branching (55%; $p=0.03$) with a minor increase in bouton number 18% ($p<0.01$). These data indicate that the increased branching induced by *flexin1* over-expression is achieved independent of the nuclear localization of the protein and is likely due to cytoplasmic Flexin1 activity

***flexin1* structure-function analysis**

Over-expression of full length *flexin1* and C-terminal domains phenocopied each other at both the synapse and in imaginal tissues of the eye and wing (Figure 7B and D). We sought to further define and localize the activity of *flexin1* over-expression within a specific domain by assaying the curly wing phenotype in the adult. The C-terminal construct comprised amino acids 315 through 499 containing three discernible domains: (1) a charged, hydrophilic polyacidic and basic portion, (2) the Flexin domain, and (3) a C-terminal amphipathic alpha helix. Several *flexin1* C-terminal constructs were made to dissect functional domains (Figure 6). To investigate a requirement for possible microtubule interaction, we generated a series of mutants in that region. We performed site-directed mutagenesis of the four C-terminal Lysines to Alanine (construct 4KA) as well as deletions of the C-terminal helix (construct E). These mutations should eliminate possible microtubule binding. Construct D contains the penultimate Flexin motif as well as the terminal helix. B:C, bearing an internal deletion of the Flexin domain, retains both the highly charged hydrophilic domain and the terminal positively charged amphipathic helix. Construct 1359 bore only the charged hydrophilic domain. The PKA/PKG site

was mutated to determine if PKA phosphorylation modulated Flexin1 activity because a screen performed in an activated PKA background also implicated *flexin1*.

Analysis of the *flexin1* constructs localized its activity to the central hydrophilic domain. PKA and PKG mutations turned out to have no difference when multiple lines of each were analyzed (data not shown). This could be due to over-expression obscuring endogenous differences. Construct D had no phenotype (data not shown). Construct B:C exhibited curly wings (data not shown). Construct E behaved like *UAS-flexin1* and *UAS-flexin1-Cterm* (Figure 7D, E, and F). Construct 1359, which contained only the hydrophilic region, also produced curly wings (Figure 7G). The C-terminal truncations revealed that any construct containing the central hydrophilic domain was sufficient to recapitulate the *flexin1* over-expression phenotype, consistent with the role of certain transcription factors where the domain responsible for activity is highly charged and modular (Si et al., 2003).

flexin1 reverse genetics

We employed multiple methods to generate *flexin1* loss-of-function mutations. An advantage of P-element insertions is their mutagenic property during excision events. In the presence of a transposase, imprecise removal of the P-element from occasionally removed flanking DNA, producing deletion mutations. The rate of deletion excisions varied highly depending upon each individual EP insertion line and was unsuccessful with $P(flexin1)^{1}$. A variation of P-element excision is male recombination (Preston et al., 1996). Male recombination was also unsuccessful because the only marker available was a recessive flanking marker, *kls*, that was difficult to score, produced a high rate of

false positives and had low fecundity. Transgenic hairpin RNAi lines were also made using inverted fragments without intervening spacers. However, the lack of any gross phenotypes made it difficult to determine if that was due to poor suppression of endogenous protein function or if the loss of *flexin1* had mild phenotypes.

We turned to classic EMS mutagenesis to create molecular lesions in *flexin1* that would behave as genetic nulls (Kurt Marek's protocol). Such mutations would not present the ambiguity in interpreting dosage sensitive loss-of-function studies that is inherent to using RNAi. Because the *P(flexin1)^{1}* sits upstream of the ORF, we could conduct a screen for mutations in the ORF by suppressing the lethality caused by *P(flexin1)^{1}*-induced full-length over-expression. Mutations in the gene or suppressors of the gene would survive. Initially, *heat-shock-Gal4* was used because we had identified over-expression lethality with that driver pulsed 1 hr daily in a 37^{0}C water bath throughout larval development. Pan-tissue heat shock implied at least one tissue where *flexin1* over-expression was lethal. Problems associated with scaling up this method were the increase number of vials altering the temperature of heat shock and the limited capacity of the water bath. A 37^{0}C dry incubator was used instead but the results were too variable. We tested other Gal4 drivers to find ones that caused complete lethality. *Tubulin-Gal4* which exhibited pan-tissue embryonic expression and lethality when driving *flexin1*, could not be used because the Gal4 line was homozygous lethal itself. Screening a mixed population would necessitate labor-intensive sorting of the balancer from the suppressors.

Some Gal4 drivers such as *24B-Gal4* had too many escapers in the background. A pilot screen using *24B-Gal4* in 5,000-9,000 progeny produced an excessive 4 false

positives in the absence of EMS compared with an expected rate of 1 hit per 5,000 to 10,000 for positive EMS mutations. Therefore a low background was important to reduce the frequency of false positives. The driver line selected was *BG57-Gal4* which in a pilot screen of over 3,000 had no background. Over-expression with the driver caused pupal lethality. Survivors were then screened by PCR of the ORF and then sequenced. About 50 *BG57-Gal4* females and homozygous isogenized EP3666 males were used per bottle. Flies were flipped into new bottles after two days. Each bottle produced several hundred progeny. Roughly 120,000 were screened per the strategy as outlined (Figure 8). About two dozen unique mosaic survivors that hatched and mated to 3rd chromosome balancers produced stocks which were then backcrossed to *BG57-Gal4*. The balancing separated somatic from germline mutations, both of which are viable in the F_0 progeny. The backcross served to uncover nonlethals. Somatic mutations would be lost during the balancing to create the stock and result in lethality in the backcross because the ORF was not mutated in the germline. Germline mutations, which we want, would survive. If there were mutations in the *flexin1* ORF, the progeny would survive – these were the lines we wanted. If the cross was pupal lethal, that indicated the mutation was not on the 3rd chromosome. Slightly over half were not lethal, suggesting that these were mutations on the 2nd or X chromosome. These lines were not analyzed further. The remaining 13 viable lines were sequenced and 11 were found to have mutations in the *flexin1* ORF. The two that did not contain mutations in the ORF may have been suppressor mutations elsewhere on the 3rd chromosome. Another possibility is that in our initial test screen, the population used was less than 3,000 progeny without a spontaneous false positive. Subsequently, we had found that *BG57-Gal4* had a low false background

rate greater than 1 in 3,000 in the absence of the mutagen. In theory, that could also account for survivors.

The *flexin1* EMS mutations fell into two classes – single point mutations and deletions (Figure 9). EMS generates deletions about 10% of the time, consistent with our findings. Single point mutations generate either missense or nonsense mutations corresponding to either substitution with a different amino acid, or a stop codon, respectively. Of the single point mutations, there were two types of substitution mutations :

1) Transition mutations of either purine to purine, or pyrimidine to pyrimidine.

2) Transversion mutations of purine to pyrimidine and vice versa.

As found by prior investigators, EMS mutagenesis produced mostly transition mutations. All EMS mutants derived from the screen were balanced with Tm6c. We focused on the five stop-codon mutations to dissect the functional domains for *flexin1*. The stop-codon mutants were further subdivided into two groups numbered by the amino acid residue where the stop codon occurred: early versus late stops. Early stop codon mutations were located at positions Q104Z, W138Z, and Q163Z. Because five methionines are sprinkled in the N-terminal region, Q104Z, W138Z, and Q163Z may still be able to express two polypeptides. The first portion would contain one nucleic acid binding motif and the second portion would contain the other motif stretching to the C-terminus. Q163Z would start with a partial nucleic acid binding motif in the second polypeptide instead of a complete domain. The late stop codon mutants Q243Z and Q333Z are expected to express one truncated N-terminal polypeptide due to an absence of methionines to initiate translation downstream of those mutations. Initial complementation experiments using a

genetic matrix of heterozygotes produced conflicting conclusions. All the stocks were homozygous lethal. Early stop mutations placed over late stop combinations were viable except for Q163Z/late stops. Late stops were lethal over each other. However, they were all viable over the Deficiency 2577 (Df 2577). One possibility for transheterozygous lethality was Q163Z behaving as an antimorphic, neomorphic, or hypomorphic mutation and the late stops being null lethals. The homozygotic lethality of the stocks could result from additional 3rd chromosome second site recessive lethals acquired in the EMS screen. It was also possible that the deficiency did not uncover the locus we expected. The *flexin1* map location is 61C9. Df 2577 spans 61A:61D3. We tested flanking recessive markers on either side of the *flexin1* locus contained within Df 2577, *kls* at 61C3-5 and *emc* at 61C9. Both mutations were uncovered, confirming the deficiency spanned the region we expected. We also placed *flexin1* stop-codon mutations Q104Z and Q333Z in *trans* with two other deficiency lines with deletions spanning the *flexin1* locus, Df 61C4;62A8 and Df 61C3-4; 61E. The progeny were also viable. Other possibilities to explain the transheterozygous lethality were antimorphic, neomorphic or haploinsufficient phenotypes arising from truncated *flexin1* mutations being expressed. However, N- and C- terminal *UAS-flexin1* constructs were viable when expressed. We outcrossed the stop codon mutations for 3 to 6+ generations after which the stocks became both homozygous and transheterozygous viable, suggesting that the starting strain used for the screen acquired a recessive pre-existing lethal mutation floating in the chromosomes.

The null EMS mutations of *flexin1* survive to adulthood with no gross morphological phenotypes. We determined that *flexin1* is not necessary for viability.

This observation correlates with a nonessential role for viability found with in the mammalian homolog CENP-B (Hudson et al., 1998; Kapoor, et al., 1998; Perez-Castro et al., 1998). The lack of an essential requirement for *flexin1* may result from functional redundancy with other homologs. Indeed, the abundance of possible functional homologs has been posited as the reason for the lack of a severe phenotype (Tawaramoto et al., 2003). Further attempts to characterize adult phenotypes of *flexin1* mutants are discussed below.

We analyzed 3rd instar synaptic morphology by quantifying normalized bouton number (Figure 10A). We observed a modest decrease in the transheterozygous combination of the late stop Q243Z/Df 2577. We measured synaptic span, a measurement of nerve terminal length and observed no change (Figure 10B) (Wan et al., 2000). Other synaptic markers and parameters such as Glutamate receptor, FasII, HRP, Synapsin staining, and bouton numbers were not grossly perturbed (data not shown). *discs-large* (*dlg*) levels at the synapse were reduced in Q163Z/Df 2577, although not to the level seen in *flexin1* over-expression.

At the synapse, *discs-large* is primarily expressed post-synaptically and localized to junctional folds. Over-expression of Flexin1 greatly decreased synaptic *dlg* levels concomitant with an increase in *dlg* throughout the muscle surface of the reticulated T-tubule system (data not shown). A reduction in synaptic *dlg* in *flexin1* mutants suggests a possible role in modulating *dlg* levels at the synapse. Assaying protein levels of *dlg* may determine if the phenomenon is accomplished at the level of translation or whether it is synaptic delivery and targeting that has been perturbed.

The null phenotype of *flexin1* suggests no essential role in development. In flies, *flexin1* may be functionally redundant with other *flexins*. *flexin3* is known to be co-expressed in muscle tissue with *flexin1*. *flexin2*, while it is expressed in overlapping and complementary tissues to *flexin1*, exhibits loss-of-function adult phenotypes similar to those of *flexin1* gain-of-function. And lastly, some genes do not have a loss-of-function much less a strong one. Perhaps it would be revealed only in an appropriately sensitized genetic environment. Analysis of *flexin1* suppressors may offer candidate backgrounds for further investigation.

Imaginal tissue over-expression of *flexin1* phenocopies *flexin2* and Notch loss-of-function

flexin1 when over-expressed in tissues where it is endogenously expressed generate phenotypes reminiscent of *flexin2* loss-of-function. Eye over-expression in *GMR-Gal4*/+;UAS-*flexin1*/+ produces a rough eye phenotype, the size of which remains wild-type (Figure 7B). We observe a comparable phenotype when *flexin2* is suppressed in the eye (Chapter 4). In the wing, *flexin1* over-expression by *MS1096-Gal4* in the wing pouch of males show strong wing size reduction, to less than one-fourth that of wild-type (data not shown). Margin bristles and venation patterns however, are retained. Differential expression by *MS1096-Gal4* on the dorsal surface of the wing disc elicited curly wings in the adult. Similar shrunk wing development is seen when *flexin2* expression is silenced by the same Gal4 driver (Chapter 4). A wing margin driver, *vestigial-Gal4*, did not produce the wing margin notching seen in *flexin2* loss-of-function. A higher temperature may elicit a detectable phenotype. However, there were occasional wings that were

reduced in size in both *flexin1* over-expression and *flexin2* loss of function mediated by the same Gal4 driver (data not shown). Because *flexin1* transcript is found in the wing disc which prefigures the adult wing and mesothorax (notum), we over-expressed *UAS-flexin1* with *scabrous-Gal4*. In the notum, *scabrous-Gal4* induces expression in the sensory organ precursor from which the large bristles, macrochaetes, develop. Wild-type scutellum contains 4 stereotypical macrochaetes on average (Gho et al., 1999; Chapter 4). When *flexin1* is over-expressed by *scabrous-Gal4*, we observed a five-fold increase in extra macrochaetes, 23.1% versus 3.9% in controls. Over 50% more scutellar macrochaetes are observed when *flexin2* is removed (Chapter 4). In multiple tissue types where *flexin1* is found, hypermorphic levels of *flexin1* phenocopy *flexin2* and *Notch* loss-of-function (Chapter 4).

DISCUSSION

Using a forward genetic approach in Drosophila we have identified the gene *flexin1* and have shown that it participates in the regulation of synaptic growth and synaptic muscle depolarization. While our analysis of *flexin1* has focused on the glutamatergic neuromuscular synapse, this gene is also expressed in the optic lobes and in regions of the central brain (though not in the motoneurons of the abdominal ganglion). In addition, other *flexin* genes are expressed in diverse tissues including *flexin2* which is expressed throughout the central nervous system. Therefore, the *flexin* genes may regulate synaptic structure and function during the development of diverse synapses throughout the nervous system.

The *flexin1* gene was first isolated based on the phenotype associated with muscle over-expression. Since *flexin1* is normally expressed in muscle this phenotype represents an over-expression phenotype rather than ectopic expression. The over-expression of full-length *flexin1* leads to increased nerve-terminal branching without an increase in bouton number. The consequence increased branching is a severe alteration of synapse morphology that is consistent with a fragmentation of the neuromuscular synapse into a population of small synaptic boutons. Electrophysiologically, however, this synapse appears normal despite a modest reduction in quantal size. Importantly, we do not observe any change in the pattern of target innervation in either the gain or loss of function genetic backgrounds. Thus, *flexin1* is sufficient to modulate the growth of the Drosophila NMJ.

Modulation of the presynaptic microtubule cytoskeleton

Associated with the increased branching due to postsynaptic *flexin1* expression is a significant reorganization of the presynaptic microtubule cytoskeleton. There is no indication, yet, as to whether postsynaptic *flexin1* over-expression causes presynaptic nerve-terminal branching with a concomitant change in microtubule rearrangement, or whether postsynaptic *flexin1* directs microtubule rearrangement which then drives the process of nerve-terminal branching. However, we have previously demonstrated that the ability of *flexin1* over-expression to induce nerve-terminal branching requires the integrity of the presynaptic microtubule cytoskeleton. Mutations in the microtubule associated protein Futsch disrupt the presynaptic microtubule cytoskeleton and impair synaptic growth (Roos et al., 2000). When *flexin1* is over-expressed in the *futsch* mutant background ($futsch^{N94}$) there is no change in nerve-terminal branching and bouton numbers are reduced as observed in $futsch^{N94}$ mutants alone (Roos et al., 2000). Thus, postsynaptic over-expression of *flexin1* requires the function of the presynaptic protein Futsch in order to achieve increased branching, supporting the hypothesis that *flexin1* is involved in a trans-synaptic signaling system that regulates presynaptic nerve-terminal branching.

A model for the coordinate regulation of pre- and postsynaptic growth; Reciprocal signaling through postsynaptic *Flexin1*

The growth of any synaptic connection including the NMJ requires coordinate changes in the pre- and postsynaptic cells. To achieve a significant increase in synapse size, such as is observed during the development of the Drosophila NMJ, synaptic growth programs

must be initiated in both the pre- and postsynaptic cells, and the effects of these programs must be coordinated. While *flexin1* over-expression is not sufficient to induce increased bouton addition, the rate of synaptic branching is dramatically increased without a change in bouton number, leading to altered synapse morphology. One might conclude from these data that *flexin1* is a branching factor, and that branching is a component of normal synaptic growth.

An alternate possibility to explain the observed increase in branching due to *flexin1* over expression is that *flexin1* is sufficient to induce a muscle-specific synaptic growth program that is not matched by a parallel increase in the presynaptic growth program. An increase in postsynaptic growth without a parallel change in presynaptic growth might be expected to alter nerve-terminal morphology without significantly altering bouton number, the observed over-expression phenotype for *flexin1*. This model adequately explains the observation that *flexin1* is sufficient to induce branching rather than bouton addition.

If true, this model poses several interesting questions. Are activity-dependent changes in synaptic branching achieved by a similar mechanism? How are the pre- and postsynaptic growth programs normally coordinated to achieve stereotypic synaptic growth? There are several examples where coordinate pre- and postsynaptic growth is enhanced. For example, the *highwire* mutation causes the Drosophila NMJ to nearly double in size but the stereotypic morphology of the synapse is retained (Wan et al., 2000). A similar process occurs with increased growth at synapses with decreased cell adhesion molecule expression (Schuster et al., 1996).

This proposed model for synaptic growth incorporates the logic of how synapse formation is thought to proceed at synaptic connections at vertebrate central and peripheral synapses. At the vertebrate NMJ the release of agrin from the motoneuron causes enhanced receptor clustering and receptor stabilization at the endplate region (Lin et al., 2001; Yang et al., 2001). Subsequently, a target-derived signal(s) then participates in the induction of the presynaptic nerve-terminal specialization (Sanes and Lichtman, 1999). Synapse formation in the vertebrate CNS may also follow a similar logic of reciprocal induction (Sanes and Lichtman, 1999; Davis et al., 2001). The model of synaptic growth that we propose here suggests that synaptic branching also involves reciprocal signaling mechanisms, utilizing both anterograde and retrograde signaling systems in which postsynaptic *flexin1* participates.

Finally, the expression of *flexin1* in the optic lobe anlage suggests that *flexin1* may participate in one of several prominent inter-cellular signaling pathways. The optic lobe anlage defines the site where retinal axons enter the central nervous system. At this site, the retinal growth cones release signaling molecules that induce the terminal differentiation of the postsynaptic neurons. Several signaling systems have been demonstrated to participate in this process including Notch, TGF-beta, EGF, hedgehog and wingless signaling pathways (Artavanis-Tsakonas et al., 1999; Huang et al., 1998; Huang and Kunes, 1998; Kaphingst and Kunes, 1994). The concentrated expression of *flexin1* at this site at the time of retinal axon innervation suggests that *flexin1* may participate in postsynaptic signal transduction for one of these signaling pathways. If over-expression of *flexin1* inappropriately activates one of these potent signaling programs in the muscle, this could achieve asymmetric growth of the neuromuscular

synapse. By extension, the diverse expression patterns of the different *flexin* genes suggests that they may be involved in achieving signal specificity for these common intercellular signaling pathways in different tissues.

Flexin1 signaling in the nucleus and cytoplasm

The over-expression of a myc-epitope tagged *Flexin1* transgene demonstrates that *Flexin1* can traffic to both the nucleus and the cytoplasm near the muscle surface. The nuclear localization correlates with the presence of the CENP-B-like DNA binding domain. When we over-express a truncated version of *Flexin1* that lacks this DNA binding domain and the conserved nuclear localization sequences the truncated protein (*Flexin1-Cterm*) is concentrated in the peri-nuclear space. Interestingly the truncated protein is sufficient to induce nerve-terminal branching suggesting that this activity is due to cytoplasmic activity of *Flexin1*. *Flexin1* may have important activities both cytoplasmically and within the nucleus. Ultimately, live visualization with a GFP-tagged protein will be required to determine whether *Flexin1* shuttles between nuclear and cytoplasmic compartments.

A number of important signaling molecules have been implicated in the regulation of synaptic structure and function that also traffic from the synapse to the nucleus. For example, the Cadherin signaling pathway has been implicated in synapse formation and plasticity (Lee et al., 2001; Tenaka et al., 2000). Within this signaling pathway, beta-catenin conveys signaling from the cell surface to the nucleus. The mad protein has a similar function during TGF-beta signaling (Bottner et al., 2001). Finally, the recent demonstration that CASK translocates from the synapse to the nucleus

suggests that this molecule has a similar signaling capacity (Hsueh et al., 2000). We hypothesize that *Flexin1* may participate in a signaling pathway by trafficking information from the muscle surface to the nucleus. The expression in the optic lobe anlage suggests that *flexin1* is a novel component of one of these well known signaling pathways, or it could be part of a novel signaling cascade that has yet to be defined.

Flexin flies, Jerky mice and CENP-B; the *flexins* define a novel gene family with similarity to a large group of genes in mouse and human.

The *flexin* gene family consists of six genes that all share an N-terminal CENP-B-like DNA binding domain and a unique C-terminal helix-loop-helix domain (Flexin domain). Sequence analysis suggests that the *flexins* are the Drosophila homologues of the mouse *jerky* gene (Ponting et al., 1998). The mouse *jerky* gene was initially defined by an insertional mutation that caused severe motor dysfunction and epilepsy (Toth et al., 1995). Subsequently, the CENP-B domains of the *jerky* protein were shown to bind mRNA and DNA (Liu et al., 2003). Recently, a human orthologue to mouse *jerky* has been proposed (*JH8*) which is found at the syntenic human locus and which has high sequence homology to mouse *jerky* (Moore et al., 2001).

The homozygous viable *jerky* mouse is highly susceptible to seizure and has impaired motor control. In addition, the heterozygous *jerky* animals are also more susceptible to chemically induced seizure than are wild type animals (Toth et al., 1995; Donovan et al., 1997). These phenotypes are associated with an increase in neural activity (Toth et al., 1995; Donovan et al., 1997). However, detailed electrophysiological, developmental and cellular analyses have not been performed on

the *jerky* mice. As with the *flexins* it will be important to determine where within the cell these proteins are mediating their effects.

A suppressor screen of P-element over-expression induced lethality efficiently identifies *flexin1* mutations

In retrospect, the EMS screen could have been improved. *BG57-Gal4* had low fecundity and high virginal eclosion mortality, so large numbers of females were wasted. *BG57-Gal4* were pupal stage lethal rendering it difficult to identify supressor candidates until they hatched. (*BG57-Gal4* was not completely lethal via UAS-*flexin1*. Because some female progeny survived, transgenic over-expression could not be used for a suppressor screen. This would be important to address the possibility that the EP was overexpressing another loci downstream of *flexin1* that was responsible for the lethality. A transgene would isolate this phenomenon.) In contrast, we subsequently determined that the homozygous viable *daughterless-Gal4* driver to be ideal for screening. The stock exhibited high fecundity and high viability. Most importantly, *daugherless-Gal4* over-expression of *flexin1* was lethal as early larval instars. Positive candidate suppressors would be easy to identify. Suppressors on other chromosomes would assist in identifying pathway interactors. In summary, the screen performed confirmed the convenience and power of EMS suppression of EP induced lethality to generate genetic lesions and obtain classes of mutations otherwise unavailable by any other method. An additional benefit is the tight genetic linkage between the lesion and the readily selectable EP phenotypic marker of red eyes.

As a consequence of the screen, we validated mutations by sequencing. In doing so, we identified over a dozen polymorphisms in *flexin1* in different commonly used strains including the standard control genotypes sequenced: *yellow-white67* (*yw67*), *w1118*, *cantonS*, EP3666, and the sequence obtained by the BDGP genome sequencing center. Our data implies possible differences in functional efficacy between the alleles. It also suggests more allelic variety exists than is commonly reported for other genes. The strain used by BDGP is more divergent from the standard genetic controls used by many laboratories. Hence some reported mutations may merely be allelic differences.

Genetic implications for the role of *flexin1* signaling

The developmental consequences of hypermorphic *flexin1* in imaginal tissue strongly resemble hypomorphic *flexin2* (Chapter 4). Intriguingly, both transcripts are expressed in overlapping time and place in imaginal tissue. The lack of a severe *flexin1* null phenotype may be attributed to functional redundancy, perhaps with *flexin2*. Additional genetic analysis may determine whether these molecules act in parallel or identical pathways via epistatic or synergistic interactions. If so, over-expression of *flexin1* in the context of *flexin2* loss-of-function would be expected to exacerbate their mutual phenotypes. Similarly, a loss-of-function *flexin1* would be expected to oppose the absence of *flexin2* assuming hypomorphic *flexin1* phenotypes are antagonistic to that of hypermorphic *flexin2*. Indeed, *flexin1* rescue of *flexin2* is sufficient to address the issue of functional conservation. However, from our studies on *flexin2*, we know that endogenous levels of *flexin1* are unable to do so.

In Chapter 4, we provide the first evidence for a CENP-B homolog, *flexin2*, to participate in Notch signaling. By implication a potential interaction may also exist between *flexin1* and the Notch pathway during intercellular signaling events. *flexin1* gain-of-function exhibits opposing phenotypes to that of Notch loss-of-function. Transcriptional effectors of Notch signaling have been shown to behave in an opposing gain-and loss-of-function manner (Lai and Rubin, 2001; Nolo et al., 2000; Kitagawa et al., 2001). Testing the fashion by which *flexin1* antagonizes Notch signaling will require genetic epistasis or enhancement analysis. The range of Notch signaling is extremely broad and may not be saturable at the levels reduced by *flexin1*. The extreme hypermorphy seen in Notch transgenic over-expression suggests *flexin1* nulls may be insufficient to antagonize Notch hypermorphs except for extremely weak alleles. Furthermore, numerous modulators of Notch signaling are known to act in a specific and limited manner (Panin and Irvine, 1998). The function of *flexin1* may be restricted to antagonize only one aspect of Notch in a gain-of-function context. If *flexin1* does impinge upon Notch, that implies exogenous levels *flexin1* are required to titrate the strong suppression mediated by *flexin2*.

To date, a large number of genes have been shown to modulate the Notch signal. An intense effort is underway in numerous laboratories to identify and characterize components of this crucial evolutionarily conserved pathway that is used continually throughout metazoan development for intercellular signaling. It will be interesting to determine if another CENP-B homology, *flexin1*, also functions in the Notch pathway.

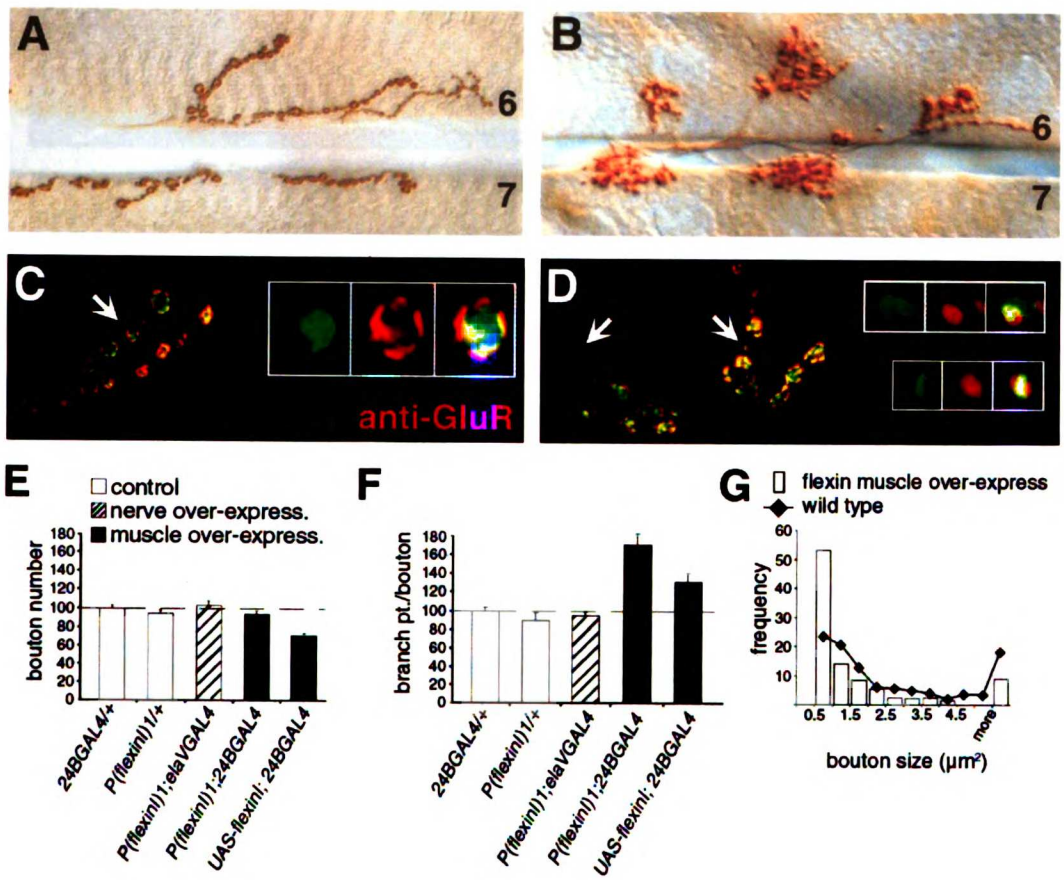

Figure 1: flexin1 synaptic gain-of-function

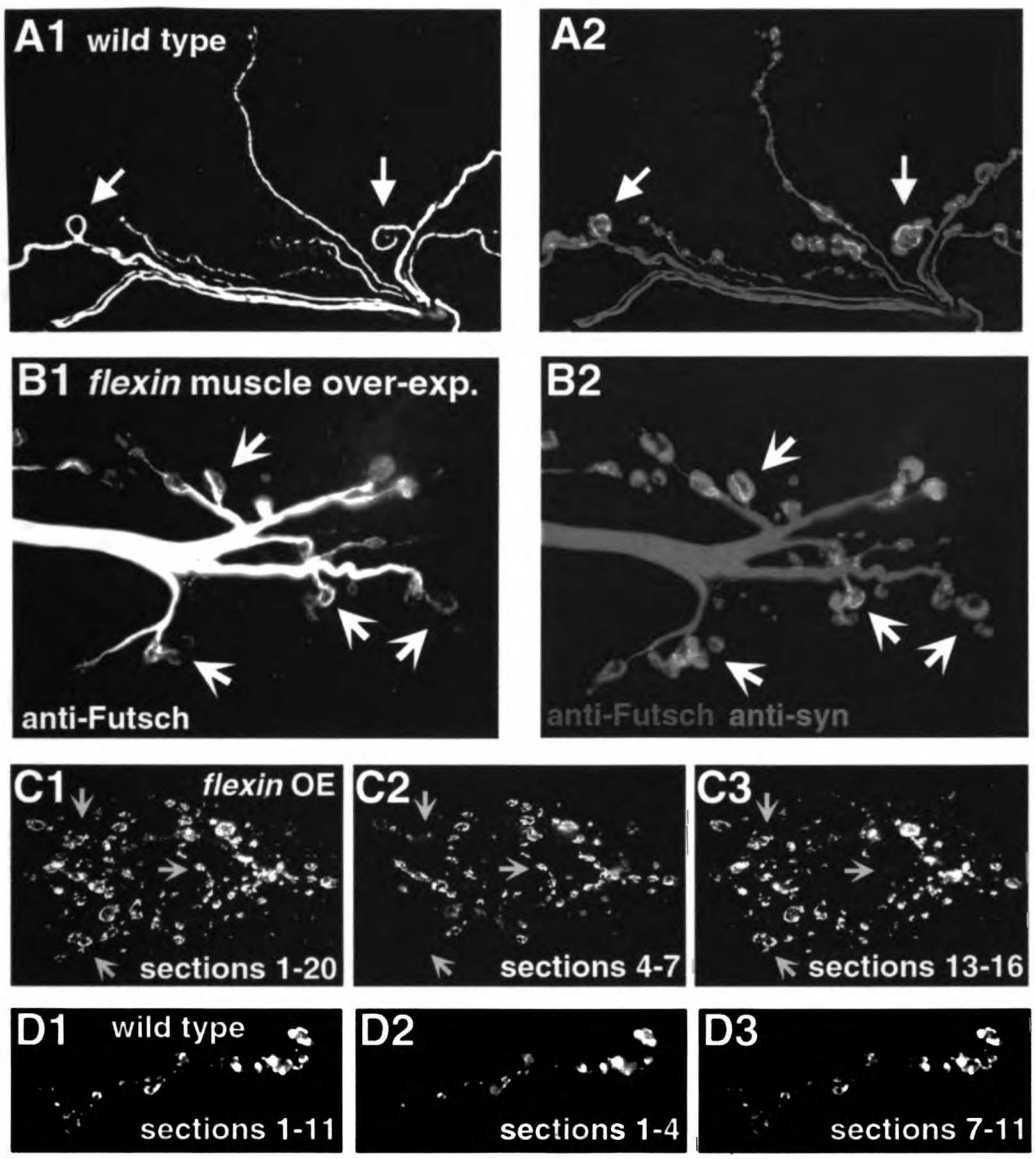

Figure 2: postsynaptic flexin1 over-expression alters presynaptic microtubule organization

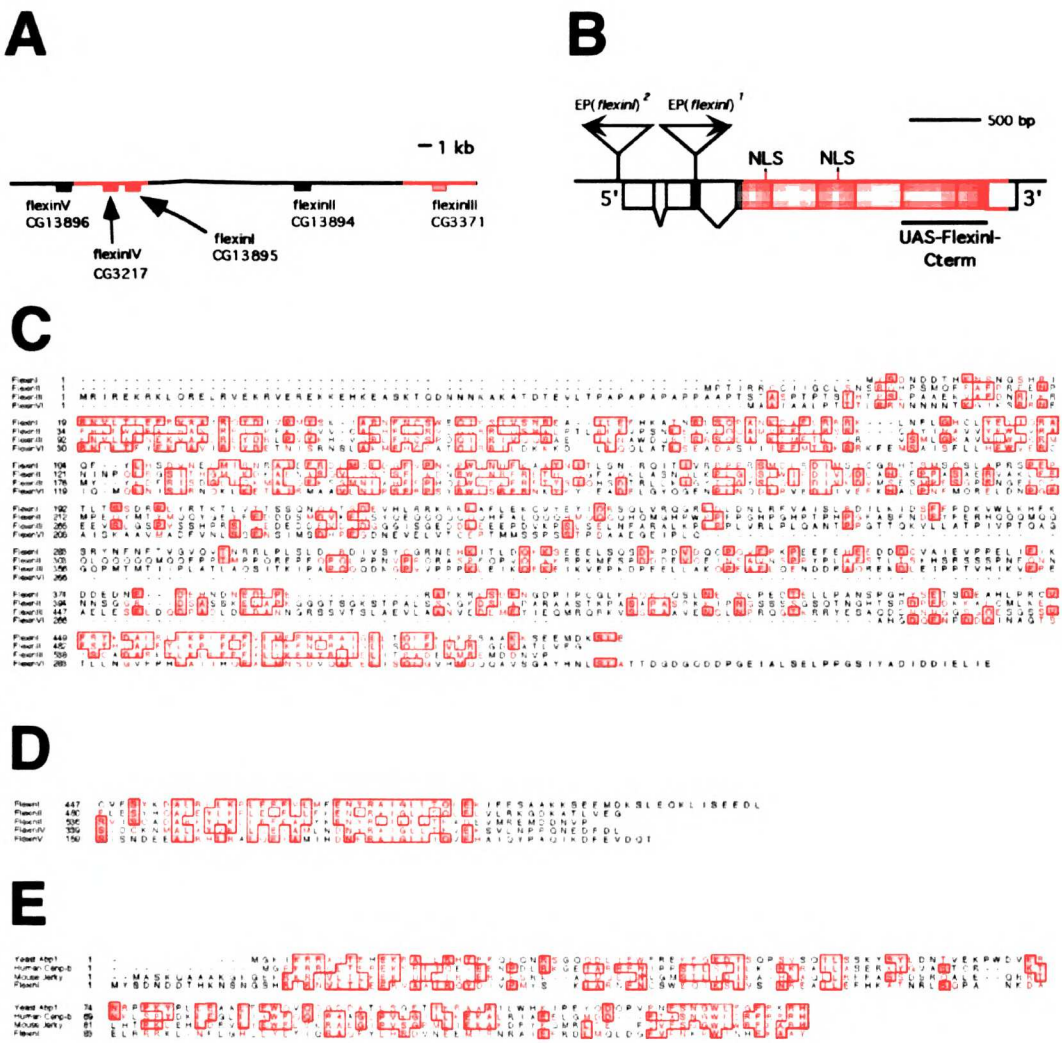

Figure 3: genomic and protein structure of the flexin gene family

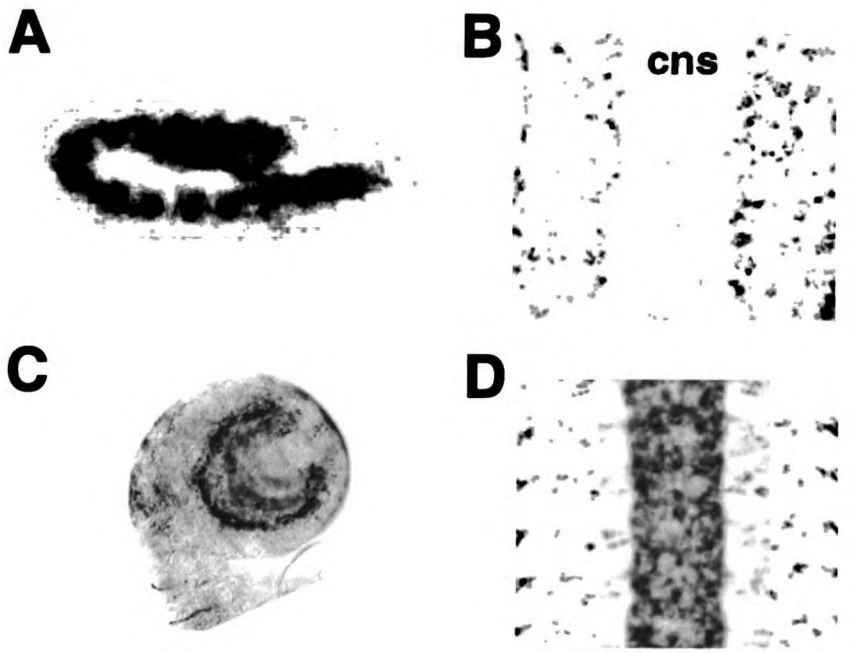

Figure 4: flexin1 in situ hybridization

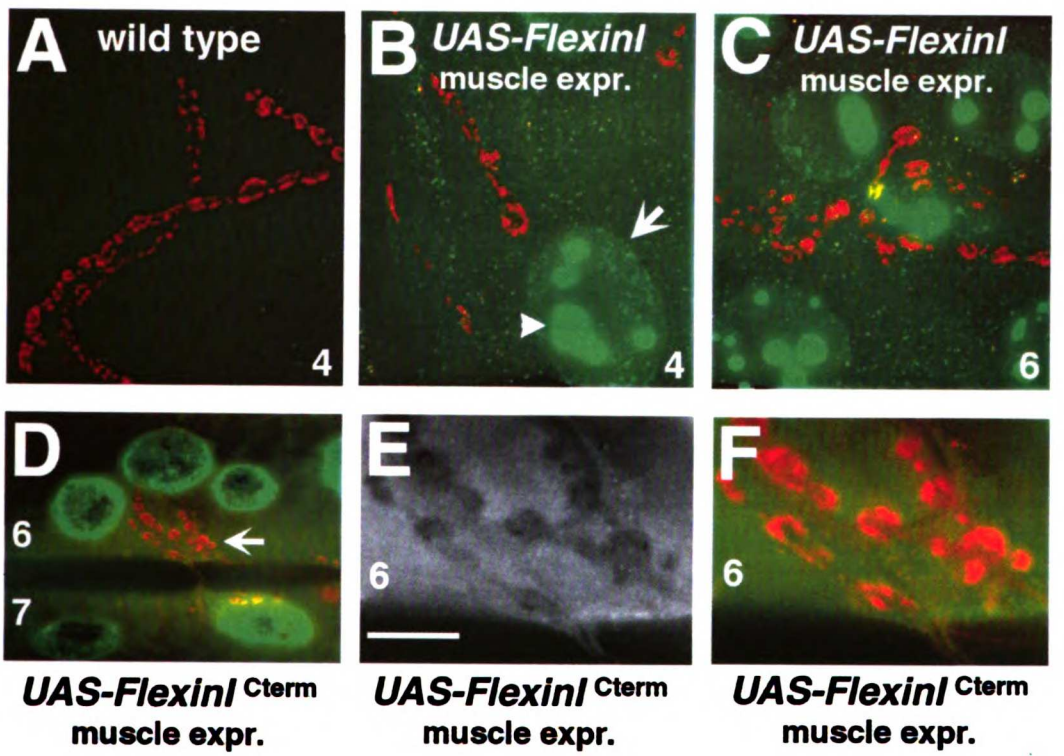

Figure 5: flexin1 subcellular localization

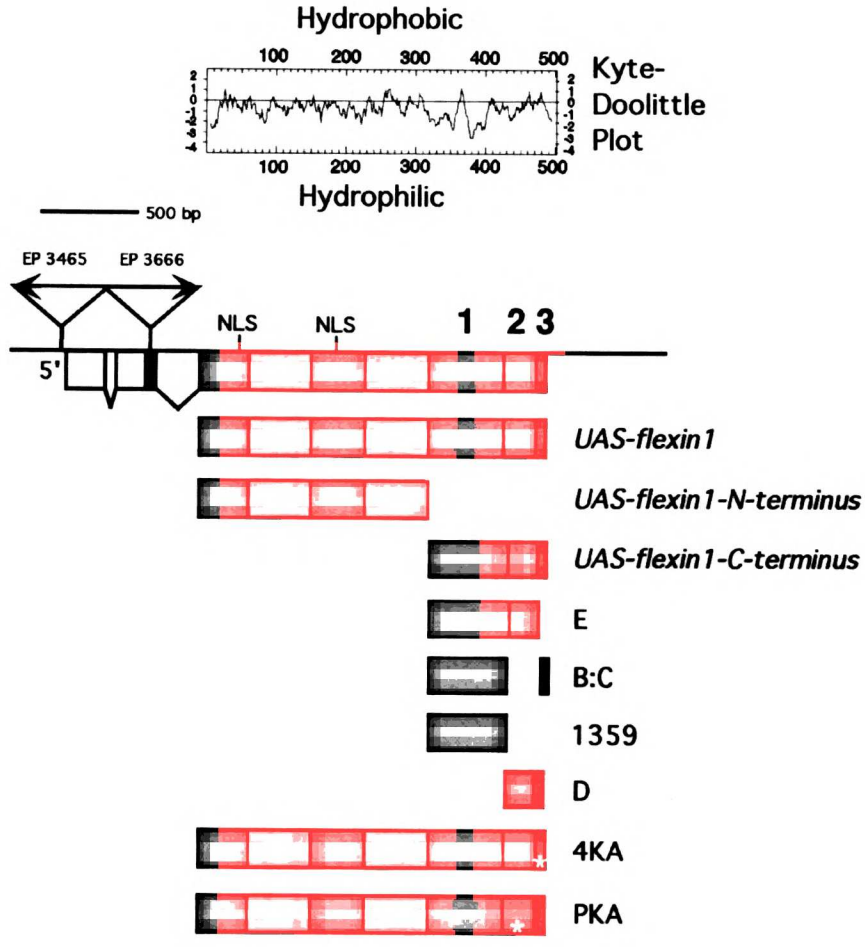

Figure 6: flexin1 constructs

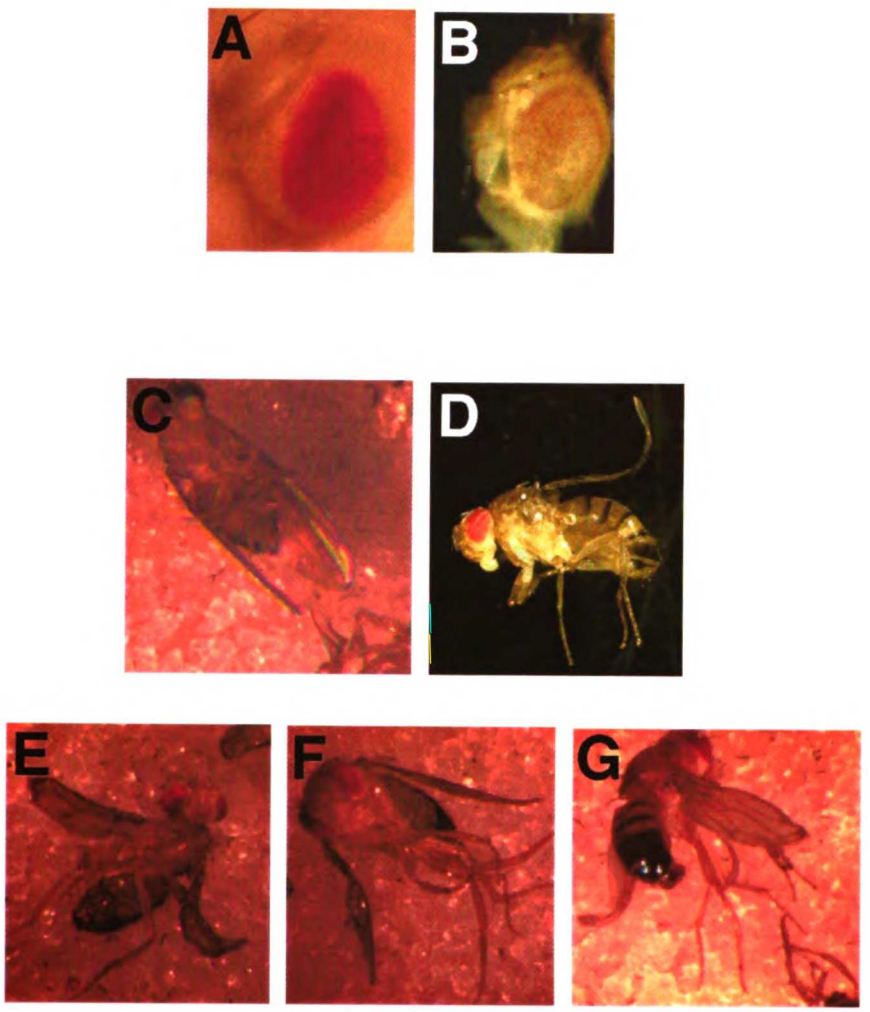

Figure 7: Imaginal Phenotypes

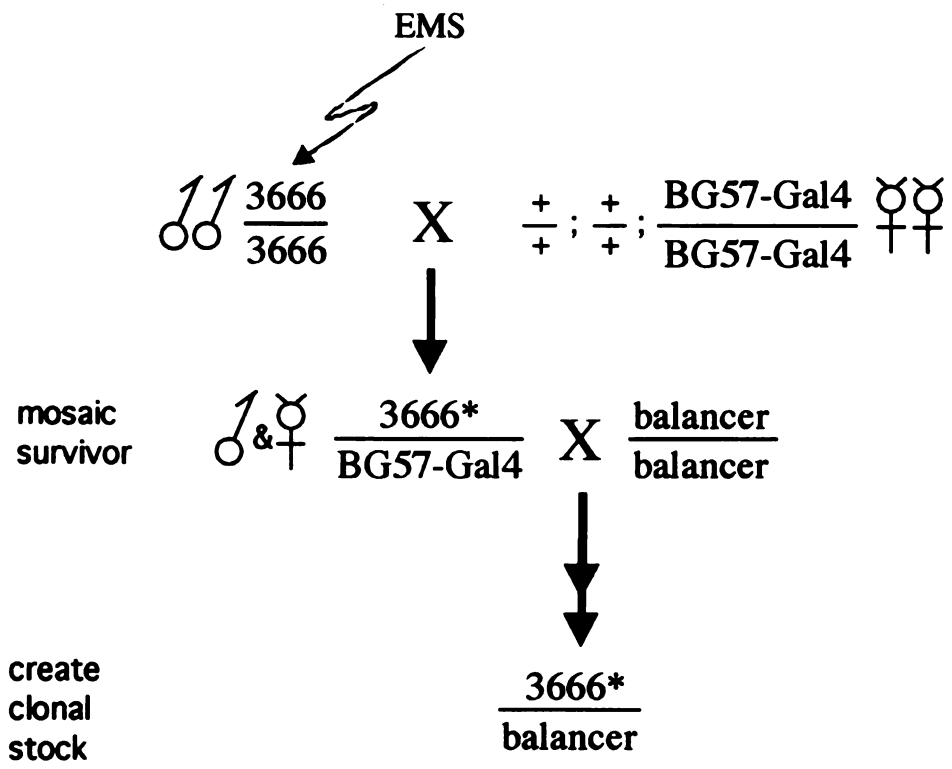

backcross to driver, keep germline non-lethals (survivors)

* indicates mutated chromosome

Figure 8: EMS Screen

(1) Single point mutations produced are primarily transition mutations :

Transition mutations (purine to purine / pyrimidine to pyrimidine)

C95Y	**TGC → TAC**
R155C	**CGC → TGC**
P161S	**CCA → TCA**
E237K	**GAG → AAG**
Q104Z	**CAG → TAG**
W138Z	**TGG → TGA**
R163Z	**CGA → TGA**
Q243Z	**CAG → TAG**
Q333Z	**CAG → TAG**

Transversion mutations (purine to pyrimidine and vice versa)

E122Y GAG → GTG

(2) Deletion mutations :

Δ355-374

Nonsense mutations : Stop codon mutations

Early Stop is defined as occurring N-terminal to possible initiation Methionines.

Late Stop occurs after possible initiation Methionines.

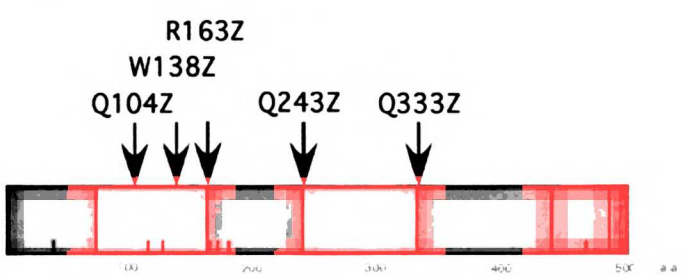

Early Stop	Late Stop
Q104Z	**Q243Z**
W138Z	**Q333Z**
R163Z	

Figure 9: EMS mutations

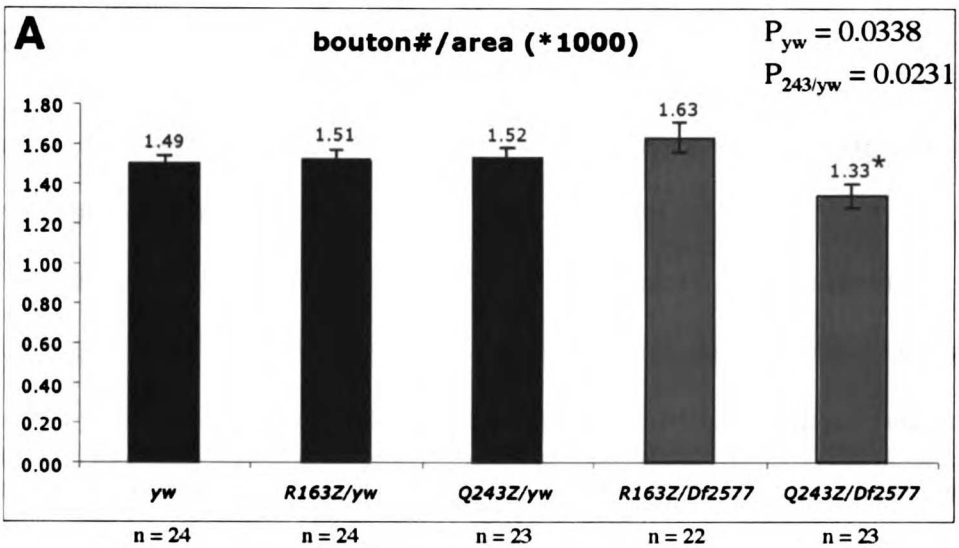

$$\text{Synaptic span} = \frac{\text{length of 2 longest branches}}{\text{length of muscle}} * 100$$

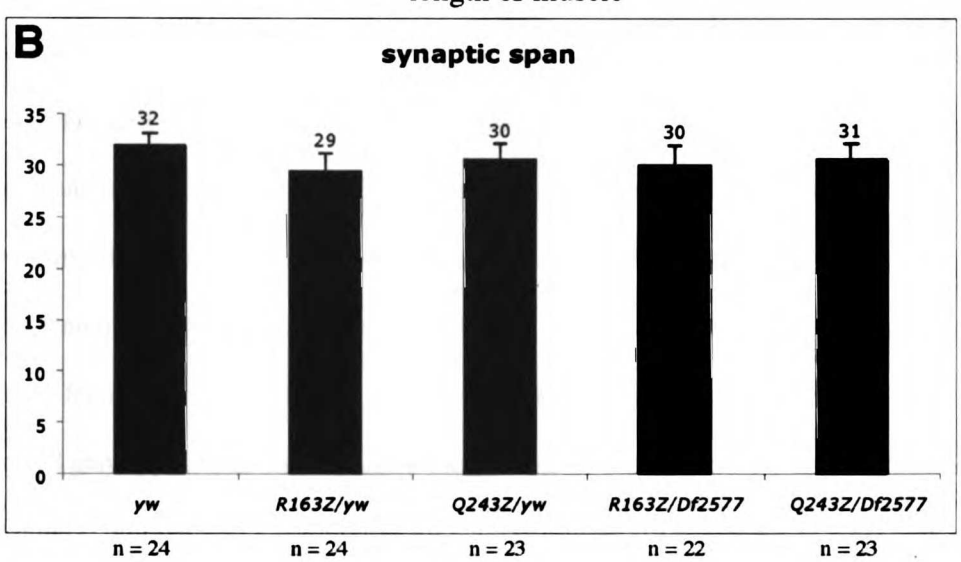

Figure 10: Quantification of synaptic morphology

FIGURE LEGENDS

Figure 1. Over-expression of *flexin1* increases nerve-terminal branching without an increase in bouton number.

(A) A wild type NMJ at muscles 6/7 in abdominal segment A3 stained with anti-synaptotagmin. (B) The NMJ at muscles 6/7 in segment A3 over-expressing Flexin1 in muscle [*P(flexin1)^{1}/24B-GAL4*]. (C) Chains of synaptic boutons are stained with anti-myc to visualize the muscle over-expression of *DGluRIIAmyc* and the presynaptic marker anti-synapsin (anti-syn). Inset: an enlarged view of the bouton indicated by the white arrow. The full genotype is *UAS-DGluRIIAmyc/+; 24B-GAL4/+*. (D) Chains of synaptic boutons stained as in C at a synapse simultaneously over-expressing both *DGluRIIAmyc* and *flexin1*. Inset: enlarged views of the single synaptic boutons indicated by the white arrows. The full genotype is *UAS-DGluRIIAmyc/+; 24B-GAL4/P(flexin1)^{1}*. (E) Quantification of bouton number for the indicated genotypes (% wt synapse size). Bouton counts were first normalized to muscle size and the averages for each genotype are presented as normalized to wild type. Only *UAS-flexin1; 24B-GAL4* is significantly different from wild type ($p<0.01$) (F) Quantification of nerve-terminal branching for the indicated genotypes. For each synapse the number of branch points were normalized to total bouton number and the averages for each genotype are presented as a percent change relative to wild type. The increased branching observed in *P(flexin1)^{1}/24B-GAL4* and *UAS-flexin1; 24B-GAL4* is statistically significant relative to wild type and genetic controls ($p<0.01$). (G) The frequency distribution of bouton sizes in wild type (N=520 boutons from 10 synapses) compared to synapses over-expressing *P(flexin1)^{1}* in muscle (N=632 boutons from 11 synapses, genotype: *P(flexin1)^{1}/24B-GAL4*). The frequency

distribution is normalized for each genotype to account for differences in sample size. The average bouton size is significantly decreased in *P(flexin1)^{1}/24B-GAL4* compared to wild type ($p<0.01$). For this analysis both type Ib and type Is boutons were measured at each synapse because it was not possible to distinguish between the two bouton types at *flexin1* over-expressing synapses.

Figure 2. Muscle over-expression of *flexin1* alters presynaptic microtubule organization and the plane of synaptic bouton addition. (A1) A confocal image of the synapse at muscles 6/7 in segment A3 of a wild type animal stained with anti-Futsch to mark the presynaptic microtubule cytoskeleton. Microtubules adopting a loop conformation are indicated by arrows. (A2) The synapse in A1 co-stained with anti-synapsin. (B1) *P(flexin1)^{1}/24B-GAL4* animal stained as in A1. Two of many microtubule loop structures are indicated by arrows. (B2) Co-staining of the synapse in B1 with anti-synapsin. Increased branching is associated with a significant increase in the number of presynaptic microtubule loops, two of which are indicated by the white arrows. (C1) A projection of a 20 confocal sections through a synapse at muscle 4 over-expressing *flexin1* stained with anti-synapsin [OE = *P(flexin1)^{1}/24B-GAL4*]. (C2) A projection of sections 4-7 of the synapse in B1 indicating the outer portion of the synapse. (C3) A projection of sections 13-16 of the synapse in B1 indicating the inner portion of the synapse. Yellow arrows indicate three areas of the synapse where a bouton is present in sections 4-7 but not in sections 13-16, or vise versa, demonstrating the presence of multiple layers of synaptic boutons. (D1-3) A similar analysis of a chain of boutons at a

wild type synapse at muscle 4. The wild type synapses in general occupy fewer sections because they do not grow into the muscle volume.

Figure 3. Genomic and Protein Structure of the *flexin* gene family

(A) The genomic organization of *flexin1* and the *flexin* gene family.

Five of the six *flexin* genes, *flexin*s 1-5, are clustered together within 40kb of each other at chromosomal band 61C-D on the left tip of the 3rd chromosome. All genes are transcribed in the same orientation, with the 5' end towards the left arm. There are no predicted intervening genes. Scale bar indicates 1 kb.

(B) *flexin1* genetic locus.

The 1908bp *flexin1* transcript contains three exons comprising an ORF (in purple) of 1497 bp (499 amino acids). Yellow indicates tandem CENP-B motifs with putative nucleic acid binding and corresponds to amino acids 86-145 & 225-288 (ncbi rpsBLAST). Red indicates the *Flexin* domain and corresponds to amino acids 447-481. "NLS" refers to predicted consensus nuclear localization sequence (RRKRK) at amino acids 85-89 and 223-227. The region used for *UAS-flexin1-Cterm* is indicated by the bar. Two EP elements are inserted within or nearby the *flexin1* locus. EP3465 ($P(flexin1)^2$)sits upstream of the 5' end of the transcript and is not oriented to drive expression of the gene. EP3666 ($P(flexin1)^1$)is situated 14bp within the ORF of *flexin1*. $P(flexin1)^1$ is oriented to drive the expression of *flexin1* in the presence of Gal4 drivers.

(C) *flexin1* family alignment.

Sequence alignment of predicted open reading frames using SeqVu for *flexins1,2,3,* and *6* which exhibit sequence conservation over N- and C-terminal regions (boxed in yellow).

Flexins exhibit high sequence similarity in both their CENB-P motif and the C-terminal *Flexin* domain, with a region of low similarity between these two motifs. *flexin6* lacks the region of low similarity and is the most divergent of the *flexins* in the *Flexin* domain. Amino acids conserved in 50% or more of the sequences are highlighted in yellow.

(D) alignment of the C-terminal motif for *flexins 1-5*. The C-terminal motif is more divergent in *flexin6*. *flexin4* and *flexin5* have well conserved *Flexin* domains, and are yet to be characterized at their 5' ends. Both are predicted by BDGP to have highly divegent N-terminal regions.

(E) alignment of CENP-B family members from different species. yeast, mouse, human. The CENP-B motif of *flexin1* is similar to the CENP-B motifs of mouse *jerky* and the human and yeast *CENP-B's*.

Figure 4. *flexin1* is expressed in muscle.

(A) In situ hybridization to wild type embryos demonstrates *flexin1* expression in the developing mesoderm including somatic muscle and gut (Stage 14-15). Note the clustered staining of muscle segment precursors along the mid-ventral length of the embryo. No expression is observed in the developing nervous system at this stage. In this sagittal view, the ventral nerve cord would form a continuous flanking border ventral to the muscle mesoderm. (anterior is to the left, dorsal is to the top).

(B) An example of *flexin1* muscle expression at a stage 15 embryonic fillet. The central nervous system is indicated as cns.

(C) Expression of *flexin1* is also observed in 3rd instar larval optic lobes. The concentrated expression in the semi-circular optic lobe anlage is clearly detected.

(D) In situ hybridization to *flexin1* in embryos that over-express of *flexin1* in the nervous system [*P(flexin1)^{1}/elaV-GAL4*]. In this example, the high level of expression driven by the source of GAL4 is revealed during rapid staining (30min) and, as a result, the endogenous expression of *flexin1* in the muscle is not observed.

Figure 5. FlexinI traffics to the both the cytoplasm and the cell nucleus. (A) An example of the wild type synapse at muscle 4 stained with anti-DAP160 (presynaptic marker; red) and anti-myc (green) to estimate endogenous muscle myc staining levels. (B) An example of *UAS-flexin1-myc* over-expression at muscle 4 stained as in A. Large myc-positive inclusions (arrow head) are present in the cell nucleus (arrow) and there is increased *flexin-myc* staining in the cytoplasm near the muscle surface. (C) An example of *UAS-flexin1-myc* over-expression at muscle 6. (D) An example of over-expression of *UAS-flexin1-Cterm* over-expression at muscle 6 and 7 stained as in A. The myc immunoreactivity is concentrated in a peri-nuclear region and is also observed to be cytoplasmic near the muscle surface. (E) A magnified view of the synapse in D at the site indicated by the arrow in D. (F) The same image in E showing co-staining for DAP160. Staining in E and F indicate staining near the muscle surface.

Figure 6. FlexinI constructs for structure-function analysis.

Genomic organization of the *flexin1* locus as described in Figure3. Aligned above is a Kyte-Doolittle representation of the *Flexin1* protein sequence. Yellow indicates homology to CENP-B. Red denotes the Flexin domain. *UAS-flexin1-C-terminus* was truncated into multiple constructs based on three motifs in order of N- to C-termini : (1)

Hydrophilic region, (2) Flexin domain, and (3) C-terminal amphipathic alpha helix. Construct 4KA contains site-directed mutagenesis of four Lysine to Alanine residues in the C-terminal amphipathic alpha helix. PKG/A construct is a mutation from a phosphorylatable Serine to either a phosphorylation mimic Glutamate, or non-phosphorylatable Alanine respectively.

Figure 7. Imaginal Phenotypes associated with hypermorphic *flexin1* in the adult eye and wing.

(A) Control adult eye. *w1118/+*; *GMR-Gal4/+* exhibit normal ommatidial development.

(B) Over-expression of *flexin1* by *GMR-Gal4 (GMR/+; UAS-flexin1/+)* induces gross ommatidial abnormalities. Absence of pigment cells causes the appearance of blotchiness.

(C) Control wing driver line *MS1096-Gal4; MS1096-Gal4* show normal straight wing morphology.

(D) Over-expression of *flexin1* in the wing disc induces wing curling in the female pictured (*MS1096-Gal4/+; UAS-flexin1/+*). In males, dosage compensation from upregulation of the X-chromosome driver *MS1096-Gal4* produce small wings (not shown).

(E) *UAS-flexin1-Cterm* phenocopies full length over-expression, demonstrating a functional domain in the C-terminal region (*MS1096-Gal4/+; UAS-flexin1-Cterm/+*).

(F) Construct E which contains the hydrophilic domain and the Flexin domain, also generate curly wings, indicating the C-terminal amphipathic helix is not necessary to generate this phenotype (*MS1096-Gal4/+; UAS-flexin1-E6/+*).

(G) Construct 1359 only bears the hydrophilic domain suggesting that we have isolated the functional component of *flexin1* to this stretch of amino acids (*MS-1096-Gal4/Y; UAS-flexin1-1359-3/+*). The Flexin domain is also dispensable for this phenotype.

Figure 8. Outline of EMS screen.

EP3666 males were mutagenized en masse and mated to *BG57-Gal4* virgins. The surviving mosaic progeny are recovered, backcrossed, and balanced. Candidate suppressors are then sequenced for mutations.

Figure 9. *flexin1* EMS mutations.

Figure illustrates the locations of the stop codon mutations used for phenotypic analysis. Hatch marks indicate Methionine residues.

Figure 10. Quantification of synapse morphology in *flexin1* mutants.

(A) A modest decrease in normalized bouton numbers is seen in the transheterozygous Q243Z/Df 2577.

(B) *flexin1* genomic mutations do not exhibit altered synaptic terminal length.

Materials and methods

Drosophila Stocks

The fly stocks were EP(3)3666, EP(3)3465, *24B-Gal4*, *yw67*, and *Df 2577* (Bloomington). Additional fly stocks were obtained from the following:

hsp70 (Nancy Bonini); *hdj1*(Parsa Kazemi-Esfarjani)

GMR-Gal4, *MS1096-Gal4*, *p35*, *hs-Gal4* (Jean-Karim Heriche)

yellow white 67, *Eyeless-Gal4*, (Sean Sweeney)

Fly culture: Fly stocks were maintained at 18^0C in standard cornmeal agar cotton-plugged vials. Grape or apple juice plates were used to collect embryos as described (BDGP). Crosses reared for analysis and dissection were raised in an incubator at 25^0C.

Identification of the *flexin1* locus:

Virgin females of a muscle expressing Gal4 (*MHC82*) were crossed to males of the Rorth EP collection of random P-element insertions. 3rd instar larvae were then dissected, stained for the synapse as described below, mounted onto slides, and visually inspected for altered synaptic morphology. EP3666, *P(flexin1)*^{1}, was identified in this manner.

Male recombination :

To select for deletion events cosegregating with the P-element given the orientation of the *flexin1* gene, we used the *kls* marker as described (Preston et al., 1996).

P-element excision :

Performed as described as per Drosophila Protocols (Sullivan et al., 2000).

Molecular Cloning

All molecular biological manipulations were done as described unless otherwise stated (Sambroook). Genomic DNA isolation (BDGP), plasmid rescue (BDGP), inverse PCR (BDGP).

Cloning of the *flexin1* ORF:

Genomic DNA flanking the EP3666 insertion was isolated by 5' and 3' inverse PCR and plasmid rescue (BDGP) resulting in 3kb, 1.4kb, and 8kb products respectively.(BDGP) 3' RACE for the 1.8kb EP induced transcript was cloned as follows: Total RNA(Qiagen) from 2 hour 37°C heat shock induced hs-gal4-3666 embryos were subject to RT (GibcoBRL). Nested PCR was performed in two 30 cycle rounds. Round 1 used PR192 (GAG TTA ATT CAA ACC CCA CGG ACA TGC) and PR199 (GAG CGG CCG CTT TTT TTT TTT TTT TV - V is AGC mixed). 1uL of Round1 was used for Round 2 with PR200 (CTC TAG ACA AGC ATA CGT TAA GTG GAT GTC) and PR199.

5' RACE (GibcoBRL) was performed on *yw67* 3rd instar larval mRNA. Total RNA was isolated by Trizol (GibcoBRL) and mRNA by Oligotex (Qiagen). cDNA was cleaned with GlassMax (Gibco) and TdT tailed (5' RACE kit, Gibco). Nested amplification was performed with GSP1 ATCTCCTCGTTCAC and GSP2 CTCTGGATGTACTCGTACAG.

PCR products were cloned into pGEM-T(Promega) and sequenced(Perkin-Elmer).

5' RACE primers

Gsp1E606AS ATCTCCTCGTTCAC

Gsp2E567AS CTCTGGATGTACTCGTACAG

Gsp3E444AS CGATTGGAGACTATGCTCTTG

IntronSpan GTGTCATCATTGTCAGAGTAC

EP3666 Sau3A1 inverse PCR plasmid rescue

Genomic DNA from adult EP3666 flies were obtained (BDGP). One-half genome equivalent was digested 2hr @37^{0}C and ligated (BDGP). Inverse PCR was done as described (BDGP). EP3666 Msp1 inverse PCR plasmid rescue was manipulated as described. EP3666 HinP1 inverse PCRplasmid rescue was also similarly performed. Msp1 and HinP1 iPCR rescue produced single bands of 1.5 and 3kb respectively. The 400bp Sau3A1 iPCR product was eluted and TA cloned (Promega) into pGEM-T and sequenced with T7 and SP6.

3666 EcoR1 3'Plasmid rescue

EP insertions bear the Kanamycin resistance gene (insert appendix pUAST). Adult EP3666 flies were grounded and genomic DNA obtained (BDGP). DNA was digested with HindIII, diluted , ligated, transformed into DH5a, and plated onto Kanamycin plates (40ug/mL) (BDGP). Clones were minipreped and digested with HindIII and the clone bearing the largest sized insert of 8kb was selected for sequencing.

PCR was used to determine orientation of 3465 and 3666 P-elements (nt p32). EP3465 not oriented to over-express, 3666 can over-express. The primers combinations pr192

and 282As or 2243AS, plac1 and 282AS or 2243AS were used. Furthermore, both EPs are expressing *flexin1* transcript via RT-PCR. (nt p74). For pr192 and plac1 sequences, see BDGP.

5'RES-2243 ACC ACC ACG ATC GGA ATC G

3666-282AS GGT GAC CAA TGT CTT TGT GC

flexin1 genetic polymorphisms

Polymorphisms were identified in: *yellow-white67* (*yw67*), *w1118*, *cantonS*, EP3666, and the sequence obtained by the BDGP genome sequencing center. We used *yw67* DNA as the source for *UAS-flexin1* from which all other constructs were derived.

Whole-mount in situ hybridization

In situ hybridization to embryos and 3rd instar larvae were done as described (BDGP). 500bp probes were synthesized with the Dig RNA Labeling Kit (Boehringer Mannheim). Embryos were left to stain for 10-14 hours before analyzing whole mounts. Larval in situs for wing discs and optic lobes were stained for 2-4 hours and mounted.

The template was made with the PCR product obtained using the following primers :

Flexin 1

Xba-N#4 5' GCTCTAGA ATGTACTCTGACAATGATGACAC 3'

T7-624AS 5'

TAATACGACTCACTATAGGGAGACCACGGTGACCAATGTCTTTGTGC 3'

Flexin 2

Flex2t7s 5' TGCCACCTCAAAGGGAACC 3'

Flex2t7as 5'

TAATACGACTCACTATAGGGAGACCACGACCAGTGTGGCCTTGTCC

Flexin 3

Flex3t7s 5' AGCATCACCAAGATTCCTGC 3'

Flex3t7as 5'

TAATACGACTCACTATAGGGAGACCACGGCACATTGTCATCCATTTCG

Whole-mount immunocytochemistry

Transgenic lines bearing myc epitope tagged constructs (see below) were crossed to 24B drivers and the larval fillets were stained with 9E10 anti-myc (1:500 Sigma), anti-DAP160 (1:200), synapsin (1:20). For DAB reactions, antibodies used were anti-FasII(1:10), anti-2210(1:50),and anti-SAP47(1:50). Branches were quantified as a process bearing at least two boutons.

Fillets were mounted in 70% glycerol and the slides visualized under a 60X oil immersion lens. Dark synaptic protuberances along the length of the terminal processes were counted as boutons. Any length of nerve terminal process containing at least two boutons was counted as a branch. Muscle size was determined by measuring the central width and length of each fiber using an ocular micrometer (Zeiss).

Quantification of boutons in *flexin1* over-expressing synapses via flourescent microscopy was performed by Dr. Graeme Davis. A bouton was identified as a presynaptic marker anti-synapsin (1:50) with a corresponding myc-tagged post-synaptic glutamate receptor staining (anti –myc 1:100). Double-labeling boutons increased

accuracy in assessing minute boutons as a developmentally mature varicosity and not as background puncta (reference on timing of synaptic insertion). By DAB or single florescent labeling, minute boutons may not have been visible above the background staining or were dismissed as background puncta (imaging methods).

Bouton counts and synaptic branch quantification were performed on HRP stained third instar larval fillets at muscle 6 or muscle 4 in abdominal segment A3. Boutons were defined as discrete puncta of staining within a chain of synaptic boutons. Bouton counts were normalized to the rectangular surface area of the muscle fiber as described previously (Schuster et al., 1996). Branching was quantified by counting branch points. A branch point is defined as a bouton that gives rise to a chain of at least two synaptic boutons.

Quantification of boutons and active zones by fluorescent microscopy was performed on a deconvolution confocal microscope (Zeiss) fitted with a high resolution CCD camera and deconvolution analysis software (3I - Intelligent Imaging Innovations). Measurements of bouton dimensions were done using the measurement tool of slidebook software (3i). Comparison of fluorescence intensities between preparations involved staining larval fillets in a common reaction tube, and imaging and deconvolution under identical conditions.

RNAi methods

Double-stranded RNAi synthesis was performed using T7Megascript (Ambion) using the following primers :

T7-1s 5'

TAATACGACTCACTATAGGGAGACCACATGTACTCTGACAATGATGACAC 3'

T7-624AS 5'

TAATACGACTCACTATAGGGAGACCACGGTGACCAATGTCTTTGTGC 3'

yw67 embryos were injected for wild-type RNAi experiments (Drosophila Protocols,2000). For injection experiments, 18 hour old embryos were dechorionated in bleach and soaked overnight in 6% sucrose, 1X Spradling, and a final RNAi concentration of 25ng/uL and allowed to develop to wandering 3rd instars on apple plates with yeast.

Transgenic Lines

Transgenic flies were made as per Drosophila Protocols, 2000. DNA obtained from a Qiagen maxiprep was coinjected with Δ2-3 plasmid in a 20 to 5 ug ratio into early stage embryos prior to cellularization. Embryos were collected on apple juice plates with a small soft paintbrush and brushed onto the surface of a non-toxic double-sided sticky tape taped to a microscope slide. Attached embryos were gently overlaid with another double-sided sticky tape slide and pressed together with light pressure and both slides pulled apart to detach the chorion. Embryos were singly removed with a pair of #5 or #3 forceps (Roboz) and aligned with posterior ends overhanging from the edge of a 0.5cm strip of double sided sticky tape.

Each construct bearing a C-terminal c-myc epitope were cloned into pUAST(Not1/Xba1) site.

UAS-*Flexin1*

N-Not1-4s 5' AGATAAGAAT GCGGCCGC ATGTACTCTGACAATGATGACAC 3'

3666Xba1Cmyc AS 5'

CGTCTAGATTACAAGTCTTCTTCAGAAATAAGCTTTTGTTCTAAGGATTTGTC

CATTTCC 3'

UAS-flexin1-Nterm

N-Not1-4s 5' AGATAAGAAT GCGGCCGC ATGTACTCTGACAATGATGACAC 3'

945MYC-AS 5'

GCTCTAGATTACAAGTCTTCTTCAGAAATAAGCTTTGCCGGCCGCAATAACTA

ACTAT 3'

UAS-flexin1-Cterm

Not-946s 5' ATAAGAATGCGGCCGCATGAATGAACACAAGATCACGCTGG 3'

3666Xba1Cmyc-AS 5' CGTCTAGATTACAAGTCTTCTTCAGAAATAAGCTTTTG

TTCTAAGGATTTGTCCATTTCC 3'

Germline transformants were done by standard methods(Spradling,1986).

Head-to-head RNAi primers (to make 556 bp RNAi template)

R1-566 AS CG GAATTC GGC GCT AAG CTG CAA GAC AT

Kpn-556 AS CGG GGTACC GGC GCT AAG CTG CAA GAC AT

N-Xho-4s CCG CTCGAG ATG TAC TCT GAC AAT GAT GAC AC

The antisense fragment PCR-ed from N-Xho-4s and R1-566 AS was inserted into pUAST in DH5a. The sense fragment made with N-Xho-4s and Kpn-566 AS was sequentially ligated into a clone bearing the first insert. Ligation products were electroporated into the recombination-deficient SURE cells.

Transgenic flies for structure-function analysis were made as described :

Construction of 4KA (site directed mutagenesis of terminal lysine residues of putative microtubule amphipathic binding motif in *UAS-flexin1-Cterm*) was made in two steps. First 3KA was constructed and then mutated to 4KA. The template source was UAS-*flexin1*.

3KA was made as follows : N-Not1-4s and 3KA-Xba-As primers amplified a 1.5kb fragment of *flexin1* from the UAS-*flexin1* template. It was digested, BAP treated, and inserted with Not1 and Xba1 into pUAST. Sequence was confirmed and the construct used as template for the last lysine mutation.

N-Not1s-4s

AGATAAGAAT GCGGCCGC ATG TAC TCT GAC AAT GAT GAC AC

3KA-Xba-AS

GC TCTAGA TTA CAA GTC TTC TTC AGA AAT AAG CTT TTG TTC TAA GGA TGC GTC CAT TTC CTC ACT CGC TGC CGC AG

Flex1-EcoR1-1KA-s

GAG GAATTC GTC CTA ATG GAG GAG AAC TAT CGA GCC ATT GGC CTG

CTC ACG CAG CTG GAG GC

Flex1-EcoR1-1KA-s and pUAST-AS were used to amplify a 137bp fragment (from 3KA template) that was digested with EcoR1 and Xba1 then inserted into pUAST similarly digested. This 137bp insert now contains 4 lysine to alanine mutations. Then the 1.4 kb fragment was digested from UAS-*flexin1* in pUAST (to avoid extraneous mutations) with flanking EcoR1 sites (one to the vector, the other internal to the ORF) and inserted into the 137 bp containing vector also digested with EcoR1. The desired orientation and frame of the 1.4kb insert next to the 137bp mutated fragment was sequence confirmed. Transgenic lines were made as described.

Construction of 1359 (*UAS-flexin1-Cterm* -Flexin, -microtubule + myc tag):

1359 myc Xba AS

TGC GTA GAA AGC TAC AAG GAC GAA CAA AAG CTT ATT TCT GAA GAA

GAC TTG TAA TCT AGA CG

Not 946s

Template from UAS-flexin was used to amplify a 0.4 kb C-terminal fragment missing the last 141 bp containing two identified motifs, NYRAIG and amphipathic helix.

Construction of B:C (*UAS-flexin1-Cterm* missing Flexin domain, + myc tag). Amplified with Pfu (Stratagene). 1359BglAS and Not946s were used to amplify a 413bp fragment. 1443Bgl-s and 3666Xba1CmycAS (primer sequence given previously) were used to amplify a 57 bp fragment from C-terminal pUAST. The two fragments were purified and

digested with BglII and ligated to each other in a 15uL reactioin. 2uL of that reaction was used as template for a second round of PCR. Both the pUAST and the 470bp fragment were digested with Not1 and Xba1 and ligated and injected as described.

1443 Bgl-s GAAGATCTTTGAGTCCGCTG

1359BglAS GAAGATCTTGTCCTTGTAGCTTTCTACGCA

Construction of D, (*UAS-flexin1-Cterm* +Flexin domain, +C-terminal alpha helix, + myc tag):

1360Not-s and 3666 CmycXba-AS were used to ampify a 140bp fragment with Pfu from C-terminal pUAST template. The insert and vector were digested with Not1 and Xba1 and ligated and injected as described.

3666 CmycXba-AS

CG TCTAGA TTA CAA GTC TTC TTC AGA AAT AAG CTT TTG TTC TAA GGA TTT GTC CAT TTC C

1360 Not-s

AGATAAGAATGCGGCCGC ATG GCA CTG CGT CTA CTG AA

Construction of E, (*UAS-flexin1-Cterm* missing C-terminal helix, + myc tag):

Not946s and 1443 myc Xba AS amplified a 497bp fragment with Pfu from C-terminal pUAST template. The insert and vector were digested Not1 and Xba1 and ligated and injected as described.

1443 myc Xba AS

GC TCTAGA TTA CAA GTC TTC TTC AGA AAT AAG CTT TTG CTC CAG CTG CGT GAG CAG

Site directed mutagenesis of putative cAMP phosphorylation site (Serine 474) in *UAS-flexin1*: PKA/PKG site to a nonphosphorylatable alanine. Primers and conditions designed per Stratagene to bp 1423 and 1424.

Phosphorylated mimic - Glutamate:

PK-G-s: GCT ACT AAA CGA AAA **GAA** GAC GAG AAC GGC GAC

PK-G-AS: GTC GCC GTT CTC GTC **TTC** TTT TCG TTT AGT AGC

Non-phosphorylatable version - Alanine:

PK-A-s: GCT ACT AAA CGA AAA **GCA** GAC GAG AAC GGC GAC

PK-A-AS: GTC GCC GTT CTC GTC **TGC** TTT TCG TTT AGT AGC

EMS Screen of *flexin1*

(Kurt Marek, personal communication)

1) Starve 3-4 day old males 12-24 hr

2) Dump flies in bottle with filter.

3) Apply EMS solution to filter in fume hood.

EMS solution:

25mM EMS = 24uL EMS stock in 10mL 5% sucrose solution

4) Mutagenize overnight in hood.

5) Mate males to virgins (aged 1-2 days)

6) Flip every 2 days for 4 days

Flies were screened by PCR as described previously using the primers:

Pr192 (BDGP)

FlexinC-term-AS 5' CGTCTAGA TGTTCTAAGGATTTGTCCATTTCC 3'

PCR products were sequenced as described.

REFERENCES

Artavanis-Tsakonas S, Rand MD, Lake RJ. Notch signaling: cell fate control and signal integration in development. Science. 1999 Apr 30;284(5415):770-6. Review.

Bianchi M, Heidbreder C, Crespi F. Cytoskeletal changes in the hippocampus following restraint stress: role of serotonin and microtubules. Synapse. 2003 Sep 1;49(3):188-94.

Briggs LJ, Stein D, Goltz J, Corrigan VC, Efthymiadis A, Hubner S, Jans DA. The cAMP-dependent protein kinase site (Ser312) enhances dorsal nuclear import through facilitating nuclear localization sequence/importin interaction. J Biol Chem. 1998 Aug 28;273(35):22745-52.

Cantallops I, Haas K, Cline HT. (2000) Postsynaptic CPG15 promotes synaptic maturation and presynaptic axon arbor elaboration in vivo. Nat Neurosci. *3*, 1004-11.

De Kerchove D'Exaerde A, Cartaud J, Ravel-Chapuis A, Seroz T, Pasteau F, Angus LM, Jasmin BJ, Changeux JP, Schaeffer L. Expression of mutant Ets protein at the neuromuscular synapse causes alterations in morphology and gene expression. EMBO Rep. 2002 Nov;3(11):1075-81. Epub 2002 Oct 22.

Dent EW, Kalil K. Axon branching requires interactions between dynamic microtubules and actin filaments.J Neurosci. 2001 Dec 15;21(24):9757-69.

Enerly E, Larsson J, Lambertsson A. Reverse genetics in *drosophila*: From sequence to phenotype using *UAS*-RNAi transgenic flies. Genesis 2002 34:152-155.

Gho M, Bellaiche Y, Schweisguth F. Revisiting the Drosophila microchaete lineage: a novel intrinsically asymmetric cell division generates a glial cell. Development. 1999 Aug;126(16):3573-84.

Goyal L, McCall K, Agapite J, Hartwieg E, Steller H. Induction of apoptosis by Drosophila reaper, hid and grim through inhibition of IAP function. EMBO J. 2000 Feb 15;19(4):589-97.

Gundersen GG, Khawaja S, Bulinksi JC. 1987. Postpolymerization detyrosination of a-tubulin: a mechanism for subcellular differentiation of microtubules. J Cell Biol 105:251-264.

Hashemolhosseini S, Kilian K, Kardash E, Lischka P, Stamminger T, Wegner M. Structural requirements for nuclear localization of GCMa/Gcm-1. FEBS Lett. 2003 Oct 23;553(3):315-20.

Hsueh YP, Wang TF, Yang FC, Sheng M. (2000) Nuclear translocation and transcription regulation by the membrane-associated guanylate kinase CASK/LIN-2. Nature. *404*, 298-302.

Huang EJ, Reichardt LF. Neurotrophins: roles in neuronal development and function. Annu Rev Neurosci. 2001;24:677-736. Review.

Hubner S, Xiao CY, Jans DA. The protein kinase CK2 site (Ser111/112) enhances recognition of the simian virus 40 large T-antigen nuclear localization sequence by importin. J Biol Chem. 1997 Jul 4;272(27):17191-5.

Hudson DF, Fowler KJ, Earle E, Saffery R, Kalitsis P, Trowell H, Hill J, Wreford NG, de Kretser DM, Cancilla MR, Howman E, Hii L, Cutts SM, Irvine DV, Choo KH. Centromere protein B null mice are mitotically and meiotically normal but have lower body and testis weights. J Cell Biol. 1998 Apr 20;141(2):309-19.

Iso T, Hamamori Y, Kedes L. HES and HERP families: multiple effectors of the Notch signaling pathway. J Cell Physiol. 2003 Mar;194(3):237-55. Review.

Kalil K, Gyorgyi S, Dent EW. 2000. common mechanism underlying growth cone guidance and axon branching. Neurobiology 44:145-158.

Kapoor M, Montes de Oca Luna R, Liu G, Lozano G, Cummings C, Mancini M, Ouspenski I, Brinkley BR, May GS. The cenpB gene is not essential in mice. Chromosoma. 1998 Dec;107(8):570-6.

Kennerdell,J.R. and Carthew,R.W. (2000) Heritable gene silencing in *Drosophila* using double-stranded RNA. *Nat. Biotechnol.*, **18**, 896–898.

Kitagawa M, Oyama T, Kawashima T, Yedvobnick B, Kumar A, Matsuno K, Harigaya K. A human protein with sequence similarity to Drosophila mastermind coordinates the nuclear form of notch and a CSL protein to build a transcriptional activator complex on target promoters. Mol Cell Biol. 2001 Jul;21(13):4337-46.

Komeili A, O'Shea EK. Roles of phosphorylation sites in regulating activity of the transcription factor Pho4. Science. 1999 May 7;284(5416):977-80.

Lai EC, Rubin GM. neuralized functions cell-autonomously to regulate a subset of notch-dependent processes during adult Drosophila development. Dev Biol. 2001 Mar 1;231(1):217-33.

Lam,G. and Thummel,C.S. (2000) Inducible expression of double-stranded RNA directs specific genetic interference in *Drosophila*. *Curr. Biol.*, **10**, 957–963.

Lee YS, Carthew RW. Making a better RNAi vector for Drosophila: use of intron spacers. Methods. 2003 Aug; 30(4): 322-9.

Liu W, Seto J, Sibille E, Toth M. The RNA binding domain of Jerky consists of tandemly arranged helix-turn-helix/homeodomain-like motifs and binds specific sets of mRNAs. Mol Cell Biol. 2003 Jun;23(12):4083-93.

Lundell MJ, Lee HK, Perez E, Chadwell L. The regulation of apoptosis by Numb/Notch signaling in the serotonin lineage of Drosophila. Development. 2003 Sep;130(17):4109-21.

Martinou I, Fernandez PA, Missotten M, White E, Allet B, Sadoul R, Martinou JC. Viral proteins E1B19K and p35 protect sympathetic neurons from cell death induced by NGF deprivation. J Cell Biol. 1995 Jan;128(1-2):201-8.

McCabe BD, Marques G, Haghighi AP, Fetter RD, Crotty ML, Haerry TE, Goodman CS, O'Connor MB. The BMP homolog Gbb provides a retrograde signal that regulates synaptic growth at the Drosophila neuromuscular junction. Neuron. 2003 Jul 17;39(2):241-54.

Mount SM, Burks C, Hertz G, Stormo GD, White O, Fields C. Splicing signals in Drosophila: intron size, information content, and consensus sequences. Nucleic Acids Res. 1992 Aug 25;20(16):4255-62.

Nedivi E, Wu GY, Cline HT. (1998) Promotion of dendritic growth by CPG15, an activity-induced signaling molecule. Science *28*, 1863-6.

Nolo R, Abbott LA, Bellen HJ. Senseless, a Zn finger transcription factor, is necessary and sufficient for sensory organ development in Drosophila. Cell. 2000 Aug 4;102(3):349-62.

Panicker AK, Buhusi M, Thelen K, Maness PF. Cellular signalling mechanisms of neural cell adhesion molecules. Front Biosci. 2003 May 1;8:d900-11

Panin VM, Irvine KD. Modulators of Notch signaling. Semin Cell Dev Biol. 1998 Dec;9(6):609-17. Review.

Perez-Castro AV, Shamanski FL, Meneses JJ, Lovato TL, Vogel KG, Moyzis RK, Pedersen R. Centromeric protein B null mice are viable with no apparent abnormalities. Dev Biol. 1998 Sep 15;201(2):135-43.

Piccin A, Salameh A, Benna C, Sandrelli F, Mazzotta G, Zordan M, Rosato E, Kyriacou CP, Costa R. Efficient and heritable functional knock-out of an adult phenotype in Drosophila using a GAL4-driven hairpin RNA incorporating a heterologous spacer. Nucleic Acids Res. 2001 Jun 15; 29(12): E55-5.

Ponting CP, Mott R, Bork P, Copley RR. Novel protein domains and repeats in Drosophila melanogaster: insights into structure, function, and evolution. Genome Res. 2001 Dec;11(12):1996-2008.

Presente A, Shaw S, Nye JS, Andres AJ. Transgene-mediated RNA interference defines a novel role for notch in chemosensory startle behavior. Genesis. 2002 Sep-Oct; 34(1-2): 165-9.

Preston CR, Sved JA, Engels WR. Flanking duplications and deletions associated with P-induced male recombination in Drosophila. Genetics. 1996 Dec;144(4):1623-38.

Reichhart JM, Ligoxygakis P, Naitza S, Woerfel G, Imler JL, Gubb D. Splice-activated *UAS* hairpin vector gives complete RNAi knockout of single or double target transcripts in *drosophila melanogaster* Genesis. 2002 Sep-Oct; 34(1-2): 160-4.

Rorth P. (1996) A modular misexpression screen in Drosophila detecting tissue-specific phenotypes. Proc Natl Acad Sci U S A. *93*, 12418-22.

Roussigne M., Cayrol C, Clouaire T, Amalric F, Girard JP. THAP1 is a nuclear proapoptotic factor that links prostate-apoptosis-response-4 (Par-4) to PML nuclear bodies. Oncogene (2003) 22, 2432-2442.

Schuster, C. M., Davis, G. W., Fetter, R. D., and Goodman, C. S. (1996a). Genetic dissection of structural and functional components of synaptic plasticity. I. Fasciclin II controls synaptic stabilization and growth, Neuron *17*, 641-54.

Si K, Lindquist S, Kandel ER. A neuronal isoform of the aplysia CPEB has prion-like properties. Cell. 2003 Dec 26;115(7):879-91.

Stewart BA, Schuster CM, Goodman CS, Atwood HL. Homeostasis of synaptic transmission in Drosophila with genetically altered nerve terminal morphology. J Neurosci. 1996 Jun 15;16(12):3877-86.

Sweeney ST, Davis GW. Unrestricted synaptic growth in spinster-a late endosomal protein implicated in TGF-beta-mediated synaptic growth regulation. Neuron. 2002 Oct 24;36(3):403-16.

Sugimoto A, Friesen PD, Rothman JH. Baculovirus p35 prevents developmentally programmed cell death and rescues a ced-9 mutant in the nematode Caenorhabditis elegans. EMBO J. 1994 May 1;13(9):2023-8.

Sullivan W, Ashburner M, Hawley RS. Drosophila Protocols. Cold Spring Harbor Laboratory Press (2000).

Suzuki N, Nakano M, Nozaki N, Egashira SI, Okazaki T, Masumoto H. CENP-B interacts with CENP-C domains containing Mif2 regions responsible for centromere localization. J Biol Chem. 2003 Nov 10 [Epub ahead of print].

Tawaramoto MS, Park SY, Tanaka Y, Nureki O, Kurumizaka H, Yokoyama S. Crystal structure of the human CENP-B dimerization domain at 1.65 A resolution. J Biol Chem. 2003 Sep 30 [Epub ahead of print].

Terskikh A, Fradkov A, Ermakova G, Zaraisky A, Tan P, Kajava AV, Zhao X, Lukyanov S, Matz M, Kim S, Weissman I, Siebert P. "Fluorescent timer": protein that changes color with time. Science. 2000 Nov 24;290(5496):1585-8.

Verzi MP, Anderson JP, Dodou E, Kelly KK, Greene SB, North BJ, Cripps RM, Black BL. N-twist, an evolutionarily conserved bHLH protein expressed in the developing CNS, functions as a transcriptional inhibitor. Dev Biol. 2002 Sep 1;249(1):174-90.

Wan HI, DiAntonio A, Fetter RD, Bergstrom K, Strauss R, Goodman CS. Highwire regulates synaptic growth in Drosophila. Neuron. 2000 May;26(2):313-29.

Zito K, Parnas D, Fetter RD, Isacoff EY, Goodman CS. Watching a synapse grow: noninvasive confocal imaging of synaptic growth in Drosophila. Neuron. 1999 Apr;22(4):719-29.

CHAPTER IV

flexin2 Restricts Central and Peripheral Neurogenesis and Participates in Notch Signaling

Abstract

We have characterized a member of the novel *flexin* family in Drosophila. *flexin2* exhibits neural and imaginal tissue expression spanning embryonic to larval stages. Via transgenic RNAi-mediated silencing, we demonstrate that *flexin2* is required for viability and is essential in neurogenic tissue throughout development. Hypomorphic embryos display CNS disorganization, revealing a role for *flexin2* in restricting neural development. Removal of *flexin2* in imaginal wing discs produces excess bristles, loss of wing margin and thickened wing veins suggesting that *flexin2* normally functions in the wing to restrict tissue growth and vein differentiation. In the notum, *flexin2* limits sense organ development. By several criteria, loss of *flexin2* phenocopies classic loss of neurogenic Notch signaling. Indeed, we observe transgenic RNAi-mediated synergistic enhancement of wing margin tissue loss in *trans* with either Notch RNAi or Notch deficiency. Genetic analysis places *flexin2* upstream of the Notch receptor-ligand interaction. Our data suggest *flexin2* participates as a positive effector in the Notch pathway.

Introduction

Coordinated cellular differentiation is fundamental to metazoan development. Extrinsic and intrinsic factors must be tightly integrated to elicit a specific developmental program (Irvine and Rauskolb, 2001). Among the most frequently utilized systems for local intercellular communication, Notch signaling orchestrates morphogenesis, patterning, growth, and cell fate (Artavanis-Tsakonas et al., 1999). The Notch pathway is evolutionarily conserved and required for cellular differentiation in all germ layers (Artavanis-Tsakonas et al., 1999). In mammals, aberrant Notch signaling leads to numerous pathologies such as cancer and developmental disorders (Robey, 1997; Egan et al., 1998; Artavanis-Tsakonas et al., 1999; Harper et al., 2003; Weng and Aster,2004).

While deceptively simple, the Notch pathway generates a remarkably diverse spectrum of responses. The developmental outcome elicited by the core components is context dependent, being influenced by specific spatio-temporal modulators (Justice and Jan, 2002; Panin and Irvine 1998). Notch has been best studied in Drosophila where numerous genes that influence the Notch signal have been identified (Panin and Irvine, 1998; Artavanis-Tsakonas et al., 1999; Greenwald,1998). During embryonic neurogenesis, neuropotent cells require Notch to restrict neural fate, hence, the "neurogenic" phenotype of neural hyperplasia seen in the absence of Notch signaling (Campos-Ortega, 1993 ; Hartenstein and Posakony, 1990; Beatus and Lendahl, 1998). In the imaginal tissue of the eye, ommatidial formation requires Notch for multiple roles (Voas and Rebay, 2004). In the pupal notum, sensory organ determination in the PNS depends upon cell-fate decisions mediated by Notch signaling (Hartenstein and Posakony, 1990; Justice and Jan, 2002). Notch is necessary for wing establishment,

growth and patterning (Klein, 2001). The restriction of wing vein differentiation is controlled by Notch (de Celis, 2003). Its obligate function is also manifested by its eponymous requirement during wing margin formation (Helms et al., 1999; Lai, 2004).

Different modes of Notch function have been described depending upon its site of action (Artavanis-Tsakonas et al., 1999). Lateral signaling mediated by stochastic Notch expression in equipotent neighbors allow restriction of cell fate to a limited subset via mutual amplification and consolidation of molecular differences (Artavanis-Tsakonas et al., 1999; de Celis and Bray, 1997). In contrast, inductive signaling occurs between non-equivalent cells whereby asymmetric receptor and ligand expression ensures a specific developmental program to be activated in the receptor-bearing cell (Artavanis-Tsakonas et al., 1999; de Celis and Bray, 1997). How Notch coordinates an appropriate response from its pleiotropic repertoire is under major investigation. Its effects are thought to be modulated at multiples levels by certain pathway components that act in a limited context, for example, that of *strawberry notch* in inductive signaling (Voas and Rebay,2004; Lai 2004; Majumdar et al., 1997). Understanding how its component members can exert tissue specific effects is critical in the study of the Notch pathway (Portin, 2002).

Here we describe the identification of a putative transcription factor, *flexin2*, as a novel component of Notch signaling that functions in a limited context. *flexin2* contains a predicted nucleic acid binding homologous to the vertebrate CENP-B family of DNA and RNA binding proteins. In *jerky* mice, loss of this CENP-B homolog causes epileptic seizures. To date, no members of the evolutionarily conserved CENP-B family have been either ascribed a signaling function or implicated in the Notch pathway. In *flexin2*, we

have uncovered an essential role for a CENP-B homolog in Notch-mediated restriction of neurogenic signaling. We find *flexin2* expression is developmentally regulated throughout embryonic and larval stages. Embryos mutant for *flexin2* exhibit neural disorganization. *flexin2* is required for embryonic and larval viability. In the adult, it is necessary for proper morphogenesis of the developing wing, eye, thorax, CNS, and sensory bristles of the PNS. In wing imaginal tissue, loss of *flexin2* promotes supernumerary notal bristles suggesting a role in lateral inhibition. We observe thickened veins in adult wings. In the wing margin, loss of *flexin2* identifies its function in mediating Notch signaling-dependent proliferation. *flexin2* genetically enhances Notch mutations in the wing margin. We conclude that *flexin2* functions synergistically in neurogenic Notch signaling during central and peripheral neurogenesis.

RESULTS

We identified *flexin2* as a homolog of *flexin1*, a gene we previously determined from our EP screen to modulate synaptic development (Sweeney and Davis, 2002; Roos et al., 2000). Drosophila *flexins* bear domains homologous to the mammalian CENP-B family whose specific *in vivo* developmental context has not been explored. Members of the *flexin* family exhibit dynamic expression patterns. Neurogenic and imaginal tissue expression of *flexin2* led us to investigate a neural function for Drosophila *flexins*.

Loss of *flexin2* Produces Wing Notching and Rough Eyes

To examine *flexin2* function, we constructed a *flexin2* RNAi transgene in a modified intron-bearing pUAST vector (pWIZ) and drove its expression using *vestigial-Gal4* (Lee and Carthew 2003; Guichard et al., 2002). *vg-Gal4* induces transcription along the dorsal-ventral boundary of the 3rd instar wing disc from which the presumptive wing blade everts during pupal development. Silencing of *flexin2* along the presumptive wing margin produces a striking "Notch-like" loss of margin tissue in adult wings (Figure 1). Strong notching, nicking, bristle loss, margin "gapping", as well as smaller wing hinge and compartment sizes are apparent in both independent transgenic lines driven by *vg-Gal4*. The RNAi generated phenotype is completely penetrant with greater homogeneous expressivity at 29^{0}C.

We assayed the requirement for *flexin2* function in another neurogenic tissue for adult phenotypes. Loss of *flexin2* in the eye disc mediated by *GMR-Gal4* produces a rough eye phenotype with a severe deficit of pigment cells, ommatidial bristles, and

disorganized ommatidia in the adult (data not shown). However, the size of the eye appears wild-type.

flexin2 Represents a Novel Family with Homology to CENP-B

The molecular organization of *flexin2* is predicted to comprise 2 exons of 322 bp and 1905 bp with an intervening intron of 3870 bp (Flybase identifier CG13894, Transcript ID CT33429). The open reading frame is predicted by Flybase to encode a protein 528 amino acids that contains a central proline and glutamine rich region (Figure 2B). By BLAST analysis, *flexin2* contains an N-terminal nucleic acid binding region homologous to the ancient metazoan CENP-B family of DNA binding proteins encompassing mouse *jerky*, human *JH8*, transposases, and shared by *THAP1-11* (Toth et al., 1995; Morita et al., 1998; Roussigne et al., 2003a; Smit and Riggs, 1996) (Figure 2B and E). (An NCBI conserved domain query, CDDv1.63 – 16482 PSSMs, also supports a nucleic acid binding function.) Residues 5-86 exhibit conserved cysteine-rich motifs found in human *THAPs 1-11* (Roussigne et al., 2003b). The CENP-B homology extends to the 165th amino acid. Sequence analysis predicts nuclear localization for *flexin2* (ProtComp, SubLoc v1.0), as demonstrated for CENP-B (Pluta et al., 1992).

The Drosophila *Flexin* family comprises six genes, five of which are clustered together at 61C9 on the third chromosome (Figure 2A). No other intervening genes are found in this cluster, suggesting an early gene duplication event. *flexin6* is located at 78C8. Family members were identified based upon the CENP-B domain and a common C-terminal motif we have designated the *Flexin* domain (Figure 2C and D). 4 *flexins* contain at least one N-terminal motif homologous to CENP-B. As with mouse *jerky*,

flexins 1 and *2* bear tandemly arranged motifs that may bind nucleic acids (Liu et al., 2003; Ponting et al., 2001).

***flexin2* is Expressed in Embryonic and Larval Stages.**

To determine the distribution of *flexin2* expression throughout development, we performed RNA in situ hybridization on embryos and larvae. *flexin2* expression is clearly detectable in all embryonic stages beginning about stage 4 when zygotic transcription initiates and a procephalic dorsoventral band appears by stage 6 (Figure 3A and B). Prominent neural expression is apparent in mid-embryonic stages 8-11 in the protocerebral and midline precursors, during the stage of neuroblast development (Figure 3C-E). In late stage embryogenesis, an intense pattern of *flexin2* highlights the CNS, the ventral midline (Figure 3F), and neurogenic imaginal tissue primordium corresponding to the wing and eye discs (Figure 3G). We dissected stage 15 embryos and examined them for their expression in the ventral nerve cord. Both glia and motoneurons exhibited robust expression (Figure 3H). Pronounced *flexin2* transcription continues in 3rd instar larval optic lobes (Figure 3I). In addition to CNS staining, abundant message manifests within the eye and antennal discs (Figure 3J). Intense staining lines the morphogenetic furrow of the eye disc. In the wing imaginal disc, *flexin2* occurs throughout the wing pouch (Figure 3K). A lower level of *flexin2* message is observed in the dorsal wing disc which prefigures the future notum and peripheral sense organs. Expression in these tissues persists during pupation. In the 24h APF (after puparium formation) notum, *flexin2* transcript is maintained in the presumptive dorsocentral and scutellar macrochaetes (Figure 3L). We also observe *flexin2* staining confined to intervein

compartments of the developing wing at 24h APF but absent from provein tissue (Figure 3Q). *flexin2* appears to be expressed in most neural and imaginal tissues and possibly epidermis. Controls with a sense probe do not show specific staining (Figure 3M, N, O, P, R).

Other *flexin* family members express in dynamic and diverse patterns (data not shown). *flexin1* initiates mesodermal transcript in mid-stage embryo at low levels. In the larva, *flexin1* is concentrated in the optic lobes within the optic anlage but absent from the ventral ganglion. *flexin1* is also detected in wing imaginal tissue. *flexin3* is ubiquitously expressed at low levels in the embryo. We confirm *flexin4* message in larval tissue by RT-PCR. We do not observe embryonic expression for *flexin5*. No expression data is available for *flexin6*.

flexin2 is Essential for Embryonic and Larval Development

A lack of somatic mutations in the *flexin2* locus necessitated our use of RNAi. For consistent results in a tissue-specific, cell-autonomous manner, we employed UAS-mediated transgenic RNAi expression (Lee and Carthew, 2003; Reichhart et al., 2002; Okajima and Irvine, 2002). Initial RNAi microinjections throughout embryogenesis revealed early embryonic lethality (data not shown) which we investigated using the *flexin2* transgenic RNAi lines *2A* and *5*, both of which behaved similarly.

UAS-flexin2-RNAi expression with the neuronal Gal4 drivers *Elav* and *c155* do not elicit phenotypes in the embryo, larvae, or adult (data not shown). Because the drivers express in post-mitotic neurons whereas the onset of *flexin2* expression begins around embryonic stage 4, we used a strong ubiquitous Gal4 expressing driver, *Tubulin-*

Gal4 (Lee and Luo, 1999; Castellijo-Lopez et al., 2004). *Tubulin-Gal4*; *UAS-flexin2-RNAi* embryos were lethal, consistent with an early requirement for *flexin2*. For technical reasons, we turned to pan-tissue *heat-shock-Gal4* to investigate the phenotype of early embryonic loss of *flexin2*. By inducing heat-shock at 2 hours, we initiated expression of *flexin2 RNAi* prior to the onset of neuroblast development. Anti-HRP staining of embryos with reduced levels of *flexin2* reveals increased neuronal staining and a moderately disorganized CNS unlike that seen in wild-type (Figure 4A and B); phenotypes displayed by hypomorphic Notch signaling. Staining for FasII identifies delayed and misrouted axonal projections at the midline (data not shown).

To determine an essential requirement for *flexin2* during larval development, we removed *flexin2* function via a weaker pan-tissue expressing *daughterless-Gal4* (*da-Gal4)* (data not shown) (Castillejo-Lopez et al., 2004). Animals were pharate pupal lethal at 22^{0}C, suggesting either that *flexin2* was incompletely silenced or unnecessary during larval development. Because Gal4 activity is higher at 29^{0}C, we shifted developing animals from 22^{0}C to 29^{0}C at the start of 1st, 2nd, and 3rd instars and allowed them to develop. Larvae fail to grow, molt, or transit each stage at which higher Gal4 expression was initiated. Instead, strong suppression of *flexin2* with either transgene results in stage arrest with the larvae maintaining their size for a week before expiring.

In the larva, *flexin2* exhibits neuronal expression. We inhibited *flexin2* function by driving the transgenic RNAi with the pre- and/or postsynaptic Gal4 drivers *Elav-Gal4*, *c155-Gal4*, *OK6-Gal4* and *BG57-Gal4*, *24B-Gal4* respectively. No gross synaptic perturbations are seen morphologically or electrophysiologically at the neuromuscular junction of 3rd instar larva except for occasional muscle fusion deficits via *OK6-Gal4* and

a modest increase in bouton number by *da-Gal4* (data not shown). This is consistent with our embryonic Gal4 results confirming that *flexin2* is an essential neuronal gene that is dispensable in post-mitotic neurons.

Loss of *flexin2* Increases Wing Vein Territory

flexin2 is expressed throughout the wing disc (Figure 3K). The above experiments demonstrate a role for *flexin2* in neurogenic and wing margin development. Neurogenic signaling is also required in wing vein determination which we investigated using the *scabrous-Gal4* driver (Mlodzik et al., 1990). In the wing imaginal disc, *sca-Gal4* directs expression along the anteroposterior axis (A-P) perpendicular to that evinced by *vg-Gal4*. The A-P axis delineates the longitudinal vein 3 (L3) in the adult wing blade (Figure 5A and D). Removal of *flexin2* during pupal wing blade development with either RNAi transgenic lines produces irregular thickening of L3 (Figure 5B and E). The L3/L4 intervein compartment appears slightly smaller. Occasionally, ectopic bristles protrude from locations corresponding to the campaniform sensilla. The reduced wing compartment size found in *vg-Gal4* driven wings is also observed in the intervein compartment between L3 and L4 in *sca-Gal4/+; UAS-flexin2-RNAi-2A/+*. These wings consistently curl upwards. Thickened L3 venation is seen with another A-P driver, *patched-Gal4* (data not shown). The strong wing pouch driver, *MS1096-Gal4* produces markedly reduced wings with thick veins throughout (Figure 5C) (Capdevila and Guerrero, 1994; Lai and Rubin, 2001). We do not detect ectopic or missing veins (de Celis, 1997; Martin-Blanco, et al., 1999). Our data suggest a role for *flexin2* in restricting the establishment of veins and a role in wing tissue proliferation, processes controlled by

Notch signaling. Vein territory delimitation is a Notch-dependent process that restricts pro-vein fate from intervein fate (de Celis, 2003). In the absence of Notch, vein patterning is normal, but thicker (de Celis, 2003). Smaller wing and compartment sizes are also consistent with reduced inductive Notch-mediated proliferation (Giraldez and Cohen, 2003; Baonza and Garcia-Bellido, 2000).

***flexin2* is Necessary to Restrict Sense Organ Development**

flexin2 is endogenously expressed in the neurogenic imaginal tissue of 3rd instar larval wing discs and pupal nota (Figure 3K and L), where the timing and location of each process conveniently defines and dissects specific gene function (reviewed in Gomez-Skarmeta et al., 2003). The wing imaginal disc produces the adult wing blade and half of the mesothorax (notum) including its attendant PNS sense organs (Koelzer and Klein, 2003). PNS bristle development has been well characterized in Drosophila. In the adult notum, each sensory bristle sensillum is comprised of four cells generated from a single precursor cell that had undergone three sequential asymmetric cell divisions (Escudero et al., 2003; Fisher and Caudy, 1998; Culi and Modolell, 1998). The two external cells visible in the adult are the hair shaft cell and the socket cell. Nestled in direct contact below are the internal cells, the neuron, sheath and glia cell which subsequently migrates away (Gho et al., 1999). The large bristles, macrochaetes, develop from an initial prepattern that selects the sensory organ precursor (SOP) (Gho et al., 1999; Culi et al., 2001). Highly conserved, stochastic events during Notch-mediated lateral inhibition restrict neural cell fate to the strongest Delta producing cell (Artavanis-Tsakonas et al., 1999; Chen et al., 1997). Thereupon, further Notch-mediated binary cell fate lineage

specification events direct normal development of external sensory bristle and socket as well as internal neuron and sheath cells (Gho et al., 1999). Four dorsocentral macrochaetes occupy invariable locations in the wild-type adult notum surrounded by a lawn of microchaetes arrayed in a stereotypical density pattern (Figure 6A). In the scutellum, four macrochaetes typically project (Figure 6A and E).

Based upon its notal expression in sense organs (Figure 3L), we have analyzed the role of *flexin2* in the notum. To eliminate *flexin2* expression in the proneural clusters of the wing imaginal disc, we used a *scabrous-Gal4* line (*sca-Gal4*). During notum development, prior to the first pI division, *sca-Gal4* directs continuous expression in proneural clusters which become the sensory organ precursors (SOP) that give rise to the adult macrochaetes (Gho et al., 1999). When *flexin2* function is suppressed via either transgenic RNAi lines, we observe excess bristle development. Loss of *flexin2* in SOP clusters produces dramatic tufting adjacent to the dorsocentral macrochaetes (Figure 6B and C). Indeed, many of the hair bristles do not resemble the stereotypical long, slender, tapering macrochaetes. Instead, the bristles are generally short, about the size of microchaetes. Additionally, the dense overgrowth render it difficult to determine whether each bristle developed with its own socket except for supernumerary bristles at the margins of the tufting where we can clearly see that each bristle retains a separate socket cell. Quantifying the ratio of hairs to sockets at the margins of the tufts may reveal possible cell fate transformations of socket to bristle cells. We do not observe severe tufting or loss of bristles in the scutellum. Extra macrochaetes, almost always with a concomitant socket cell, grew in close proximity to the wild-type bristles (Figure 6F, J). Scutellar expression of *flexin2* RNAi with *patched-Gal4* also produced excess

bristle-socket pairs with a reduced scutellum size suggesting that excess sensory organs develop at the expense of epidermal tissue (data not shown).

While we observe dorsocentral tufting, it is important to note that the excess bristles continue to point in the same direction. Notal bristles are aimed in an anterior to posterior direction. The maintenance of wild-type bristle orientation suggests normal *frizzled*-mediated (*Fz*) planar cell polarity. *Fz* activity is required during the first asymmetric cell division of the sensory organ precursor. Defective *Fz* signaling produces random bristle orientation (Adler, 2002; Okajima and Irvine 2002; Roegiers et al., 2001). We conclude that *flexin2* is not required for planar cell polarity.

To address whether supernumerary bristles are generated through cell fate transformation or a failure in lateral inhibition, we assayed for Elav-positive neurons over the course of pupal sense organ development in the absence of *flexin2* (Justice and Jan, 2002; Okajima and Irvine, 2002; Huang et al., 1991). Transforming internal cells of the normal sensillum into external cells would leave the sense organs devoid of neurons. Conversely, relief of lateral inhibition would generate excess sensilla, each containing one internal neuron per macrochaete. In the pupal mesothorax, reduced levels of *flexin2* promote development of extra scutellar and dorsocentral neurons, but only in the vicinity of extant ones. At 48h APF, we observe a dramatic increase in neurons adjacent to the dorsocentral bristles but not at 24h APF (data not shown). In the scutellum, four Elav-positive neurons are visible at 24h APF in controls (SEM 0, n=10) (Figure 6G and I) whereas we detect an average of six neurons (SEM 0.15, n=13), 50% more, in *sca-Gal4;UAS-flexin2-RNAi-5* (Figure 6H and I) (p value=0.00037). In adult *sca-Gal4;UAS-flexin2-RNAi-5* scutellum, we observe an average of 6.9 bristles (SEM 0.4, n=31) versus

4.1 (SEM 0.04, n=80) in controls (Figure 6J) (p value=$3.5x10^{-7}$). That each macrochaete retains a neuron is suggested by the near one-to-one correlation between neuron number and bristle number suggesting that lineage specification has not been perturbed. The results from both *flexin2* RNAi lines support a failure in lateral inhibition as the mechanism for extra sensilla that contain the normal complement of external and internal cells.

Additional evidence that *flexin2* does not function in cell fate transformation was seen in the background of the strong PNS driver, *neuralized-Gal4* (Boulianne et al., 1991; Usui and Kimura, 1993; Huang et al., 1991). *neuralized-Gal4* expresses after SOP formation when lateral inhibition decisions have already been made (Pickup et al., 2002; Roegiers F pers. comm.). Thus its onset of expression occurs during lineage specification. *UAS-flexin2-RNAi-2A* expression via *neuralized-Gal4* do not produce viable adults. Pupae develop until eclosion upon which a few attempt to eclose but fail regardless of the transgene used. The lethality may stem from a failure to secret cuticle. We dissected eclosion-lethal adults. At this stage, the adult notum and bristles are fully developed. These nota do not exhibit bristle defects and appear wild-type in bristle number and pattern (Figure 6D). Macrochaetes retain their stereotypical locations with each bristle shaft accompanied by a socket suggesting that loss of *flexin2* after lateral inhibition does not interfere with sensillum development. We conclude from our observations that *flexin2* is required prior to lineage specification to restrict excess SOPs. *flexin2* function in the notum is dispensable after lateral signaling events.

flexin2 Interacts Genetically with Notch

Removal of *flexin2* in the wing, notum, eye, and embryo phenocopies Notch loss-of-function. To test for a genetic interaction with Notch signaling, we obtained both *UAS-Notch* and *UAS-Notch-RNAi* transgenic flies to facilitate genetic manipulations in a spatio-temporal specific manner (Figure 7A and B) (Presente et al., 2002; Enerly et al., 2002). Our intent was to create heterozygous lines bearing *UAS-Notch-RNAi; UAS-flexin2-RNAi* strains to maintain as a stock and cross to other Gal4 drivers. We were surprised to find that transheterozygotes exhibited notched wings in the absence of a source for Gal4 (Figure 7D and E). The enhancement was robust and highly penetrant in both transheterozygous combinations of *UAS-Notch-RNAi* and *UAS-flexin2-RNAi* alleles tested (Figure 7G). The expressivity of the genetic enhancement was comparable to haploinsufficient Notch (Axelrod et al., 1996). No other Notch phenotypes were evident in adult eyes or notum. Homozygous parental stocks of *UAS-Notch-RNAi* and *UAS-flexin2-RNAi* rarely showed notched wings. Furthermore, we did not observe wing margin enhancement of the *UAS-flexin2-RNAi* lines with other control *UAS-RNAi* lines tested (data not shown).

We sought to confirm the transgenic RNAi enhancement by placing the *UAS-flexin2-RNAi* in *trans* with a heterozygous classical Notch loss-of-function mutation, *Df(1)N-264-105* (Presente et al., 2002). On average, 27% (SEM 0.04, n=8 trials) of the female progeny in control *Df(1)N-264-105/ yw,* exhibited distal tip notching on at least one wing (Figure 7C and H). We analyzed female progeny *Df(1)N-264-105/+;UAS-flexin2-RNAi-5/+* for a genetic interaction (Figure7 F and H). An average of 54% of the

progeny bore wing notching along the distal tip (SEM 0.08, n=6 trials, p value=0.0177). Our genetic enhancement data suggest *flexin2* participates in Notch signaling.

Having demonstrated a genetic interaction with the Notch pathway, we attempted to determine whether *flexin2* was upstream or downstream of the Notch receptor-ligand interaction. Rescue of either mutation with a full-length transgene to wild-type levels would suggest mutual participation in the same pathway. However, we did not possess a full-length *flexin2* transgene to rescue Notch hypomorphs. We performed the converse experiment; rescue of *flexin2* loss-of-function with full-length Notch. We co-expressed full-length Notch transgene together with a *UAS-flexin2-RNAi-5* in the wing disc using *MS1096-Gal4*. We observed greatly reduced pupal wings at 24h APF, identical to that in *MS1096-Gal4/+; UAS-flexin2-RNAi-5* (data not shown). Because that stage is lethal in Notch overexpression by *MS1096-Gal4*, we looked in 3rd instar larvae at the wandering stage. Normal wing discs were observed when *MS1096-Gal4* drove *flexin2* RNAi. Overgrown wing pouches were seen in Notch overexpression alone. Coexpression by *MS1096-Gal4* of both full-length Notch and *flexin2* RNAi also exhibited overgrown wing pouches (data not shown). A wide range of Notch overexpression exists that is not readily saturable (Artavanis-Tsakonas et al., 1999). Vanishingly small amounts of activated Notch are sufficient to elicit a nuclear Notch response. Thus full-length Notch overexpression manifests as an extremely strong hypermorph, overshooting the amount needed to rescue the reduction of Notch signaling caused by loss of *flexin2*. Transient expression or weaker gain-of-function Notch alleles may suffice to rescue the phenotype to wild-type levels. A possible interpretation of the data is that *flexin2* may be upstream

of or parallel to the Notch receptor-ligand interaction. Epistatic analysis utilizing a Notch pathway hypomorph with an opposing phenotype may resolve this issue.

DISCUSSION

We initially identified *flexin2* as a Drosophila homolog of the vertebrate CENP-B family. Loss-of-function *flexin2* phenocopies the classical haploinsufficient Notch in the wing margin. We further investigated the requirement for *flexin2* in neurogenic tissue and find loss-of-function phenotypes that also recapitulate mutations in the Notch pathway. In the wing margin, *flexin2* genetically enhances Notch mutations. Our results implicate an *in vivo* role in a critical genetic pathway for an evolutionarily conserved class of molecules. We also identify a previously unknown function for these molecules as possible regulators of neurogenic development.

flexin2 Encodes a CENP-B Domain with Putative Nucleic Acid Binding Function

flexin2 is a prototypic member of a novel family of genes designated the *flexin* family (Roos et al., 2000). *flexin2* contains extensive homology to the mammalian DNA binding family, CENP-B and its zinc-finger bearing relative, *THAP*. That *flexin2* bears sequence conservation to CENP-B family members suggests an evolutionarily conserved function. In mice the CENP-B member, *jerky*, has been shown *in vitro* to bind both RNA and DNA (Liu et al., 2003). Mutations in the human homologue *JH8*, is associated with a form of human idiopathic generalized epilepsy (Moore et al., 2001). Similarly, members of the mammalian *THAP* family are thought to possess DNA binding activity (Roussigne et al., 2003).

A structural feature found in the middle region of *flexin2* is a stretch of proline and glutamine rich residues. These domains have been demonstrated to be the hallmarks of nuclear transcription factors (Si et al., 2003; Iso et al., 2003; Verzi et al., 2002).

Transcriptional components in Notch signaling have similar structural organization to *flexin2* – an N-terminal DNA binding domain followed by a central portion of polynucleic acid repeats (Iso et al., 2003). Multiple lines of sequence evidence suggest nuclear localization and putative transcriptional function for *flexin2*. While *THAP* and CENP-B proteins have been characterized for their nuclear roles, to date, no members of these families have been shown to participate in a specific developmental pathway. We demonstrate here the first evidence for participation by members of this ancient family in the evolutionarily conserved Notch signaling.

flexin2 is Essential in Neural Precursors Throughout Drosophila Development

We have identified *flexin2* to be a member of the *flexin* family and confirmed that our genomic prediction was not a pseudogene via RNA in situ hybridization. The dynamic spatiotemporal expression pattern in neurogenic imaginal tissue suggests that *flexin2* expression may be important in multiple organs. Transgene-mediated RNAi suppression of *flexin2* uncovered an essential role in embryonic development. In particular, it is required in neurogenic tissue prior to neuroblast differentiation but not in post-mitotic neurons. We were able to dissect the timing of its requirement up to mid-embryogenesis. Notch-mediated lateral inhibition events that specify neural and ectodermal precursors during embryogenesis correspond to the time frame of *flexin2* expression. Similarly, in larval imaginal tissues where Notch signaling has been well characterized, *flexin2* transcript is also found at the morphogenetic furrow in the eye disc, the sensory organ precursors in the wing disc, as well as the intervein compartments in the pupal wing (Brennan and Moses, 2000; de Celis et al, 1997b; de Celis, 2003).

flexin2 is also required throughout larval and pupal development. In the larval CNS where we observed high levels of *flexin2* transcript, a pulse of neural development occurs during each instar. Failure of neurogenic tissue to develop results in stage arrest (Tissot and Stocker, 2000; Rayburn et al., 2003). *flexin2* message is apparent in neurogenic imaginal tissues that give rise to adult structures including wing, eye, and notum. We examined *flexin2* function in detail in the wing and notum where its expression in the dorsal wing disc implicates a role in proneural clusters.

flexin2 Participates in Notch Signaling

The wing margin is exquisitely tuned to the reception of Notch signal (de Celis and Bray, 1997). A heterozygous reduction of Notch can be robustly displayed and sensitively assayed. Indeed, mutations in Notch signaling frequently display dosage-sensitive interactions with each other (Lai and Rubin, 2001). Notch has an inductive role between non-equivalent cells in wing margin formation and growth contrary to that of its repressive role in embryonic CNS development (Portin 2002; Tsuda et al., 2002; Lai and Rubin 2001; Rulifson and Blair, 1995; Neumann and Cohen, 1996). When removed from the wing margin by *vg-Gal4, flexin2* mutants produce margin notching and bristle loss identical to a reduction of one copy of Notch (Axelrod et al., 1996). Genetic dissection of pathway interactions using RNAi has been previously demonstrated in Drosophila (Kiger et al., 2003; Liebl et al., 2003). We have taken a similar approach using leaky transgenes. A basal level of UAS-mediated transgenic expression with phenotypic consequences in the absence of Gal4 has been previously noted in Drosophila (Quinn et al. 2003, Jaramillo et al. 2004, Schuster et al. 1996). While homozygous parental strains

of *flexin2* RNAi or Notch RNAi rarely manifested any phenotypes, heterozygous combinations of one copy each of *flexin2* RNAi and Notch RNAi sufficed to mediate genetic enhancement to a level reminiscent of haploinsufficient Notch.

Genetic interaction in a signaling pathway has classically been determined by epistasis or genetic enhancement using somatic alleles. Epistatic interpretation of RNAi data has been demonstrated to be comparable to traditional epistasis performed with genomic mutations in Drosophila (Goto et al., 2003; Lum et al. 2003). Classical genetic enhancement is generally considered evidence of mutual participation in a genetic pathway if transheterozygous loss-of-function mutations produce synergistic interactions greater than either mutation alone. Genetic enhancement through the use of injected RNAi has been documented in Drosophila (Liebl et al., 2003). Our data support interpreting transgenic RNAi enhancement as a genetic interaction. A convenient advantage of transgenic RNAi is that dosage sensitivity can be manipulated by copy number.

RNAi enhancement in a defined somatic mutant background has been shown to be effective for determining genetic interactions (Withee et al., 2004). We corroborated our mutual RNAi enhancement by placing *flexin2* RNAi in the sensitized background of the classical Notch loss-of-function, *Df(1)N-264-105*. The loss of margin tissue in both Notch deficiency and Notch RNAi enhancement suggests that the genetic interactions seen with Notch RNAi is specific to a perturbation of Notch signaling (Figure 7G and H). We conclude that appropriately sensitized RNAi alleles may be used to test for genetic interactions in a signaling pathway. This may be particularly useful in analyzing genes

for which no dominant negatives, somatic loss-of-function mutations or gain-of-function alleles are available.

Effects on Differentiation and Proliferation in the Wing

Vein and intervein development have been well characterized (Bray 1998; Artavanis-Tsakonas et al., 1999). Vein differentiation involves Notch restriction of vein thickness along vein-intervein territories (Bray 1998). The process of vein width refinement is Notch dependent and analogous to lateral inhibition in SOP development (Johannes and Preiss, 2002; Huppert et al., 1997; de Celis et al., 1997). The mutant thick vein phenotype observed in *sca-Gal4/+;UAS-flexin2-RNAi-2A/+* is reminiscent of phenotypes displayed by loss-of-function mutations in neurogenic genes involved in Notch signaling (de Celis, 2003; Ahmed et al., 2003). The extra L3 venation in *sca-Gal4/+;UAS-flexin2-RNAi-2A/+* flies appears to come at the expense of intervein tissue producing a slightly smaller L3/L4 intervein compartment consistent with a lack of lateral inhibitory Notch (Figure 5E). Our expression data suggests *flexin2* normally acts to limit vein fate by acting in pro-vein anlage during early pro-vein formation to restrict vein territory, or during later vein formation in the intervein cells immediately flanking the Delta-expressing vein cells to inhibit vein differentiation (Huppert et al., 1997; de Celis, 2003).

The smaller wing size in *MS1096-Gal4/+;UAS-flexin2-RNAi-2A/+* phenocopies the lack of wing tissue proliferation seen in loss of inductive Notch-mediated proliferation. (Go et al., 1998; Giraldez and Cohen, 2003). Similarly, we observe a reduced wing hinge size when *vg-Gal4* expresses *flexin2* RNAi. By 24h APF, mutant

MS1096-Gal4/+;UAS-flexin2-RNAi-2A/+ wing is observed to be less than half the size of wild-type yet still retaining the stereotypical vein patterning (data not shown). We have demonstrated that *flexin2* is necessary for proper wing margin formation. Our observations are consistent with a proliferative role for *flexin2* in intervein tissue.

Effects on Neurogenesis

Our data indicate that *flexin2* is essential for normal bristle number in the notum. Mutant bristle shafts develop complete with an accompanying socket cell. Furthermore, the almost one-to-one correlation between scutellar neuron number to scutellar macrochaete and socket pair suggests that extra bristle and socket pairs do not come at the expense of cell fate transformation. An explanation consistent with duplicated sensilla that exhibit complete development including shaft, socket, and neuron, would be *flexin2* acting to during lateral inhibition but not in cell fate transformation. Various components that modulate Notch signaling have been shown to influence only one aspect. Genes that are known to affect only lateral inhibition, but not SOP lineage decisions include *O-fucotransyltransferase1* (Okajima and Irvine, 2002). Alternatively, genes such as Numb have been shown to act only during cell fate transformation (Lu et al., 2000). *strawberry-notch* acts only in inductive Notch signaling but not in lateral inhibition (Tsuda et a., 2002). Our results imply a function for *flexin2* to restrict peripheral neurogenesis via lateral inhibition.

A similar process of neural precursor restriction occurs in embryonic central neurogenesis (Urbach and Technau, 2004; Kunisch et al., 1994). Notch signaling is required during central neurogenesis in the neuroectoderm to ensure an appropriate

balance between neuroblast and epidermoblasts by limiting neural precursors in the vicinity of prospective neuroblasts (Kunisch et al., 1994; Seugnet et al., 1997). Robust *flexin2* expression is seen in the time and place where neuroblast precursors are specified throughout stages 8-11 (Campos-Ortega, 1995). *flexin2* is essential prior to and during, but not after, neuroblast formation. The disorganized CNS and increased neuronal staining seen in embryonic *flexin2* loss-of-function is reminiscent of mutations that reduce Notch signaling (Escudero et al., 2003). As in the adult peripheral nervous system, *flexin2* appears to act primarily in lateral signaling events in the developing central nervous system.

Across a spectrum of tissues where we examined *flexin2* function, the resulting phenotypes recapitulated loss of neurogenic Notch function (Artavanis-Tsakonas et al., 1999). *flexin2* represents a new addition to the pantheon of genes that impinge upon the Notch pathway. Many such genes have been demonstrated to exhibit opposing gain-of-function and loss-of-function phenotypes (Panin and Irvine, 1998; Lai and Rubin, 2001; Nolo et al., 2000). In particular, these components frequently act as part of a multi-protein complex involved in transcriptional regulation (Lai and Rubin, 2001; Kitagawa et al., 2001). We hypothesize *flexin2* overexpression to confer opposing phenotypes from that described for its loss-of-function based upon its predicted nuclear nucleic acid binding structure. Furthermore, as with other Notch interacting genes, the complex interplay of multiple developmental signaling pathways offer additional avenues through which crosstalk can mediate *flexin2* activity. The remarkable conservation of developmental pathways between Drosophila and mammals suggests a likely role to explore for mammalian counterparts of the *flexin* proteins.

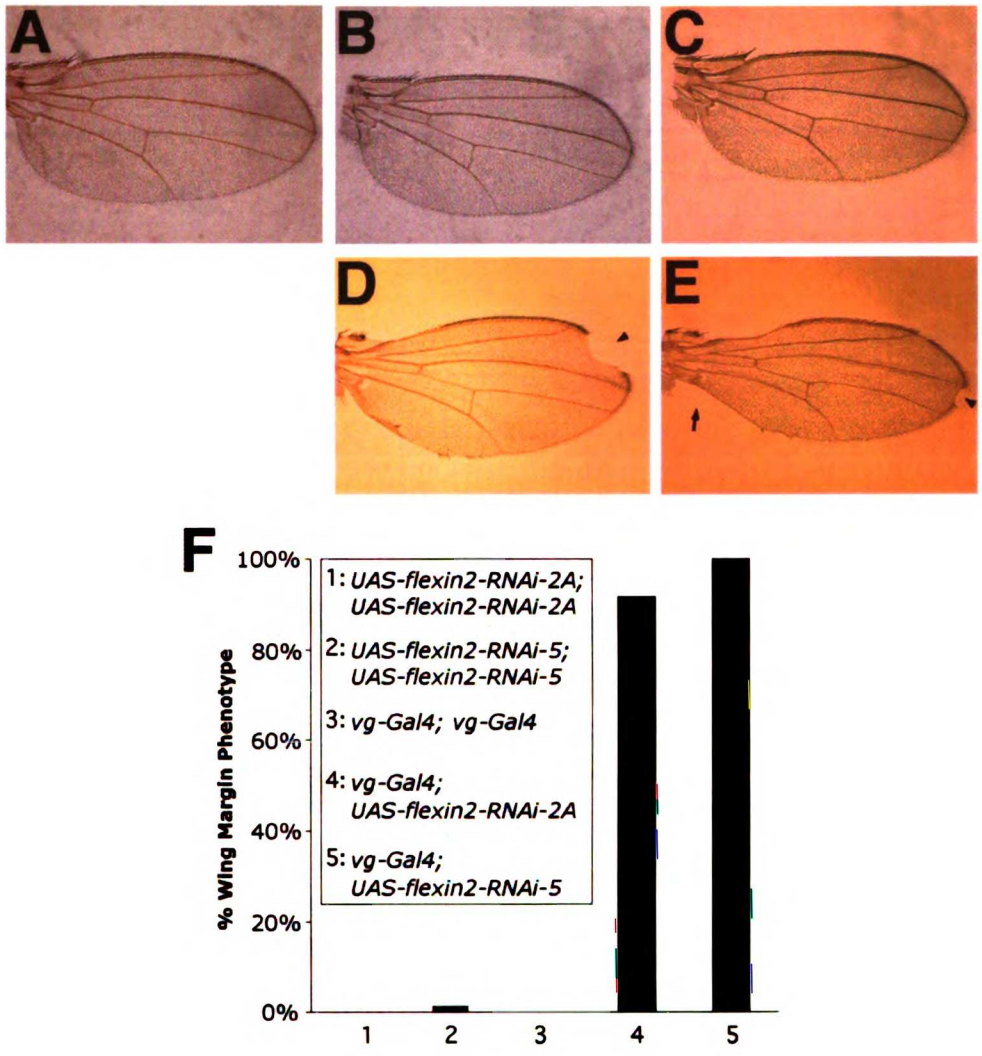
A
B
C
D
E
F
100%
80%
60%
40%
20%
0%
% Wing Margin Phenotype
1: UAS-flexin2-RNAi-2A; UAS-flexin2-RNAi-2A
2: UAS-flexin2-RNAi-5; UAS-flexin2-RNAi-5
3: vg-Gal4; vg-Gal4
4: vg-Gal4; UAS-flexin2-RNAi-2A
5: vg-Gal4; UAS-flexin2-RNAi-5
1
2
3
4
5

Figure 1

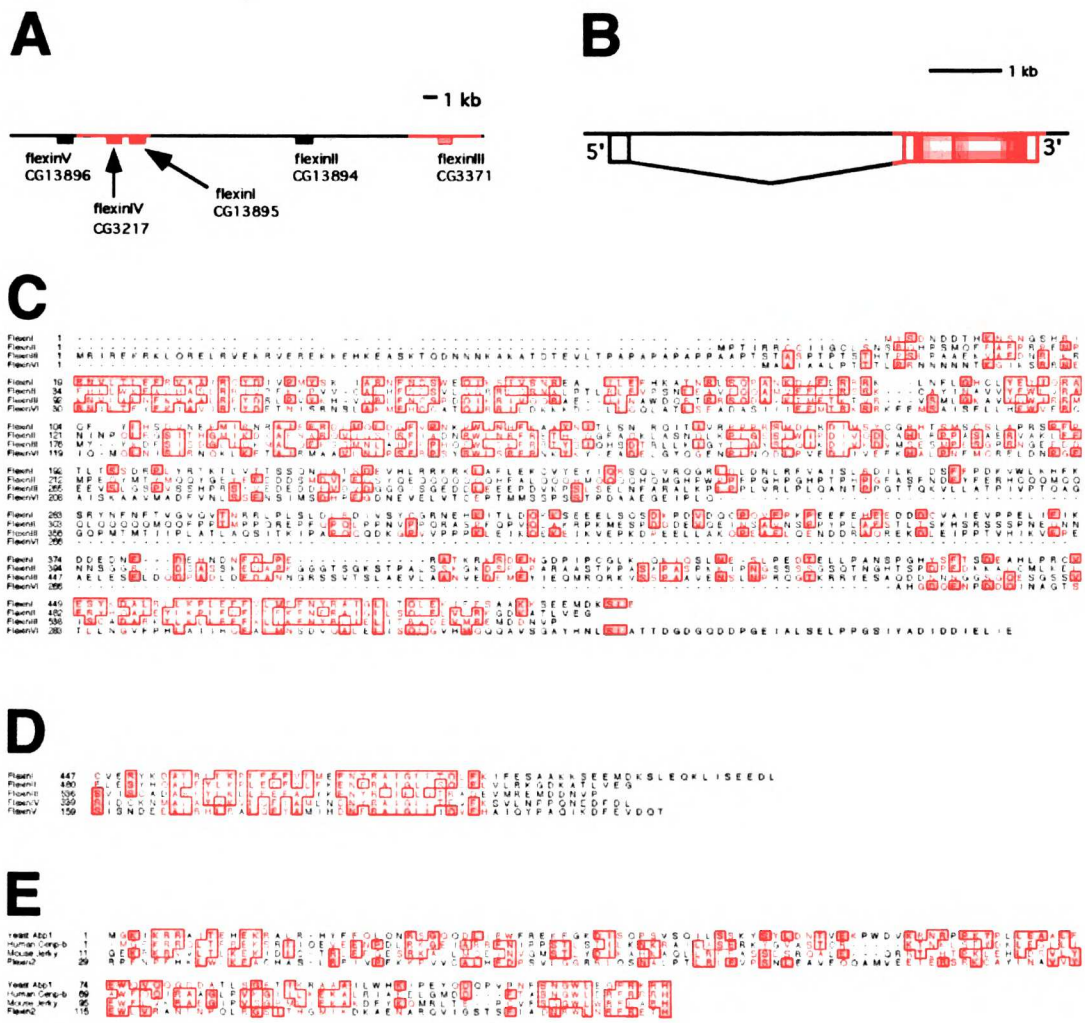
A
1 kb
flexinIV
CG13896
flexinIV
CG3217
flexinI
CG13895
flexinII
CG13894
flexinIII
CG3371
B
1 kb
5'
3'
C
D
E

Figure 2

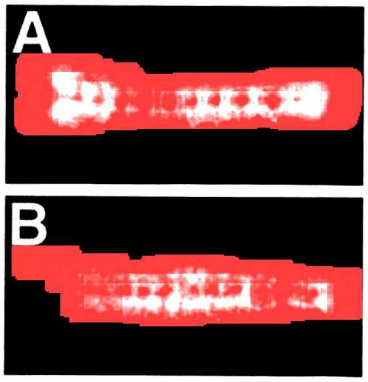

Figure 3

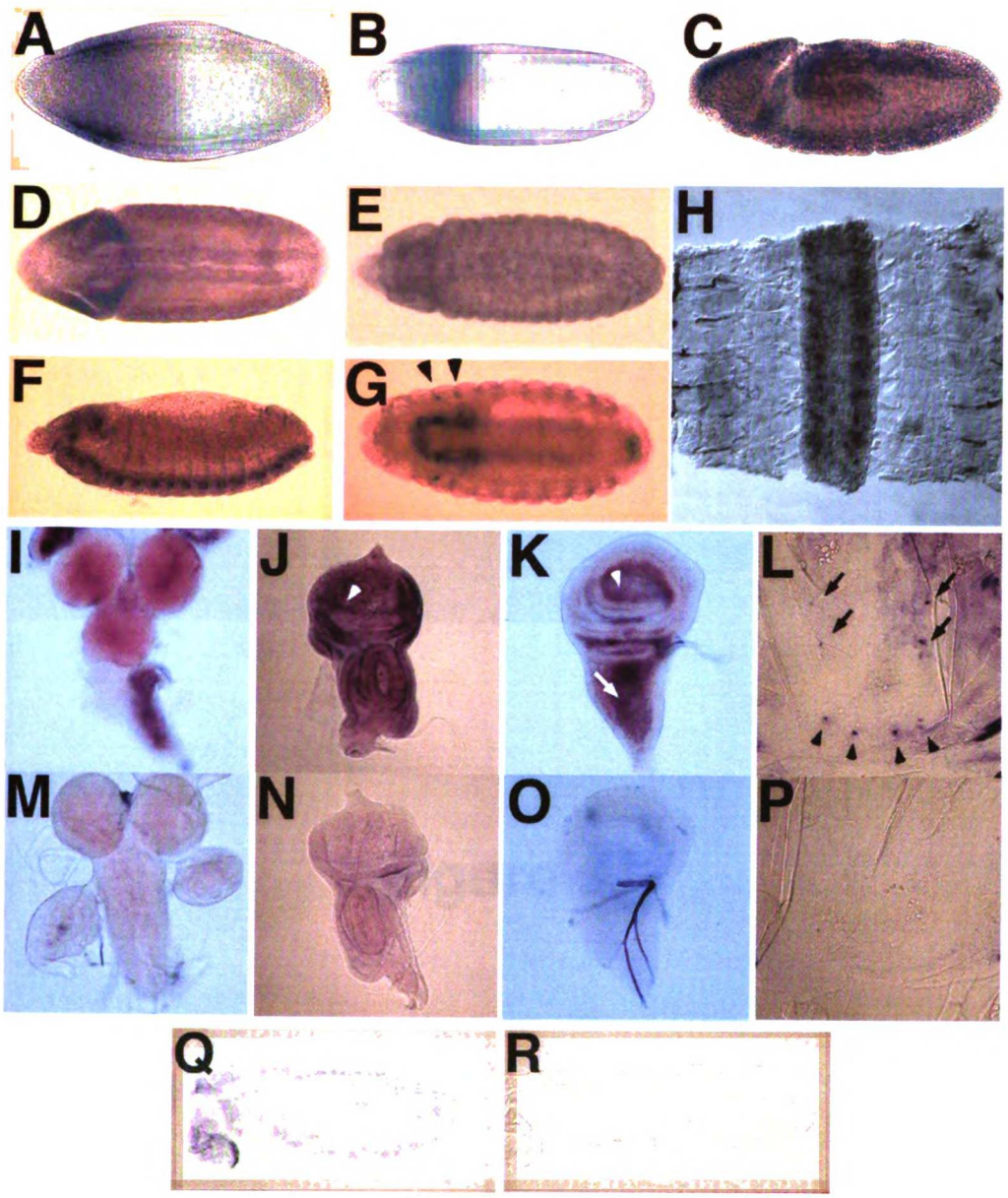

Figure 4

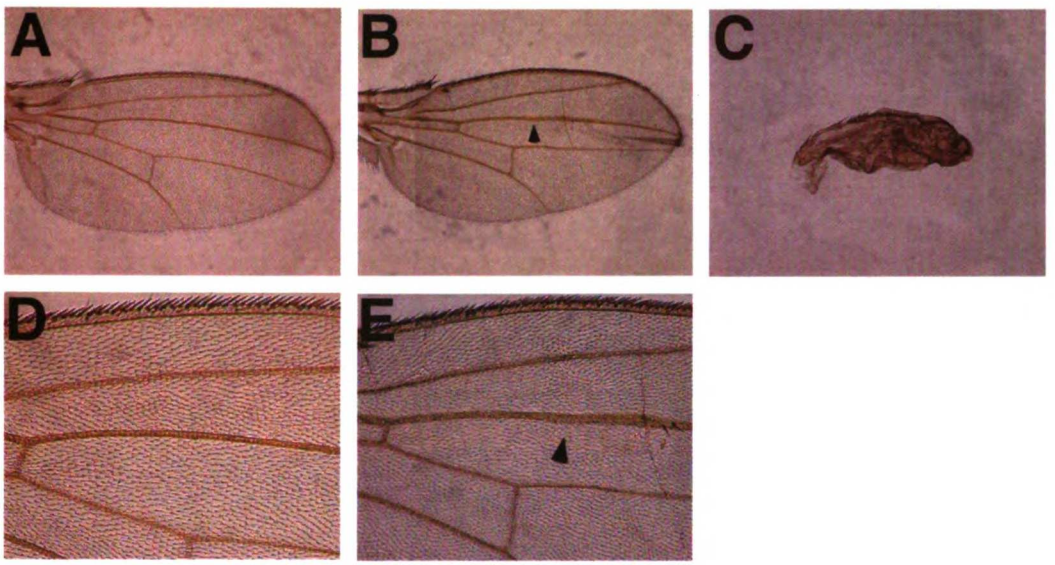

Figure 5

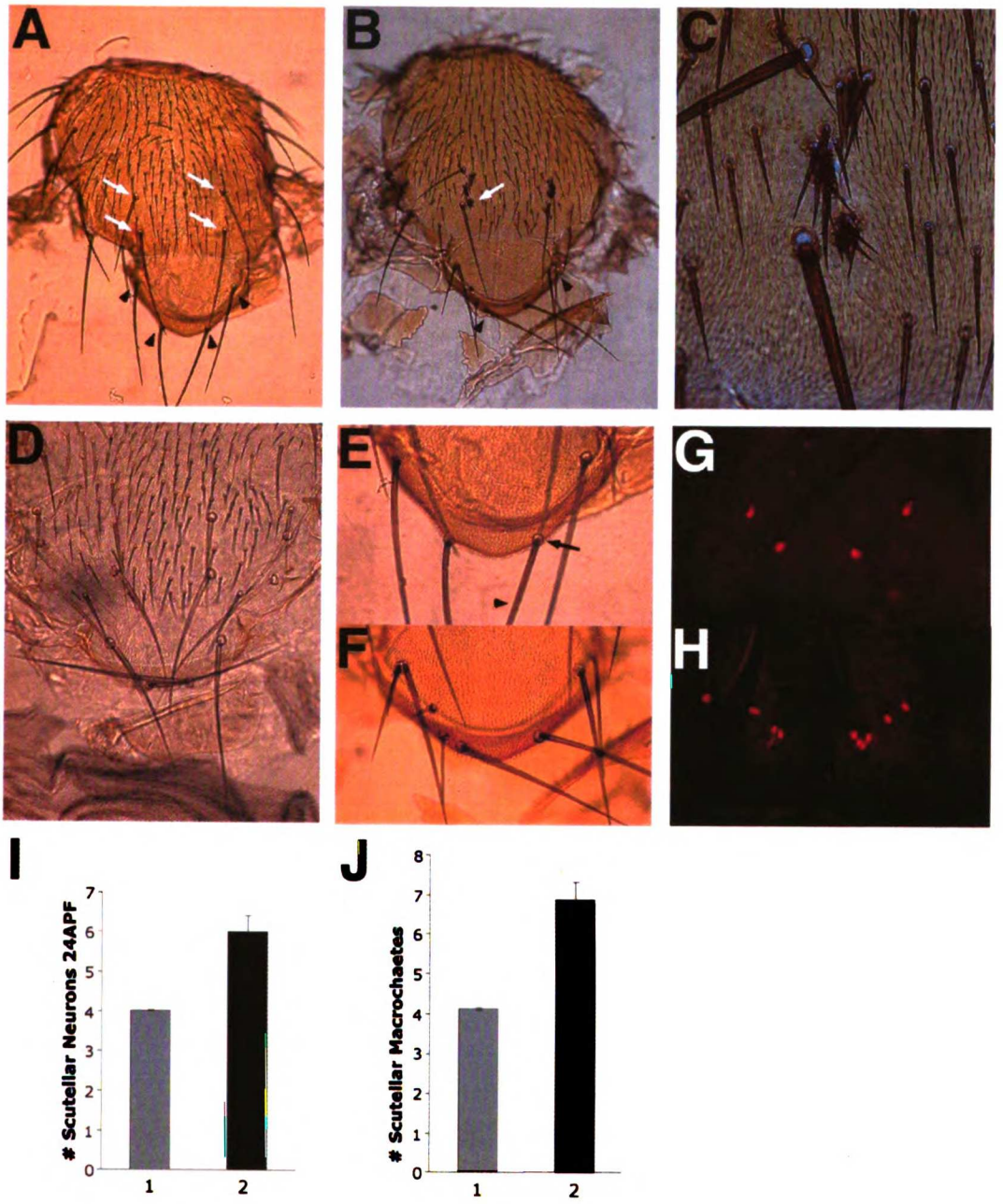
A
B
C
D
E
F
G
H
I
Scutellar Neurons 24APF
0
1
2
3
4
5
6
7
1
2
J
Scutellar Macrochaetes
0
1
2
3
4
5
6
7
8
1
2

Figure 6

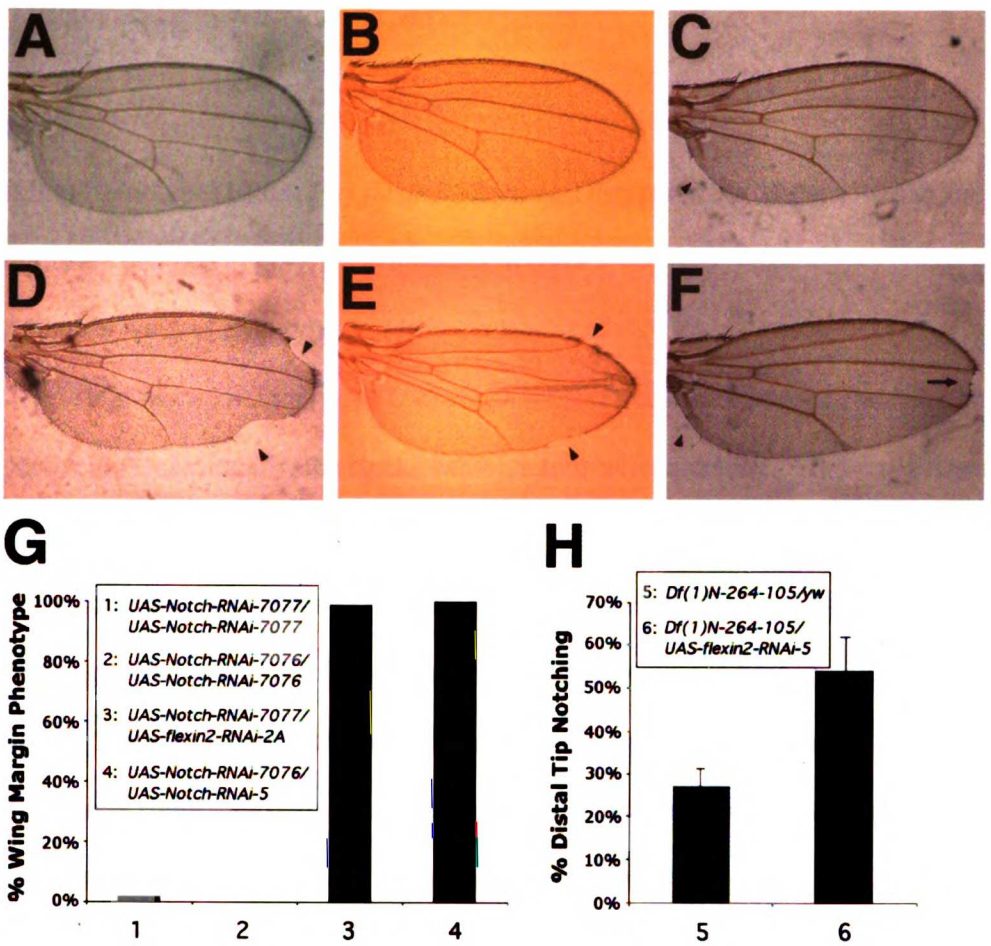
A
B
C
D
E
F
G
% Wing Margin Phenotype
100%
80%
60%
40%
20%
0%
1: UAS-Notch-RNAi-7077/ UAS-Notch-RNAi-7077
2: UAS-Notch-RNAi-7076/ UAS-Notch-RNAi-7076
3: UAS-Notch-RNAi-7077/ UAS-flexin2-RNAi-2A
4: UAS-Notch-RNAi-7076/ UAS-Notch-RNAi-5
1
2
3
4
H
% Distal Tip Notching
70%
60%
50%
40%
30%
20%
10%
0%
5: Df(1)N-264-105/yw
6: Df(1)N-264-105/ UAS-flexin2-RNAi-5
5
6

Figure 7

Figure legends

Figure 1

Imaginal Phenotypes Elicited by *flexin2* Silencing Disrupts Wing Margin Formation. Controls are denoted in gray, experimentals in black.

(A) Control wing of wild-type *w1118*.

(B, C) Wings of two homozygous *UAS-flexin2-RNAi* transgenic lines, *2A* and *5* respectively. Occasionally, the stocks exhibit minor wing notching. Flies were raised at 25^0C.

(D, E) Expression of *UAS-flexin2-RNAi, 2A* and *5* respectively, directed by *vestigial-Gal4* along the wing margin. We observe wing nicks, wing notching, and loss of margin bristles or "gapping" along both posterior and anterior wing margins (arrow). The wing blade appears significantly smaller near the thoracic insertion site (arrowhead). Both transgenic insertions yield similar phenotypes when driven by *vg-Gal4*.

(F) Quantification of wing margin phenotypes induced by *vg-Gal4* expression scored as being notched or "gapping,"missing margin bristles. (For genotypes 1-5, n = 0/152, 2/143, 0/81, 55/60, 46/46 respectively)

Figure 2.

The genomic and protein structure of the *flexin* gene family.

(A) Five of the six *flexin* genes are clustered together within 40kb of each other at chromosomal band 61C9. All genes are in the same orientation, with the 5' end on the left.

(B) The yellow box indicates the region of homology shared by *flexins 1,2,3* and *6*. The red box indicates the C-terminal Flexin domain. White domains are predicted noncoding sequences.

(C) *flexins* are characterized by a high similarity in their CENB-P motif and Flexin domain, with a region of low similarity between these two motifs. *flexin6* lacks the region of low similarity and is the most divergent of the *flexins* in the Flexin domain. Amino acids conserved in 50% or more of the sequences are highlighted in yellow.

(D) *flexin4* and *flexin5* have well conserved Flexin domains, and are yet to be characterized at their 5' ends.

(E) The N-terminal portion of *flexin2* bears similarity to the CENP-B motifs of mouse *jerky* and the human and yeast *CENP-B's*.

Figure 3

flexin2 Expression Pattern During Embryogenesis (A-H), Larval Development (I-K), and Early Pupation (L,Q). Embryos are shown anterior to the left and dorsal up unless otherwise indicated. Sense controls have no detectable patterns (data not shown).

(A) Stage 4 embryo exhibits procephalic ectodermal expression.

(B) A procephalic dorsoventral band arises in a stage 6 embryo.

(C) Stage 9 embryo. Staining is evident in the neuroblast precursors and along ectodermal germ band.

(D) Ventral view of stage 9 embryo during midgut invagination. Expression manifests throughout the procephalic region of the embryo.

(E) Stage 11 embryo. Ventral view of the nerve cord which exhibits *flexin2* message. Neuroectodermal tissue and peripheral sense organs appear to stain at weaker levels.

(F) Stage 15 embryo. Intense neural expression is visible along the ventral nerve cord.

(G) Stage 16 embryo ventral view. Note expression in the anterior spots flanking the ventral nerve cord containing the precursors to the presumptive wing and eye imaginal discs (arrowheads). The ventral nerve cord continues to express high levels of *flexin2*.

(H) Image of dissected late stage 15 embryo. *flexin2* message is apparent in ventral nerve cord and absent in muscle. Tracheal staining is non-specific. Anterior is up.

(I, J, K) In late 3rd instar larva, intense *flexin2* expression is evident in the optic lobes (I), and eye-antennal imaginal disc (J). Concentrated staining lines the morphogenetic furrow of the eye disc (J, arrowhead). The wing pouch where the wing blade everts exhibits high levels of *flexin2* (K, arrowhead). Additional expression is detected in the dorsal portion of the wing imaginal disc that gives rise to the adult notum and scutellum (K, arrow).

(L,Q) Pupal expression of *flexin2*.

flexin2 is found in the developing sense organs corresponding to the presumptive dorsocentral (arrows) and scutellar macrochaetes (arrowheads) of the pupal notum at 24h APF (after puparium formation) (L). In the same stage of the pupal wing, we observe refined expression localized to the intervein tissue (Q).

(M, N, O, P, R) Controls performed with sense probes do not stain specifically.

Figure 4

Neuronal phenotypes associated with loss of *flexin2* in the embryo. Ventral view, anterior is to the right.

(A) Control wild-type *yw67* embryos stained with anti-HRP-Cy3.

(B) Embryonic CNS disorganization seen in *heat-shock-Gal4/ UAS-flexin2-RNAi-5* embryos.

Figure 5

Loss of neurogenic signaling mediated by *flexin2* RNAi expression during pupal wing vein development. All flies were raised at 25^0C.

(A) Adult wing blade of control *w1118*.

(B) Thick vein phenotype of longitudinal vein 3 resulting from *sca-Gal4* expression of *UAS-flexin2-RNAi-2A* RNAi along the A-P axis of the wing imaginal disc (arrowhead). Image was taken in separate frames and merged together.

(C) *MS1096-Gal4* expresses strongly in the 3rd instar wing pouch producing severe wing blade hypoplasia in *MS1096-Gal4/+; UAS-flexin2-RNAi-2A/+* flies. Wings are shrunken and nearly absent in males. Margin bristles appear normal. Veins are grossly thickened.

(D) Higher magnification view of wild-type wing above showing longitudinal vein L3.

(E) Higher magnification view of *sca-Gal4/+;UAS-flexin2-RNAi-2A/+* L3 vein (arrowhead). Note thickened vein. Extra vein material appears to come at the expense of the L3/L4 intervein compartment.

Figure 6

Notum phenotypes associated with *flexin2* suppression. Anterior is up in (A-H). Transgenic lines containing the *UAS-flexin2 RNAi* transgene were crossed to the *sca-Gal4* driver which directs expression in proneural clusters. Inactivating *flexin2* during SOP lateral inhibition promotes excess bristle development. All flies were raised at 25^0C.

(A) Dorsal view of *w1118* adult mesothorax control notum with four scutellar macrochaetes in their stereotypical locations (white arrows). Four dorsocentral macrochaetes are also apparent in the notum (black arrowheads).

(B) *sca-Gal4; UAS-flexin2-RNAi-2A* flies exhibit completely penetrant, severe tufting of bristles in dorsocentral areas (white arrow) and duplicated macrochaetes in the scutellum (black arrowheads). Tufting is also apparent in notopleural sites. In strong scutellar suppression at 29^0C or *patched-Gal4* or *dpp-Gal4* backgrounds, adults show extensive tissue loss, resulting in a reduced scutellum size (data not shown). Extraneous scutellar macrochaetes are usually shorter in length. Bristles surrounding dorsocentral macrochaetes are frequently microchaetes of variable size. Both *flexin2* RNAi transgenic lines behaved identically.

(C) Magnified view of the dorsocentral notum shown in (B). *sca-Gal4; UAS-flexin2-RNAi-2A* flies exhibit extra bristles of various sizes. We were unable to resolve bristles in the center of the tufts for socket cells due to extreme overgrowth. Those at the periphery of the tufts however, appear to maintain one socket cell per bristle shaft.

(D) Notum from eclosion-lethal *neuralized-Gal4*-driven *UAS-flexin2-RNAi-2A*. *neuralized-Gal4* expresses strongly in the SOPs during lineage specification. The density

of notum microchaetes appear wild-type as do both dorsocentral and scutellar macrochaete number.

(E) Magnified view of wild-type scutellum shown in (A). The external portion of each sense organ is comprised of a single bristle hair shaft (arrowhead) and a socket cell (arrow).

(F) Magnified view of the *flexin2* RNAi-expressing scutellum shown in (B). Extra macrochaete shafts complete with corresponding socket cells are apparent near their stereotypical wild-type locations. Occasional twinning and shaft length variation observed may result from the later development of additional sense organs.

(G, H) anti-Elav(red) staining for macrochaetae neurons in the pupal scutellum at 24h APF.

(G) Control *UAS-flexin2-RNAi-5/ UAS-flexin2-RNAi-5* 24h APF pupal scutellum displays four neurons, one per sensillum.

(H) *sca-Gal4; UAS-flexin2 RNAi-5* 24h APF scutellum manifests clusters of Elav-positive cells where normally only one would be present at each of the four locations. Nine neurons are visible in the micrograph.

(I) Quantification of Elav-positive neurons at 24h APF for the genotypes shown in (G) and (H). Controls are denoted in gray, experimentals in black for both (I) and (J).

(J) Quantification of adult scutellar macrochaetes for the same genotypes as in (G) and (H). The average number of macrochaetes correlates strongly with neuron number.

Figure 7

flexin2 loss-of-function genetically enhances *Notch* loss-of-function in the wing margin.

(A, B) Control homozygous transgenic lines bearing *UAS-Notch-RNAi, 7077* and *7076* respectively. Notching is rarely observed in the stocks quantified in (G).

(D, E) Transheterozygous wing margin enhancement of *UAS-Notch-RNAi* by *UAS-flexin2-RNAi* in the absence of Gal4. Classical Notch haploinsufficient phenotypes are almost completely penetrant in both independent allelic combinations (arrowheads). Genotype in (D) is *UAS-Notch-RNAi-7077/ UAS-flexin2-RNAi-2A;* that in (E) is *UAS-flexin2-RNAi-5/+; UAS-Notch-RNAi-7076/+*. Intervein compartments appear slightly smaller in *UAS-flexin2-RNAi-5/+; UAS-Notch-RNAi-7076/+* wings, producing a crinkled appearance.

(C) Control *Df(1)N-264-105/+; yw* wings have a higher frequency of posterior margin loss without concomitant distal notching (arrow). Image was taken in separate frames and merged together.

(F) *Df(1)N-264-105/+; UAS-flexin2-RNAi-5/+* recapitulate classical Notch and show increased frequency of distal tip notching (arrowhead). Image was taken in separate frames and merged together.

(G) Quantification of mutual RNAi enhancement of *UAS-Notch-RNAi* by *UAS-flexin2-RNAi.* Wing margin phenotype is scored as being notched or missing margin bristles, "gapping". (for genotypes 1-4, n = 4/215, 0/61, 149/151, 126/126) Controls are denoted in gray, experimentals in black for both (G) and (H).

(H) Quantification of distal wing notching in *Df(1)N-264-105* enhanced by *UAS-flexin2-RNAi-5.*

MATERIALS AND METHODS :

Preparation of tissues:

Adult nota were dissected in 80% isopropanol, mounted in Hoyer's medium, and cleared at 60^{0}C overnight (Justice et al., 2003; Drosophila Protocols, 2000). White prepupae were collected for staging. Pupal nota were staged 15, 24, and 48 hours after puparium formation (APF), dissected in PBS, then fixed in Bouin's solution for 1 minute. Preps were washed, stained in PBT, and mounted in VectaShield. Adult wings were dissected in 80% isopropanol and mounted in 70% glycerol. Light microscopy was performed on a Zeiss Axioscope 40.

Immunohistochemistry: The following antibodies were used: rat anti-Elav 7E8A10 (1:50; Developmental Studies Hybridoma B, University of Iowa), anti-Mouse-Cy3 (1:400), anti-HRP-Cy3 (1:500).

Immunoflourescence: Imaging was performed on a Zeiss Axioscope 40 and taken with a Nikon 4500 digital camera.

In situ hybridization:

In situ hybridization was performed as previously described (BDGP) with the primers described below. For *flexin2* sense and antisense reactions, internal controls of RNAi expressing transgenic larvae, *MS1096-Gal4/+; UAS-flexin2-RNAi-5/+*, were included. These larvae exhibited staining in both experiments.

flexin2 antisense probe:

Flex2-ORF-801-S : cccatggccaccgtttcca

Flex2-T7-RNAi-AS : TAATACGACTCACTATAGGGAGACCAC

ctcttaaccctcgaccagtg

flexin2 sense probe control:

Flex2-T7-S :

TAATACGACTCACTATAGGGAGACCAC catcaacagcaaatgcaacagc

Flex2-AS : ctcttaaccctcgaccagtg

flexin1 antisense probe:

Xba-N#4 5' GCTCTAGA ATGTACTCTGACAATGATGACAC 3'

Flex1-T7-624AS 5'

TAATACGACTCACTATAGGGAGACCACGGTGACCAATGTCTTTGTGC 3'

flexin3 antisense probe:

Flex3-RNAi-S: ccacacccattgttccgacg

Flex3-T7-RNAi-AS :

TAATACGACTCACTATAGGGAGACCAC cactgtttggagcattctacg

flexin4 antisense probe:

Flex4-S : gctgtaagaggtgtgaatacc

Flex4-T7-RNAi-AS :

TAATACGACTCACTATAGGGAGACCAC atcgaaatcctcgttctgagg

flexin5 antisense probe:

Flex5-S : gaagtggtgtacatccaacac

Flex5-T7-RNAi-AS :

TAATACGACTCACTATAGGGAGACCAC cgtttgatccacctcgaagtc

flexin6 antisense probe:

Flex6-S : ccatccggatggcagctgt

Flex6-T7-RNAi-AS :

TAATACGACTCACTATAGGGAGACCAC ttactcgatcaattcgatgtcat

Molecular Biology:

Standard methods for DNA manipulation were done as described (Sambrook et al., 1989). Primers were obtained from Elim Biopharmaceuticals. Sequencing of plasmids and PCR products were also performed by Elim Biopharmaceuticals.

Primers used in this study :

UAST-s : TTG AAT ACA AGA AGA GAA CTC TG

UAST-AS : TAT GTC ACA CCA CAG AAG TAA G

Sense fragment : Nhe1 / Xba1

flex2-UAS-Nhe1-701-s cgc gcg GCT AGC atg taa agg agc aga gct atc aa

flex2-UAS-Xba-1150-AS cgc gcg TCT AGA gac tgt gct tgc tgg tta agg

Antisense fragment : Not1 / Xho1

flex2-UAS-Anti-Not-1150-s ggataagaat GCGG CCGC gac tgt gct tgc tgg tta agg

flex2-UAS-Anti-Xho-701-ASgcg ccg CTC GAG atg taa agg agc aga gct atc aa

Construction of *UAS-flexin2* RNAi lines:

flexin2 RNAi was cloned into the modified pUAST vector, pWIZ, which contains an internal intron. The plasmid was obtained from Lee, Y.S. and Carthew, R.W. pWIZ vector was digested with Xba1, CIP treated, and gel purified. The 450 bp sense insert corresponding to bp 701-1150 with flanking Nhe1 and Xba1 sites respectively was PCR

amplified (Promega) from genomic DNA using flex2-UAS-Nhe1-701-s and flex2-UAS-Xba-1150-AS, then digested (NEB), gel purified (Qiagen), ligated (NEB) into the digested pWIZ vector, and transformed into DH5α (Invitrogen). Sixteen colonies were screened by PCR using the pUAST-s and pUAST-AS primers for inserts and re-screened for sense-oriented insertion with the flex2-UAS-Nhe1-701s and pUAST-AS primers. Plasmid DNA obtained from a positive clone was digested with Not1, Xho1, and BAP as the vector for the second insert. The antisense insert was similarly PCR amplified with flex2-UAS-Anti-Not-1150-s and flex2-UAS-Anti-Xho-701-AS then TA cloned (Promega) into pGEM-T Easy Vector. Blue/white screening was employed to identify a positive clone for both sequence confirmation and digestion of the insert using Not1 and Xho1. The digested antisense insert was ligated into the pWIZ bearing the sense insert and transformed into DH5α. Colonies were screened using pUAST-s and flex2-UAS-Anti-Xho-701-AS primers. A positive clone bearing both the second and first inserts was AvrII digested and sequence and orientation confirmed by sequencing with pWIZ compatible pUAST-s and pUAST-AS primers. Maxiprep DNA with Δ2,3 DNA was coinjected as described (Sullivan et al., 2000). Germline transformants possessing white$^+$ eyes were individually crossed to *w1118* to generate stocks (Sullivan et al., 2000). *UAS-flexin2-RNAi-2A* and *UAS-flexin2-RNAi-5* were the two transgenic line used in this study. Both lines behaved similarly and were used interchangeably.

Fly genetics :

Fly lines for *UAS-Notch-RNAi 7076, 7077* and *Df(1)N-264-105/Fm1,lz[+]*,were obtained from Bloomington. Other strains used were *MS1096-Gal4* and *heat-shock-Gal4* obtained

from Jean-Karim Heriche, *scabrous-Gal4* and *neuralized-Gal4* from Fabrice Roegiers in YN Jan lab (Gho et al., 1999) and *vestigial-Gal4* from Sean Sweeney. Crosses were done in a 25^{0}C incubator except where noted.

Larval temperature shifts were performed in a 29^{0}C incubator. Each day's collection of *da-Gal4;UAS-flexin2-RNAi* eggs were allowed to develop at 22^{0}C for 1, 2, 3, 4, or 5 days of larval development. At the end of each period at 22^{0}C, vials were moved to 29^{0}C for the remainder of development.

For the *heat-shock-Gal4* experiments, virgin *UAS-flexin2-RNAi-5* females were mated en mass to *heat-shock-Gal4* males. Embryos were collected at 25^{0}C for 1 hour, aged for 2 hours at 25^{0}C, then placed in a 29^{0}C incubator for 10 hours. Embryos were fixed and stained for the nervous system with anti-HRP-Cy3.

Wing margin phenotypes were scored as a loss of either margin tissue or margin bristles except for the genetic enhancement experiments in somatic mutant backgrounds denoted below.

Df(1)N-264-105/+;UAS-flexin2-RNAi-5/+ progeny were generated by crossing female *Df(1)N-264-105/Fm1,lz[+]* to *UAS-flexin2-RNAi-5* males at 29^{0}C and selecting against the Bar-marked balancer Fm1. Female progeny were analyzed for wing margin phenotypes. Controls for the *Df(1)N-264-105/+;UAS-flexin2-RNAi-5/+* cross were performed by crossing female *Df(1)N-264-105/Fm1,lz[+]* to *yw67* males and selecting for non-Bar eyed *Df(1)N-264-105/yw; +/+*females. For crosses using *Df(1)N-264-105/Fm1,lz[+]*, we did not score for posterior margin gapping which we define as occurring between L5 and the posterior wing hinge insertion site. Due to the wide

expressivity of the notch phenotype, the strongest enhancement was most clearly manifested in the distal tip of the wing blade encompassing L2 and L4.

References

Adler PN. Planar signaling and morphogenesis in Drosophila. Dev Cell. 2002 May;2(5):525-35. Review.

Ahmed A, Chandra S, Magarinos M, Vaessin H. Echinoid mutants exhibit neurogenic phenotypes and show synergistic interactions with the Notch signaling pathway. Development. 2003 Dec;130(25):6295-304.

Artavanis-Tsakonas S, Rand MD, Lake RJ. Notch signaling: cell fate control and signal integration in development. Science. 1999 Apr 30;284(5415):770-6. Review.

Axelrod JD, Matsuno K, Artavanis-Tsakonas S, Perrimon N. Interaction between Wingless and Notch signaling pathways mediated by dishevelled. Science. 1996 Mar 29;271(5257):1826-32.

Baonza A, Garcia-Bellido A. Notch signaling directly controls cell proliferation in the Drosophila wing disc. Proc Natl Acad Sci U S A. 2000 Mar 14;97(6):2609-14.

Beatus P, Lendahl U. Notch and neurogenesis. J Neurosci Res. 1998 Oct 15;54(2):125-36. Review.

Boulianne, G. L., de la Concha, A., Campos-Ortega, J. A., Jan, L. Y. and Jan, Y. N. (1991). The Drosophila neurogenic gene neuralized encodes a novel protein and is expressed in precursors of larval and adult neurons. *EMBO J.* 10, 2975-2983.

Bray S. Notch signalling in Drosophila: three ways to use a pathway. Semin Cell Dev Biol. 1998 Dec;9(6):591-7. Review.

Brennan CA, Moses K. Determination of Drosophila photoreceptors: timing is everything. Cell Mol Life Sci. 2000 Feb;57(2):195-214. Review.

Campos-Ortega JA. Genetic mechanisms of early neurogenesis in Drosophila melanogaster. Mol Neurobiol. 1995 Apr-Jun;10(2-3):75-89. Review.

Capdevila, J., and Guerrero, I. Targeted expression of the signaling molecule decapentaplegic induces pattern duplications and growth alterations in Drosophila wings. EMBO J. 1994 Oct 3;13(19):4459-68.

Castillejo-Lopez C, Arias WM, Baumgartner S. The fat-like gene of Drosophila is the true orthologue of vertebrate fat cadherins and is involved in the formation of tubular organs. J Biol Chem. 2004 Jun 4;279(23):24034-43. Epub 2004 Mar 26.

Chen H, Thiagalingam A, Chopra H, Borges MW, Feder JN, Nelkin BD, Baylin SB, Ball DW. Conservation of the Drosophila lateral inhibition pathway in human lung cancer: a hairy-related protein (HES-1) directly represses achaete-scute homolog-1 expression. Proc Natl Acad Sci U S A. 1997 May 13;94(10):5355-60.

Culi J, Martin-Blanco E, Modolell J. The EGF receptor and N signalling pathways act antagonistically in Drosophila mesothorax bristle patterning. Development. 2001 Jan;128(2):299-308.

Culi J, Modolell J. Proneural gene self-stimulation in neural precursors: an essential mechanism for sense organ development that is regulated by Notch signaling. Genes Dev. 1998 Jul 1;12(13):2036-47.

De Celis JF. Pattern formation in the Drosophila wing: The development of the veins. Bioessays. 2003 May;25(5):443-51. Review.

(a) De Celis JF, Bray S. Feed-back mechanisms affecting Notch activation at the dorsoventral boundary in the Drosophila wing. Development. 1997 Sep;124(17):3241-51.

(b) De Celis JF, Bray S, Garcia-Bellido A. Notch signalling regulates veinlet expression and establishes boundaries between veins and interveins in the Drosophila wing. Development. 1997 May;124(10):1919-28.

Egan SE, St-Pierre B, Leow CC. Notch receptors, partners and regulators: from conserved domains to powerful functions. Curr Top Microbiol Immunol. 1998;228:273-324. Review.

Enerly E, Larsson J, Lambertsson A. Reverse genetics in Drosophila: from sequence to phenotype using UAS-RNAi transgenic flies. Genesis. 2002 Sep-Oct;34(1-2):152-5.

Escudero LM, Wei SY, Chiu WH, Modolell J, Hsu JC. Echinoid synergizes with the Notch signaling pathway in Drosophila mesothorax bristle patterning. Development. 2003 Dec;130(25):6305-16.

Fisher A, Caudy M. The function of hairy-related bHLH repressor proteins in cell fate decisions. Bioessays. 1998 Apr;20(4):298-306. Review.

Gho M, Bellaiche Y, Schweisguth F. Revisiting the Drosophila microchaete lineage: a novel intrinsically asymmetric cell division generates a glial cell. Development. 1999 Aug;126(16):3573-84.

Giraldez AJ, Cohen SM. Wingless and Notch signaling provide cell survival cues and control cell proliferation during wing development. Development. 2003 Dec;130(26):6533-43.

Go MJ, Eastman DS, Artavanis-Tsakonas S. Cell proliferation control by Notch signaling in Drosophila development. Development. 1998 Jun;125(11):2031-40.

Gomez-Skarmeta JL, Campuzano S, Modolell J. Half a century of neural prepatterning: the story of a few bristles and many genes. Nat Rev Neurosci. 2003 Jul;4(7):587-98. Review.

Goto A, Blandin S, Royet J, Reichhart JM, Levashina EA. Silencing of Toll pathway components by direct injection of double-stranded RNA into Drosophila adult flies. Nucleic Acids Res. 2003 Nov 15;31(22):6619-23.

Greenwald I. LIN-12/Notch signaling: lessons from worms and flies. Genes Dev. 1998 Jun 15;12(12):1751-62. Review.

Guichard A, Srinivasan S, Zimm G, Bier E. A screen for dominant mutations applied to components in the Drosophila EGF-R pathway. Proc Natl Acad Sci U S A. 2002 Mar 19;99(6):3752-7.

Harper JA, Yuan JS, Tan JB, Visan I, Guidos CJ. Notch signaling in development and disease. Clin Genet. 2003 Dec;64(6):461-72. Review.

Hartenstein V, Posakony JW. A dual function of the Notch gene in Drosophila sensillum development. Dev Biol. 1990 Nov;142(1):13-30.

Helms W, Lee H, Ammerman M, Parks AL, Muskavitch MA, Yedvobnick B. Engineered truncations in the Drosophila mastermind protein disrupt Notch pathway function. Dev Biol. 1999 Nov 15;215(2):358-74.

Huang F, Dambly-Chaudiere C, Ghysen A. The emergence of sense organs in the wing disc of Drosophila. Development. 1991 Apr;111(4):1087-95.

Huppert SS, Jacobsen TL, Muskavitch MA. Feedback regulation is central to Delta-Notch signalling required for Drosophila wing vein morphogenesis. Development. 1997 Sep;124(17):3283-91.

Irvine KD, Rauskolb C. Boundaries in development: formation and function. Annu Rev Cell Dev Biol. 2001;17:189-214. Review.

Iso T, Kedes L, Hamamori Y. HES and HERP families: multiple effectors of the Notch signaling pathway. J Cell Physiol. 2003 Mar;194(3):237-55. Review.

Jaramillo AM, Zheng X, Zhou Y, Amado DA, Sheldon A, Sehgal A, Levitan IB. Pattern of distribution and cycling of SLOB, Slowpoke channel binding protein, in Drosophila. BMC Neurosci. 2004 Jan 27;5(1):3.

Justice N, Roegiers F, Jan LY, Jan YN. Lethal giant larvae acts together with numb in notch inhibition and cell fate specification in the Drosophila adult sensory organ precursor lineage. Curr Biol. 2003 Apr 29;13(9):778-83.

Justice NJ, Jan YN. Variations on the Notch pathway in neural development. Curr Opin Neurobiol. 2002 Feb;12(1):64-70. Review.

Johannes B, Preiss A. Wing vein formation in Drosophila melanogaster: hairless is involved in the cross-talk between Notch and EGF signaling pathways. Mech Dev. 2002 Jul;115(1-2):3-14.

Kiger A, Baum B, Jones S, Jones M, Coulson A, Echeverri C, Perrimon N. A functional genomic analysis of cell morphology using RNA interference. J Biol. 2003;2(4):27. Epub 2003 Oct 01.

Kitagawa M, Oyama T, Kawashima T, Yedvobnick B, Kumar A, Matsuno K, Harigaya K. A human protein with sequence similarity to Drosophila mastermind coordinates the nuclear form of notch and a CSL protein to build a transcriptional activator complex on target promoters. Mol Cell Biol. 2001 Jul;21(13):4337-46.

Klein T. Wing disc development in the fly: the early stages. Curr Opin Genet Dev. 2001 Aug;11(4):470-5. Review.

Koelzer S, Klein T. A Notch-independent function of Suppressor of Hairless during the development of the bristle sensory organ precursor cell of Drosophila. Development. 2003 May;130(9):1973-88.

Kunisch M, Haenlin M, Campos-Ortega JA. Lateral inhibition mediated by the Drosophila neurogenic gene delta is enhanced by proneural proteins. Proc Natl Acad Sci U S A. 1994 Oct 11;91(21):10139-43.

Lai EC. Notch signaling: control of cell communication and cell fate. Development. 2004 Mar;131(5):965-73. Review.

Lai EC, Rubin GM. neuralized functions cell-autonomously to regulate a subset of notch-dependent processes during adult Drosophila development. Dev Biol. 2001 Mar 1;231(1):217-33.

Lee T, Luo L. Mosaic analysis with a repressible cell marker for studies of gene function in neuronal morphogenesis. Neuron. 1999 Mar;22(3):451-61.

Lee YS, Carthew RW. Making a better RNAi vector for Drosophila: use of intron spacers. Methods. 2003 Aug; 30(4): 322-9.

Liebl EC, Rowe RG, Forsthoefel DJ, Stammler AL, Schmidt ER, Turski M, Seeger MA. Interactions between the secreted protein Amalgam, its transmembrane receptor

Neurotactin and the Abelson tyrosine kinase affect axon pathfinding. Development. 2003 Jul;130(14):3217-26.

Liu W, Seto J, Sibille E, Toth M. The RNA binding domain of Jerky consists of tandemly arranged helix-turn-helix/homeodomain-like motifs and binds specific sets of mRNAs. Mol Cell Biol. 2003 Jun;23(12):4083-93.

Lu B, Jan L, Jan YN. Control of cell divisions in the nervous system: symmetry and asymmetry. Annu Rev Neurosci. 2000;23:531-56. Review.

Lum L, Yao S, Mozer B, Rovescalli A, Von Kessler D, Nirenberg M, Beachy PA. Identification of Hedgehog pathway components by RNAi in Drosophila cultured cells. Science. 2003 Mar 28;299(5615):2039-45.

Majumdar A, Nagaraj R, Banerjee U. strawberry notch encodes a conserved nuclear protein that functions downstream of Notch and regulates gene expression along the developing wing margin of Drosophila. Genes Dev. 1997 May 15;11(10):1341-53.

Martin-Blanco E, Roch F, Noll E, Baonza A, Duffy JB, Perrimon N. A temporal switch in DER signaling controls the specification and differentiation of veins and interveins in the Drosophila wing. Development. 1999 Dec;126(24):5739-47.

Mlodzik M, Baker NE, Rubin GM. Isolation and expression of scabrous, a gene regulating neurogenesis in Drosophila. Genes Dev. 1990 Nov;4(11):1848-61.

Moore T, Hecquet S, McLellann A, Ville D, Grid D, Picard F, Moulard B, Asherson P, Makoff AJ, McCormick D, Nashef L, Froguel P, Arzimanoglou A, LeGuern E, Bailleul B. Polymorphism analysis of JRK/JH8, the human homologue of mouse jerky, and description of a rare mutation in a case of CAE evolving to JME. Epilepsy Res. 2001 Aug;46(2):157-67.

Morita R, Miyazaki E, Fong CY, Chen XN, Korenberg JR, Delgado-Escueta AV, Yamakawa K. JH8, a gene highly homologous to the mouse jerky gene, maps to the region for childhood absence epilepsy on 8q24. Biochem Biophys Res Commun. 1998 Jul 20;248(2):307-14. Erratum in: Biochem Biophys Res Commun 1998 Sep 18;250(2):536.

Neumann CJ, Cohen SM. A hierarchy of cross-regulation involving Notch, wingless, vestigial and cut organizes the dorsal/ventral axis of the Drosophila wing. Development. 1996 Nov;122(11):3477-85.

Nolo R, Abbott LA, Bellen HJ. Senseless, a Zn finger transcription factor, is necessary and sufficient for sensory organ development in Drosophila. Cell. 2000 Aug 4;102(3):349-62.

Okajima T, Irvine KD. Regulation of notch signaling by o-linked fucose. Cell. 2002 Dec 13;111(6):893-904.

Panin VM, Irvine KD. Modulators of Notch signaling. Semin Cell Dev Biol. 1998 Dec;9(6):609-17. Review.

Pickup AT, Lamka ML, Sun Q, Yip ML, Lipshitz HD. Control of photoreceptor cell morphology, planar polarity and epithelial integrity during Drosophila eye development. Development. 2002 May;129(9):2247-58.

Pluta AF, Saitoh N, Goldberg I, Earnshaw WC. Identification of a subdomain of CENP-B that is necessary and sufficient for localization to the human centromere. J Cell Biol. 1992 Mar;116(5):1081-93.

Ponting CP, Mott R, Bork P, Copley RR. Novel protein domains and repeats in Drosophila melanogaster: insights into structure, function, and evolution. Genome Res. 2001 Dec;11(12):1996-2008.

Portin P. General outlines of the molecular genetics of the Notch signalling pathway in Drosophila melanogaster: a review. Hereditas. 2002;136(2):89-96. Review.

Presente A, Shaw S, Nye JS, Andres AJ. Transgene-mediated RNA interference defines a novel role for notch in chemosensory startle behavior. Genesis. 2002 Sep-Oct;34(1-2):165-9.

Quinn L, Coombe M, Mills K, Daish T, Colussi P, Kumar S, Richardson H. Buffy, a Drosophila Bcl-2 protein, has anti-apoptotic and cell cycle inhibitory functions. EMBO J. 2003 Jul 15;22(14):3568-79.

Rayburn LY, Gooding HC, Choksi SP, Maloney D, Kidd AR 3rd, Siekhaus DE, Bender M. amontillado, the Drosophila homolog of the prohormone processing protease PC2, is required during embryogenesis and early larval development. Genetics. 2003 Jan;163(1):227-37.

Reichhart JM, Ligoxygakis P, Naitza S, Woerfel G, Imler JL, Gubb D. Splice-activated *UAS* hairpin vector gives complete RNAi knockout of single or double target transcripts in *drosophila melanogaster* Genesis. 2002 Sep-Oct; 34(1-2): 160-4.

Robey E. Notch in vertebrates. Curr Opin Genet Dev. 1997 Aug;7(4):551-7. Review.

Roegiers F, Younger-Shepherd S, Jan LY, Jan YN. Two types of asymmetric divisions in the Drosophila sensory organ precursor cell lineage. Nat Cell Biol. 2001 Jan;3(1):58-67.

Roos J, Hummel T, Ng N, Klambt C, Davis GW. Drosophila Futsch regulates synaptic microtubule organization and is necessary for synaptic growth. Neuron. 2000 May;26(2):371-82.

(a) Roussigne M., Cayrol C, Clouaire T, Amalric F, Girard JP. THAP1 is a nuclear proapoptotic factor that links prostate-apoptosis-response-4 (Par-4) to PML nuclear bodies. Oncogene (2003) 22, 2432-2442.

(b) Roussigne M, Kossida S, Lavigne AC, Clouaire T, Ecochard V, Glories A, Amalric F, Girard JP. The THAP domain: a novel protein motif with similarity to the DNA-binding domain of P element transposase. Trends Biochem Sci. 2003 Feb;28(2):66-9.

Rulifson EJ, Blair SS. Notch regulates wingless expression and is not required for reception of the paracrine wingless signal during wing margin neurogenesis in Drosophila. Development. 1995 Sep;121(9):2813-24.

Schuster CM, Davis GW, Fetter RD, Goodman CS. Genetic dissection of structural and functional components of synaptic plasticity. I. Fasciclin II controls synaptic stabilization and growth. Neuron. 1996 Oct;17(4):641-54.

Seugnet L, Simpson P, Haenlin M. Transcriptional regulation of Notch and Delta: requirement for neuroblast segregation in Drosophila. Development. 1997 May;124(10):2015-25.

Si K, Lindquist S, Kandel ER. A neuronal isoform of the aplysia CPEB has prion-like properties. Cell. 2003 Dec 26;115(7):879-91.

Smit, A.F. and Riggs, A.D. (1996) Tiggers and DNA transposon fossils in the human genome. PNAS USA, 93, 1443-1448.

Sullivan W, Ashburner M, Hawley RS. Drosophila protocols. Cold Spring Harbor Laboratory Press (2000).

Sweeney ST, Davis GW. Unrestricted synaptic growth in spinster-a late endosomal protein implicated in TGF-beta-mediated synaptic growth regulation. Neuron. 2002 Oct 24;36(3):403-16.

Tissot M, Stocker RF. Metamorphosis in Drosophila and other insects: the fate of neurons throughout the stages. Prog Neurobiol. 2000 Sep;62(1):89-111. Review.

Toth M, Grimsby J, Buzsaki G, Donovan GP. Epileptic seizures caused by inactivation of a novel gene, jerky, related to centromere binding protein-B in transgenic mice. Nat Genet. 1995 Sep;11(1):71-5. Erratum in: Nat Genet 1996 Jan;12(1):110.

Tsuda L, Nagaraj R, Zipursky SL, Banerjee U. An EGFR/Ebi/Sno pathway promotes delta expression by inactivating Su(H)/SMRTER repression during inductive notch signaling. Cell. 2002 Sep 6;110(5):625-37.

Urbach R, Technau GM. Neuroblast formation and patterning during early brain development in Drosophila. Bioessays. 2004 Jul;26(7):739-51.

Usui K, Kimura KI. Sequential emergence of the evenly spaced microchaetes on the notum of Drosophila. Roux's Archives of Developmental Biology. 1993: (20):151-158.

Weng AP, Aster JC. Multiple niches for Notch in cancer: context is everything. Curr Opin Genet Dev. 2004 Feb;14(1):48-54. Review.

Withee J, Galligan B, Hawkins N, Garriga G. Caenorhabditis elegans WASP and Ena/VASP Proteins Play Compensatory Roles in Morphogenesis and Neuronal Cell Migration. Genetics. 2004 Jul;167(3):1165-76.

Verzi MP, Anderson JP, Dodou E, Kelly KK, Greene SB, North BJ, Cripps RM, Black BL. N-twist, an evolutionarily conserved bHLH protein expressed in the developing CNS, functions as a transcriptional inhibitor. Dev Biol. 2002 Sep 1;249(1):174-90.

Voas MG, Rebay I. Signal integration during development: insights from the Drosophila eye. Dev Dyn. 2004 Jan;229(1):162-75. Review.

APPENDIX I

Drosophila Futsch Regulates Synaptic Microtubule Organization and is Necessary for Synaptic Growth

Neuron, Vol. 26, 371–382, May, 2000, Copyright ©2000 by Cell Press

Drosophila Futsch Regulates Synaptic Microtubule Organization and Is Necessary for Synaptic Growth

Jack Roos,* Thomas Hummel,† Norman Ng,* Christian Klämbt,† and Graeme W. Davis*‡
*Dept. Biochemistry and Biophysics
Programs in Cell Biology and Neuroscience
University of California, San Francisco
San Francisco, California 94143
†Institut fuer Neurobiologie
Universitaet Muenster
Badestrasse 9
D-48149 Muenster
Germany

Summary

We present evidence that Futsch, a novel protein with MAP1B homology, controls synaptic growth at the *Drosophila* neuromuscular junction through the regulation of the synaptic microtubule cytoskeleton. Futsch colocalizes with microtubules and identifies cytoskeletal loops that traverse the lateral margin of select synaptic boutons. An apparent rearrangement of microtubule loop architecture occurs during bouton division, and a genetic analysis indicates that Futsch is necessary for this process. *futsch* mutations disrupt synaptic microtubule organization, reduce bouton number, and increase bouton size. These deficits can be partially rescued by neuronal overexpression of a *futsch* MAP1B homology domain. Finally, genetic manipulations that increase nerve-terminal branching correlate with increased synaptic microtubule loop formation, and both processes require normal Futsch function. These data suggest a common microtubule-based growth mechanism at the synapse and growth cone.

Introduction

The precise modification of nerve-terminal morphology is essential for the correct wiring and plasticity of neuronal circuitry. One mechanism for the addition of new synapses to a nerve terminal involves the sprouting of new synaptic boutons (Casadio et al., 1999; Engert and Bonhoeffer, 1999). Recently, at the *Drosophila* neuromuscular junction (NMJ), it has been suggested that one mechanism for nerve-terminal sprouting involves the division of preexisting synaptic boutons (Zito et al., 1999). These results further suggest that division of a synaptic bouton into thirds (or greater subdivisions) may be a mechanism for generating a branchpoint in the nerve terminal (Zito et al., 1999). Recent evidence suggests that in the hippocampus, synaptic morphological change is associated with the consolidation of long-term synaptic plasticity (Engert and Bonhoeffer, 1999; Toni et al., 1999). In particular, the sprouting of new postsynaptic spines that contact preexisting presynaptic boutons may be a mechanism for generating new synaptic contacts (Engert and Bonhoeffer, 1999; Toni et al., 1999).

Nerve-terminal plasticity achieved through processes such as nerve-terminal sprouting will require precisely controlled and spatially regulated modifications to the nerve-terminal cytoskeleton. The cytoskeletal rearrangements that drive bouton division and the signaling events that control this process are not known. In principle, localized remodeling of the cytoskeleton could achieve the spatial precision required for synapse-specific, activity-dependent plasticity (Grant et al., 1995; Halpain et al., 1998; Rohatgi et al., 1999; Wills et al., 1999a, 1999b). Specificity could be further refined if only a small subset of synapses, at any given time, has the capacity for cytoskeletal rearrangement.

The regulation of the neuronal cytoskeletal at the growth cone has been studied extensively (Tanaka and Sabry, 1995; Luo et al., 1997; Suter and Forscher, 1998; Gallo and Letourneau, 1999; Wills et al., 1999a, 1999b). Recently, it has been demonstrated that the regulation of microtubule organization within the growth cone may be an important determinant of growth cone motility. The macroscopic organization of microtubules within the growth cone is dynamic as revealed by the formation and destruction of hairpin loop structures that incorporate a large portion of the growth cone microtubules (Tanaka et al., 1991; Dent et al., 1999). Of particular interest is the demonstration that the formation of microtubule hairpin loops is correlated with the cessation of growth cone motility and the opening (or destruction) of these loops is correlated with the reestablishment of motility (Dent et al., 1999). These data are strengthened by the observation that the transition of a motile growth cone to a stable synaptic contact is also correlated with the formation of a hairpin microtubule loop within the growth cone as it transforms into a synapse (Tsui et al., 1984). Thus, regulated microtubule architecture appears to be an essential element in the control of growth cone morphology and motility as well as synapse formation. The molecular regulation of these microtubule based structures, however, is not known.

In the present study, we implicate a novel protein, Futsch, in the regulation of the synaptic microtubule cytoskeleton and provide genetic evidence that Futsch is necessary for synaptic growth. Hummel et al. (2000 [this issue of *Neuron*]) have identified Futsch as a novel *Drosophila* cytoskeletal-associated protein of 5327 amino acids that has homology with vertebrate MAP1B at the N and C termini. Futsch is associated with the dendritic, axonal, and nerve-terminal cytoskeleton. Futsch is shown to associate with microtubules in vitro, and a genetic analysis demonstrates that Futsch is necessary for axonal and dendritic growth. Here we demonstrate that Futsch colocalizes with microtubules and is necessary for the organization of synaptic microtubule cytoskeleton. We further demonstrate that Futsch is necessary for normal synaptic growth, implicating the synaptic microtubule cytoskeleton in this process.

Of particular interest, we identify microtubule hairpin loops within a small subset of synaptic boutons at the

‡To whom correspondence should be addressed (e-mail: gdavis@biochem.ucsf.edu).

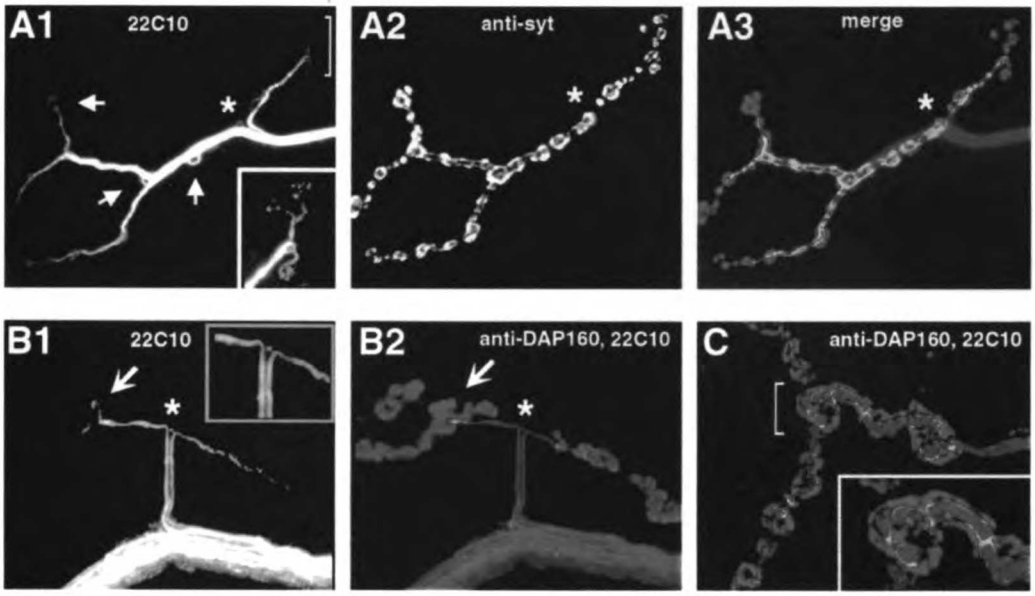

Figure 1. Loops of Futsch Immunoreactivity Are Observed within a Subset of Synaptic Boutons at Muscle 4

(A1) mAb 22C10 (anti-Futsch) reveals a core cytoskeleton within the axon that is continuous with the nerve terminal. Two type 1b axons innervate muscle 4 and arborize in opposite directions from the site of muscle contact (asterisk). Cytoskeletal loops identified by Futsch immunoreactivity (22C10) are observed at a subset of boutons (arrows) and are always observed at end-terminal boutons (see inset).

(A2) Antisynaptotagmin staining and the merged image (A3) show the position of Futsch loops within the terminal.

(B1) The two nerves innervating muscle 4 are stabilized on the muscle (inset) and extend on the muscle surface before boutons are elaborated.

(B2) Loops are only observed within synaptic boutons (arrow).

(C) mAb 22C10 (green) is localized close to but below the plasma membrane as defined by antibody staining for dynamin-associated protein (DAP160, red). The immunofluorescent image shown was deconvolved using Delta-Vision algorithms to eliminate out-of-plane fluorescent scatter.

Drosophila neuromuscular synapse. Synaptic microtubule loops are subsynaptic specializations that identify unique boutons within the *Drosophila* neuromuscular synapse. We provide evidence that synaptic microtubule loops are stabilized by Futsch. We provide further evidence that loops are associated with stable synaptic boutons, while the dispersion or destruction of these loops is associated with boutons undergoing division or sprouting. These synaptic microtubule loops are highly reminiscent of microtubule loops present within the growth cone, implying a fundamental similarity between the mechanisms of growth cone motility and the mechanisms of synaptic growth and branching.

Results

Futsch Identifies Unique Cytoskeletal Structures at Select Synaptic Boutons

At the *Drosophila* NMJ, Futsch protein is associated with a cytoskeletal core within the synaptic terminal that is continuous with the axonal cytoskeleton. This cytoskeletal core is composed of multiple fibers, consistent with Futsch binding the microtubule cytoskeleton of the axon and nerve terminal (Figures 1A and 1B). Futsch is localized close to but below the nerve-terminal plasma membrane. Synaptic terminals double stained for Futsch and the synaptic plasma membrane protein DAP160 (dynamin-associated protein 160; Roos and Kelly, 1999) do not show overlapping staining. Rather, Futsch is a discrete core of staining just inside the plasma membrane as defined by DAP160 (Figure 1C). Further evidence that Futsch colocalizes with microtubules is presented below.

Examination of Futsch staining at the nerve terminal using deconvolution confocal microscopy reveals periodic loop structures within a subset of synaptic boutons (loops are present within 24% ± 3% of boutons at the wild-type synapse on muscles 6 and 7 and 22% ± 3% of boutons at muscle 4; Figures 1A and 1B, arrows). These loops appear at stereotypic locations within the synapse at every abdominal muscle, though for the purpose of visualization, we have focused our analysis on muscle 4. Futsch-positive loops are present within all types of synaptic boutons, including type 1b, type 1s, and type II (see Keshishian et al., 1996 for bouton-type definition). We have restricted our analysis to type 1b boutons.

Synaptic microtubule loops are highly enriched at points of nerve-terminal branching (~90% of observed branchpoints include a loop), and loops are always present within the terminal bouton(s) at the end of each chain of synaptic boutons (Figure 1A, arrows and inset). The

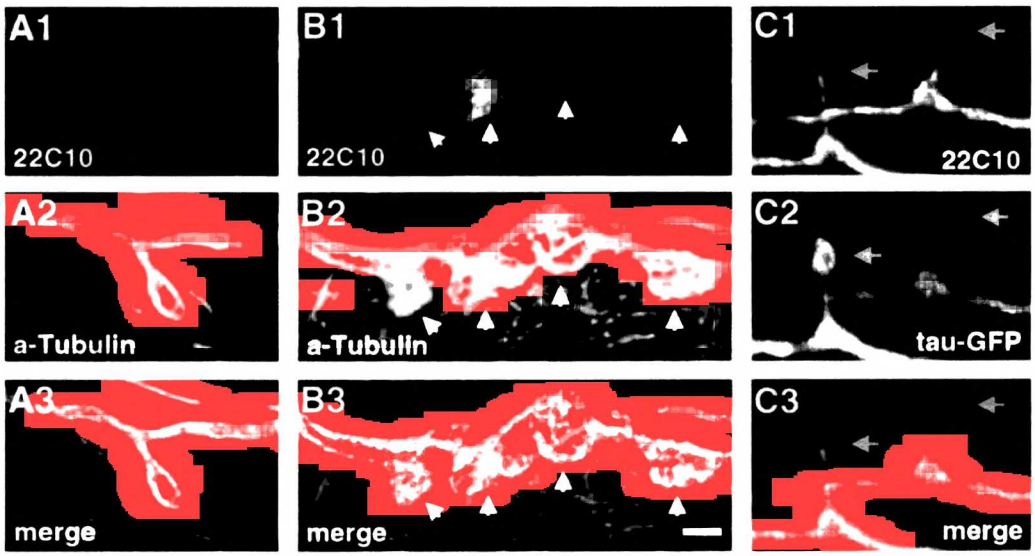

Figure 3. Futsch Colocalizes with Microtubules

(A) Colocalization of anti-Futsch (22C10; A1, green) and anti-α-tubulin (A2, red) at a synaptic terminal. In the merged image (A3, merge), note that muscle microtubules do not show 22C10 immunoreactivity, demonstrating the specificity of antibody staining.

(B) Colocalization of anti-Futsch (22C10; B1, green) and α-tubulin (red) persist in the *futsch*^{N94} hypomorphic mutant synapse despite the disorganization of the synaptic microtubule cytoskeleton. An arrowhead indicates each synaptic bouton.

(C) A synaptic terminal is shown that has been stained for anti-Futsch (22C10; C1) and that also contains overexpressed tau-GFP (*UAS-tau-GFP; elaV-GAL4* larval genotype; C2). These two proteins colocalize (merge) within synaptic loop structures (arrows) at the synapse (tau-GFP is green). Every synaptic cytoskeletal loop that was observed showed colocalization of anti-Futsch and tau-GFP.

Futsch Is Necessary for Microtubule Organization and Synaptic Growth

Two homozygous viable mutations in *futsch* were identified by Hummel et al. (2000). Both mutations alter synaptic growth (Figure 4). There is no detectable Futsch immunoreactivity in the *futsch*^{K68} mutation. *futsch*^{N94} is a hypomorphic mutation that reduces protein expression to ~20% wild-type levels (based on reduced fluorescence intensity). The *futsch*^{N94} mutation also disrupts the subcellular localization of Futsch. In *futsch*^{N94}, Futsch immunoreactivity fills up the volume of every synaptic bouton rather than being restricted to a cytoskeletal core (Figure 4C). Microtubule localization is also disrupted in these *futsch* mutations. In both *futsch*^{N94} and *futsch*^{K68}, synaptic microtubules no longer form a filamentous cytoskeletal shaft that runs through the nerve terminal, and microtubule loop formation is absent (Figure 4F and 4G). Rather, tubulin staining in these mutants is punctate and diffuse, filling up the volume of every synaptic bouton within the NMJ (Figures 4F and 4G). The diffuse, punctate tubulin staining in these mutants is identical to the diffuse anti-Futsch (22C10) staining observed in *futsch*^{N94} (Figure 4; compare [C] with [F] and [G]). Double staining for Futsch and α-tubulin demonstrates that colocalization persists even when the microtubules are dispersed in these mutations (Figure 3B). Finally, there is a qualitative disruption of both anti-Futsch and tubulin staining in *futsch*^{N94}/+ heterozygous larvae; microtubule loops are not as clearly defined at the lateral margin of select synaptic boutons (data not shown). Taken together, these data demonstrate that *futsch* is necessary for microtubule organization within synaptic boutons. These data also support the conclusion that *futsch* is necessary for the formation or stabilization of microtubule-based loop structures.

Synaptic morphology is severely altered in viable *futsch* mutant backgrounds, indicating that Futsch-dependent microtubule organization is necessary for normal synaptic growth and development (Figure 4). In *futsch*^{N94} and *futsch*^{K68}, there is a reduction in bouton number and an increase in bouton size (Figures 4B and 4C). Bouton number is reduced from an average of 64.8 (±4.1) boutons at muscle 4 in wild type to 37.9 (±3.5) in *futsch*^{N94} and 40.8 (±3.2) in *futsch*^{K68} ($p < 0.001$). We do not observe a change in muscle size in these mutations. There is also a modest but statistically significant reduction in bouton number in *futsch*^{N94}/+ heterozygous larvae (51.2 ± 3.3 boutons at muscle 4; $p < 0.01$). This correlates with a qualitative disruption in microtubule organization at the NMJ in these heterozygous larvae (described above). In parallel with the observed decrease in bouton number, we observed that the average bouton size and the distribution of bouton sizes within the synapse are dramatically increased in both *futsch* alleles (Figure 4H; see legend for average bouton sizes). Mutant nerve-terminals at muscle 4 rarely have branchpoints. However, this may be a consequence of the drastic reduction in bouton number.

Genetic rescue experiments demonstrate that *futsch*

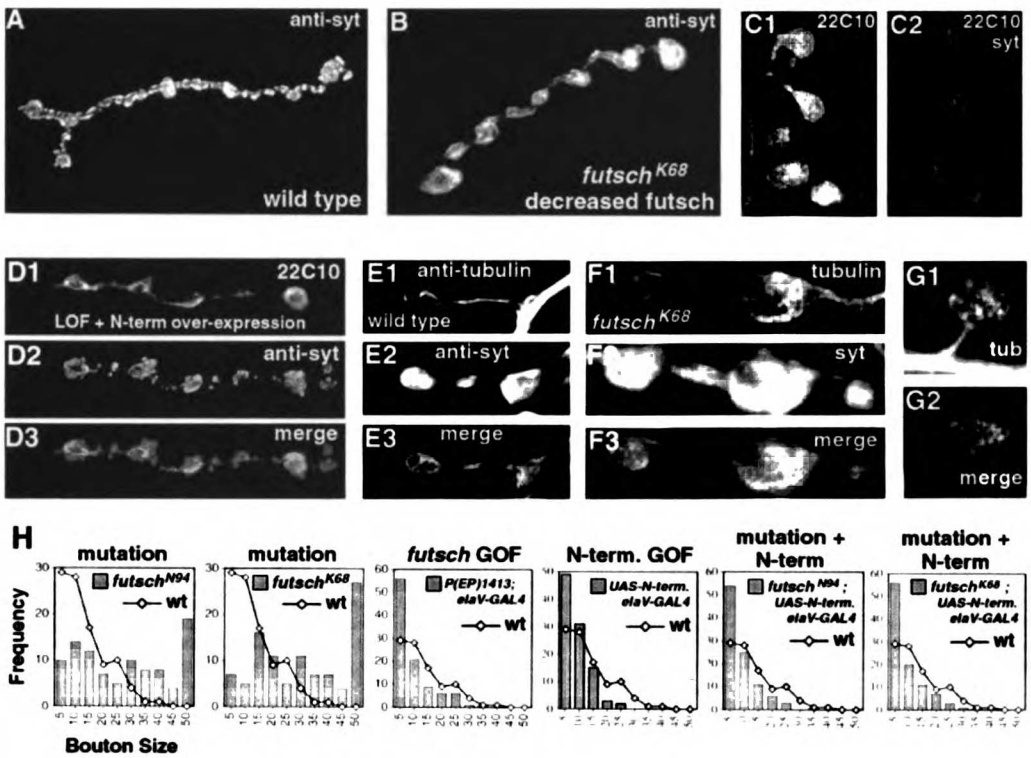

Figure 4. Futsch Is Necessary for Normal Synaptic Growth and Development

(A) The wild-type synapse at muscle 4 is shown stained with antisynaptotagmin.

(B) The synapse on muscle 4 is shown in the *futsch*^{K68} mutation that eliminates *futsch* protein as detected by mAb 22C10 immunoreactivity. Synaptic boutons are fewer and larger.

(C) Select synaptic boutons are shown at muscle 4 in the *futsch*^{N94} mutation that significantly reduces mAb 22C10 staining (C1; exposure time is ~20× longer for these images compared to all other mAb 22C10 images presented in the manuscript). The mAb 22C10 staining is mislocalized in *futsch*^{N94}, being distributed throughout every bouton (C2; merged image of anti-Futsch in green with antisynaptotagmin in red to delineate the synaptic bouton).

(D) Image of the synapse at muscle 4 in *futsch*^{N94} with overexpression of N-terminal Futsch (LOF + N-term overexpression) in all neurons (driven by *elaV-GAL4*). Anti-DAP160 is shown in red, anti-Futsch in green.

(E) Anti-α-tubulin identifies microtubule loops within synaptic boutons of a wild-type terminal. An end-terminal loop is revealed at the end of a chain of synaptic boutons.

(F and G) Tubulin staining is mislocalized in the *futsch*^{K68} mutation (F) and *futsch*^{N94} (G), appearing punctate and diffusing to fill the volume of every synaptic bouton.

(H) Quantification of bouton size is shown based on measurement of the longest bouton dimension multiplied by the perpendicular planar axis. A line indicating the wild-type size distribution is superimposed on each graph. Shown are bouton sizes measured at synapses in the *futsch* homozygous-viable mutants *futsch*^{K68} and *futsch*^{N94} (mutation) at synapses overexpressing full-length Futsch in all nerves (*futsch* GOF; ep(X)1419; *elaV-GAL4*) and at mutant synapses that also overexpress the *futsch* N-terminal microtubule binding domain (mutant + N-term). Bouton sizes with areas larger than 50 μm^2 are grouped in a single bin. Average bouton sizes for each genotype are as follows: wild type = 9.1 μm^2, *futsch*^{N94} = 22.2 μm^2, *futsch*^{K68} = 26.8 μm^2, P(EP)1419/*elaV-GAL4* = 7.1 μm^2, *UAS-Nterm/elaV-GAL4* = 6.4 μm^2, *futsch*^{N94}*; UAS-Nterm/elaV-GAL4* = 6.4 μm^2, *futsch*^{K68}*; UAS-Nterm/elaV-GAL4* = 6.8 μm^2.

(A)–(D) are the same magnification. (E)–(G) are each at the same magnification (~2× magnification compared to that shown for [A]–[D]).

loss-of-function is responsible for the observed disruption in microtubule organization and is responsible for the observed deficits in synaptic growth and development. We are able to achieve a partial rescue of the *futsch* mutant phenotype by overexpression of the N-terminal, predicted microtubule-binding domain of Futsch (Hummel et al., 2000). At present, a full-length cDNA is not available for the large 5327 amino acid transcript. Overexpression of the *UAS-Nterminal-Futsch* construct in the *futsch*^{N94} and *futsch*^{K68} mutant backgrounds reverted the mutant phenotype to nearly wild type (Figure 4D). Bouton numbers were increased from an average of 37.9 (±3.5) in *futsch*^{N94} to an average of 51.4 (±3.6) in *futsch*^{N94} larvae that also overexpress the N-terminal construct neuronally (*futsch*^{N94}*; UASN-term/+; elaV-GAL4*). In *futsch*^{K68}, bouton number was increased from 40.9 (±3.2) to 52.3 (±2.9) by the N-terminal rescue ($p < 0.01$). Thus, average bouton numbers are partially

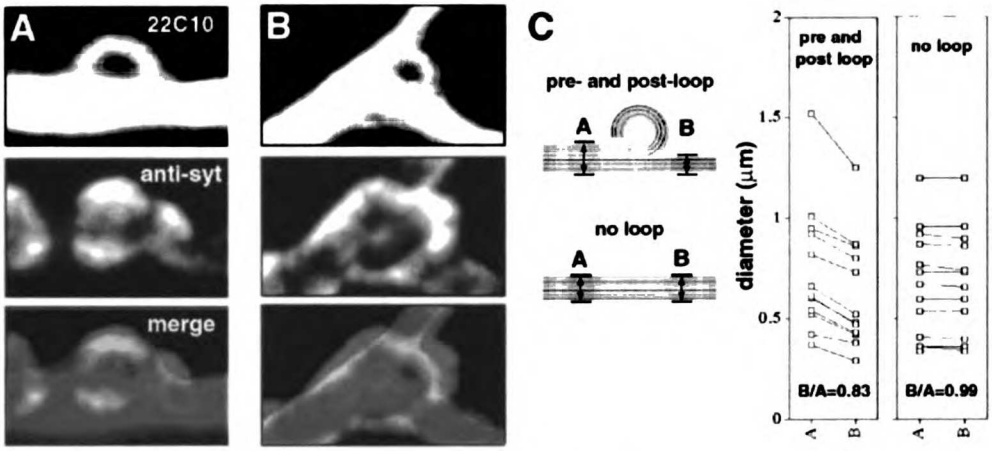

Figure 5. Microtubules within a Loop Do Not Rejoin the Major Nerve-Terminal Cytoskeletal Shaft

(A) High magnification view of an individual synaptic loop showing both mAb 22C10 and antisynaptotagmin (anti-syt) and the merged image (22C10 in green and synaptotagmin in red).

(B) Staining identical to that shown in (A), showing a loop present at a nerve-terminal branchpoint.

(C) Measurements of the diameter of mAb 22C10 staining in the nerve-terminal shaft were taken 0.5 μm before (A) and 0.5 μm after (B) loops at various positions within the NMJ (pre- and post-loop). Alternatively, measurements were taken at two sites (A and B) separated by 4 μm (larger than the average loop diameter) at various positions along the NMJ without an interposed loop (no loop). The diameter of the 22C10-positive cytoskeletal shaft is consistently and significantly reduced following a Futsch-positive loop (pre- and post-loop) compared to the normal attenuation of the cytoskeleton without an interposed loop (no loop). The calculated ratio of measurements taken from site A and site B are shown at the bottom of the graph.

rescued by N-terminal overexpression [wild-type bouton number = 64.8 (±4/1)], although there remain statistically fewer boutons in the rescues compared to wild type ($p < 0.01$).

The abnormally large average bouton size observed in the *futsch* mutants is also rescued by overexpression of the N terminus in the mutant backgrounds (Figure 4H; mutant + N-term). As a control, we demonstrate that neuronal overexpression (in a wild-type background) of either full-length Futsch or the N-terminal MAP1B homology domain of Futsch do not alter bouton number and do not affect the organization of synaptic microtubules (bouton numbers: full-length overexpression in wild-type background = 69.8 ± 3.2 and N-terminal overexpression in a wild-type background = 71.3 ± 3.0). There is, however, a slight reduction in average bouton size due to Futsch overexpression (Figure 4H; see also legend). We were able to drive overexpression of full-length Futsch in these experiments (despite not having a full-length cDNA) by taking advantage of a P(UAS) transposable element present in the 5′ regulatory region of *futsch* that can initiate *futsch* overexpression in the presence of a tissue-specific source of GAL4 (see Hummel et al., 2000). Thus, the N-terminal, predicted microtubule-binding domain of *futsch* is sufficient to partially rescue bouton number and bouton size in the *futsch* mutant backgrounds.

In addition to rescuing bouton number and bouton size, overexpression of the N-terminal domain of Futsch in the *futsch* mutant background partially rescues the organization and localization of microtubules within the mutant nerve terminal. Microtubules, while still having a punctate appearance, now localize to the periphery of the bouton rather than uniformly filling the volume of the bouton (ascertained with both 22C10 and antitubulin staining; compare Figure 4D1 with 4C1, 4G1, and 3A). We conclude that *futsch* is necessary for microtubule organization at the nerve terminal and that the N-terminal predicted MAP1B homology domain participates in this process. Furthermore, these data suggest that the correct organization of microtubules within the nerve terminal is necessary for the normal growth of synaptic boutons and for the normal addition of synaptic boutons to the synapse during development.

Microtubule Loops Persist throughout Development

A remarkable feature of microtubule organization at the nerve terminal is the formation of loop structures within select synaptic boutons. A small number of microtubule loops appear periodically along the nerve terminal. We observe that these intraterminal loops are closer together the further out they are along a chain of boutons. The average interloop distance in the proximal half of the nerve terminal (closer to the site of innervation) is 12.1 μm, and this decreases to 4.4 μm in the distal half of the nerve terminal. In addition, examination of microtubule loops at the second instar synapse (~2 days earlier in development) reveals that loops are on average closer together and that the loops are composed of a narrower gauge filament of Futsch (data not shown). This is consistent with loops forming during synaptic growth and then becoming stabilized structures within the nerve terminal. As the nerve terminal grows, more cytoskeleton is predicted to be added to

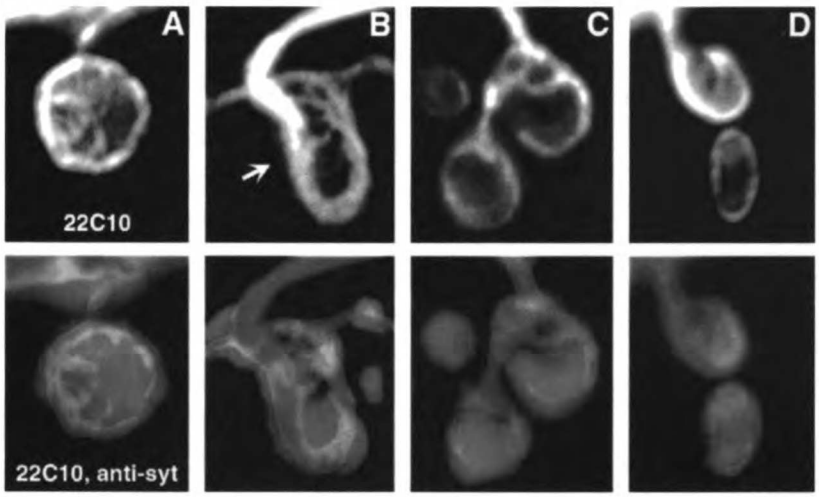

Figure 6. Predicted Progress of Synaptic Bouton Division

A series of different synaptic boutons (A–D) predicted to be at progressive stages of bouton division are shown from left to right. Each bouton is double stained for mAb 22C10 (top panel) and antisynaptotagmin (bottom panel showing the merged image with 22C10 in green and synaptotagmin in red). An arrow in (B) shows the predicted site of bouton cleavage during division and indicates the strands of Futsch-positive cytoskeleton that extend across the bouton at this point.

the synapse, and the gauge within the loops will be increased. In addition, boutons that are formed early in development will be separated by larger distances due to the expansion of the synapse with the growth of the muscle (Zito et al., 1999). Thus, loops formed early in development will be present in the proximal half of the NMJ and are predicted to be separated by larger distances, as observed.

Microtubules within Loops Do Not Rejoin the Major Cytoskeletal Core

An analysis of loop morphology demonstrates that microtubules within a loop do not rejoin the major cytoskeletal strand within the nerve terminal (Figure 5). We measured the diameter of the Futsch immunoreactivity 0.5 μm before and 0.5 μm after loop structures. We compared these measurements with diameters taken at two points separated by 4 μm (larger than the average diameter of a loop) at various positions along the nerve terminal without an interposed loop. Diameter measurements were taken after deconvolution of the nerve-terminal staining to reduce error associated with out-of-plane fluorescence scatter. The diameter of the main shaft of Futsch immunoreactivity is significantly reduced at the distal side of a loop compared to the proximal side (Figure 5C), whereas there is no change in the diameter of Futsch immunoreactivity over a similar distance of nerve terminal without an interposed loop. One essential role for Futsch as a microtubule-associated protein (MAP) could be to stabilize the microtubules at the free end of such a loop. The disruption of microtubule organization and loop formation in the *futsch* mutations supports this hypothesis.

Synaptic Microtubule Loops Identify Sites of Bouton Division

Live visualization of *Drosophila* neuromuscular synapses demonstrates that synaptic bouton division is a mechanism for bouton addition and branchpoint addition to the NMJ during development (Zito et al., 1999). This process is termed division as opposed to spouting because previously existing active zones are partitioned between newly formed boutons (Zito et al., 1999). Boutons that are predicted to be undergoing division can be identified by an irregular, hourglass-like shape (Zito et al., 1999). Examination of such bouton profiles demonstrates that these boutons not only contain microtubule loops, but these loops appear to be undergoing rearrangement (Figure 6). While dynamic rearrangement can only be proven by in vivo live observation, the irregular and highly variable branched microtubule structure is suggestive of an active process.

Examination of Futsch staining within numerous putative dividing boutons suggests a sequence for the process of bouton division (Figure 6). At the earliest stages of division, Futsch strands reach across the center of a loop within a bouton (Figure 6A). The strands of Futsch become more elaborate within boutons that have an hourglass-like shape, indicative of boutons that are midway through the process of division (Figure 6B). In many cases, strands of Futsch protein cross the middle of the dividing bouton precisely at the site where cleavage is predicted (Figure 6B, arrow). At the final stages of bouton division, two adjacent loops are produced in the neighboring newly divided boutons by the division of the original loop (Figures 6C and 6D). As the synapse grows, these new adjacent loops stabilize and later separate from one another as the synapse expands on the

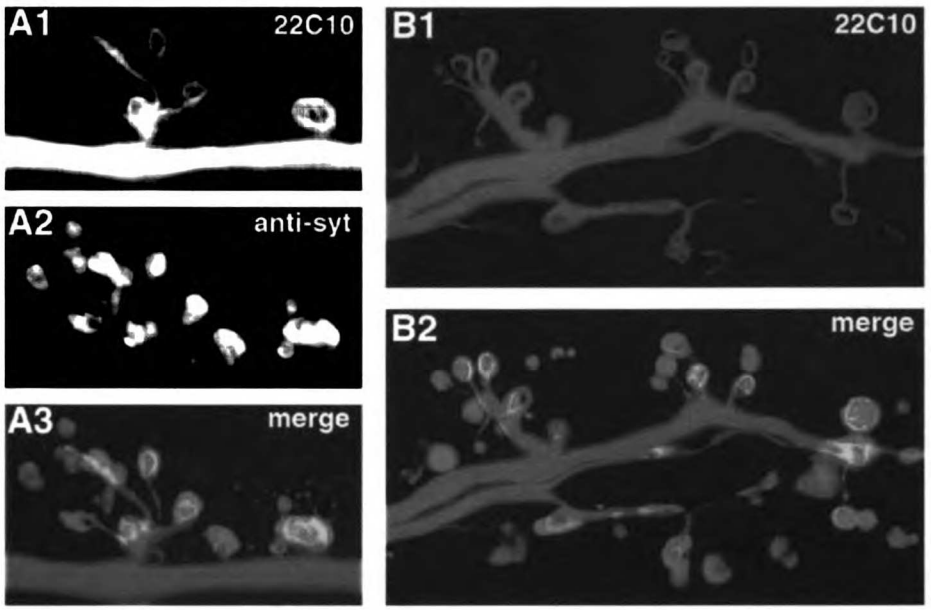

Figure 7. The Number of Presynaptic Futsch-Positive Loops Are Increased at Synapses Overexpressing *flexin* in All Muscle

(A) A synapse at muscles 6 and 7 double stained for mAb 22C10 (A1), antisynaptotagmin (A2), and the merged image showing the increase in loop number due to *flexin* overexpression.

(B) A synapse at muscles 6 and 7 showing a dramatic increase in Futsch loops due to postsynaptic *flexin* overexpression [(B1) mAb 22C10; (B2) merged image with antisynaptotagmin].

muscle surface, generating the stereotyped periodicity of loops within the synapse.

Interestingly, microtubule loops are always observed to lie in the same plane as the muscle fiber surface. If Futsch is involved in the process of bouton division, then the plane of the microtubule loop may also determine the plane of bouton division. This would prevent bouton division from occurring into the volume of the muscle fiber, which is never observed at the wild-type synapse.

Increased Synaptic Loop Formation Correlates with Increased Nerve-Terminal Branching

To support the conclusion that bouton division occurs at microtubule-based loops and is a mechanism of synaptic growth, we have taken advantage of a genetic background that increases the number of microtubule loops at the synapse. *flexin* is a novel *Drosophila* muscle protein (N. N. and G. W. D., unpublished data). Overexpression of *flexin* in muscle during postembryonic development causes a dramatic increase in nerve-terminal branching (Figure 7; N. N. and G. W. D., unpublished data). There is a two-fold increase in the occurrence of microtubule loops at *flexin* overexpressing synapses (Figure 7; 50% ± 4% of boutons contain a loop at *flexin* overexpressing synapses as compared to 22% ± 6% at wild-type synapses). This correlates with an approximate two-fold increase in nerve-terminal branch formation (N. N. and G. W. D., unpublished data). Thus, *flexin* appears to act as a muscle-derived signal to increase nerve-terminal branching. *flexin*-induced branching is correlated with increased organization of presynaptic microtubule loop structures.

Since Futsch is expected to act cell autonomously, elevated branching induced by *flexin* overexpression in muscle ought to be suppressed in a *futsch* mutant background. This was confirmed by the demonstration that muscle overexpression of *flexin* does not alter the *futsch*^{N94} mutant phenotype (overexpression of *flexin* being driven by the strong muscle promoter *24B-GAL4* [Davis et al., 1997]). There remains a reduction in bouton number (31.6 ± 4.1 boutons per synapse compared to wild type = 64.8 ± 4.1) and an increase in the average bouton size (26.6 μm^2 ± 6.6 compared to wild type = 9.3 μm^2) in *futsch*^{N94}*; flexin/24B-GAL4* larvae. Thus, normal *futsch* expression is necessary for the increased loop formation and increased branching observed when *flexin* is overexpressed in muscle.

Discussion

We have analyzed the role of a novel *Drosophila* gene, *futsch*, at the larval neuromuscular synapse. We demonstrate that *futsch* is necessary for the organization of microtubules within the nerve terminal. We further demonstrate that *futsch* is necessary for normal synaptic development, implicating a Futsch-dependent regulation of the microtubule cytoskeleton in this processes. Futsch may be particularly important for regulating the formation and stability of microtubule loops within synaptic boutons. Analysis of loop morphology and apparent loop dynamics suggests that rearrangement of these

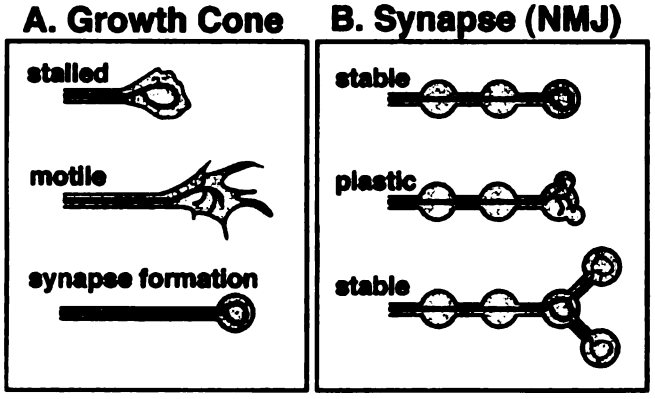

Figure 8. Microtubule Loop Specializations Implicate Common Growth Mechanisms at the Growth Cone and the End-Terminal Synaptic Bouton

(A) Regulated formation and disruption of microtubule loops correlates with growth cone motility (Dent et al., 1999). Microtubules within a stalled growth cone acquire a loop conformation. Resumed growth cone motility correlates with disruption of the loop conformation. Synapse formation, the transition of a motile growth cone to a stable synaptic contact, is once again correlated with the acquisition of a microtubule loop conformation within the newly formed synapse.

(B) At the developing *Drosophila* NMJ, the formation and reorganization of synaptic microtubule loops correlates with the division of select synaptic boutons. Bouton division (plastic) is correlated with the reorganization of microtubule loops. This bouton division is capable of branchpoint generation within the synapse. Microtubule loops are reestablished in the newly formed synaptic boutons.

microtubule-based loops is a critical component of the process of bouton division and for subsequent nerve-terminal growth and branching. We present a model in which Futsch participates in the regulation of synaptic growth by controlling the formation and rearrangement of microtubule-based loops that are present within a small subset of the synaptic boutons within each synapse (Figure 8). The presence of similar microtubule loops within growth cones, implicated in the process of growth cone motility, suggests a fundamental similarity between the mechanisms of synaptic growth and the mechanisms of growth cone dynamics.

A Model for Synaptic Growth Requiring Regulated Microtubule Loop Architecture

Our data indicate that the subsynaptic microtubule loops, identified by Futsch and tubulin immunoreactivity, are sites of bouton division within the neuromuscular synapse. Loops occur at stereotypic locations that are, or once were, sites of active bouton division including branchpoints and terminal boutons (Zito et al., 1999). In addition, examination of numerous putative dividing bouton profiles supports the conclusion that there is a progressive alteration in the microtubule-based loop architecture that is involved in the process of bouton division (Figure 6). Further genetic analysis, described below, supports this model. Ultimately, however, this model will have to be addressed by live, in vivo, visualization of synaptic microtubules during synaptic growth.

Genetic analysis of *futsch* function demonstrates that both microtubule organization and bouton division require wild-type Futsch. We observe fewer and larger boutons as well as impaired microtubule organization in *futsch* mutants. By analogy with cell division, this is the expected phenotype if bouton division were impaired. Genetic rescue experiments indicate that *futsch* can drive the processes of microtubule organization. Bouton size and number as well as microtubule organization are partially rescued by overexpression of the N-terminal MAP1B homology domain of *futsch*.

Further genetic analysis indicates that bouton division and subsequent nerve-terminal branching can be promoted by exogenous factors but require wild-type Futsch. There is a remarkable correlation between increased branching due to postsynaptic *flexin* overexpression and an increase in the number of presynaptic microtubule loops. Since the division of preexisting boutons occurs at loop-bearing boutons and since bouton division can generate nerve-terminal branching, our data present a correlation between increased loop formation and increased bouton division. Both elevated loop formation and increased branching require wild-type *futsch*, since *flexin* overexpression does not alter the *futsch* mutant phenotype. Although Futsch-dependent regulation of microtubule architecture predicts sites of apparent bouton division and appears necessary for this process, it remains to be determined whether microtubule rearrangement can drive this process.

Our hypotheses concerning the role of synaptic microtubule loops during bouton division is supported by analysis of similar structures observed within the growth cones of neurons in cell culture. Nearly identical microtubule loops (observed by injection of fluorescently labeled tubulin into cultured neurons) are observed within growth cones that have paused during their migration (Tsui et al., 1984; Tanaka and Kirschner, 1991; Dent et al., 1999). Resumed growth cone motility correlates with the disruption of the loop structure into fan-like conformations (Dent et al., 1999). Thus, highly organized loops within growth cones and within synaptic boutons are correlated with stability or lack of change, and the disruption of these loops is associated with motility and plasticity. Therefore, a switch from a stable mode to the active process of bouton division could be controlled by the regulated destabilization of microtubule loops (Figure 8).

A Molecular Switch for the Initiation of Morphological Synaptic Plasticity

It is likely that the dynamics of microtubule loops are controlled by a MAP. The small diameter of microtubule loops observed in growth cones and at the *Drosophila*

synapse indicates that a MAP is necessary to hold the microtubules in such a conformation. The predicted force necessary to bend polymerized tubulin into a loop with a diameter of ~3 μm is greater that the predicted buckling force of a microtubule (Gittes et al., 1993; Dogterom and Yurke, 1997). That vertebrate MAP1B may be involved in microtubule loop formation is supported by the demonstration that MAP1B overexpression in vitro induces the formation of wavy microtubule conformations (Pedrotti et al., 1996; Togel et al., 1998). Vertebrate MAPs including MAP1B are regulated by phosphorylation (Gordon-Weeks, 1997). Thus, phosphorylation could represent a switch capable of inducing rapid changes in microtubule loop conformation within a growth cone or synaptic bouton.

In vertebrates, phosphorylated MAP1B is enriched in growth cones (Bloom et al., 1985; Mansfield et al., 1991; Gordon-Weeks et al., 1993). The phosphorylation-dependent regulation of MAP1B and the subsequent effects on microtubule function are complex. Phosphorylation by casein kinase II appears to increase the affinity of MAP1B for microtubules (Aletta et al., 1988; Brugg and Matus, 1988; Diaz-Nido et al., 1988). Phosphorylation of MAP1B by glycogen synthase kinase 3-β (GSK3β) appears to maintain microtubules in a state of dynamic instability that is considered necessary for growth cone motility and migration (Goold et al., 1999; see review by Tanaka and Kirschner, 1995). It has been suggested that phosphorylation of MAP1B by GSK3β could act as a molecular switch to confer dynamic instability to microtubules, thereby promoting growth cone dynamics (Goold et al., 1999). In one model, phosphorylated Futsch could promote bouton division by promoting the dynamic instability of the microtubules within synaptic loops. Dephosphorylation of Futsch could decrease microtubule dynamics, promote loop formation, and switch synaptic boutons into a stable mode. If phosphorylation of Futsch is regulated by activity-dependent signaling, then the phosphorylation of Futsch could act as a permissive switch for activity-dependent plasticity at specific subsynaptic locations.

MAPs, Bouton Division, and Activity-Dependent Synaptic Plasticity

Recent results from studies of synaptic plasticity in the vertebrate brain indicate that the sprouting of new dendritic spines may be correlated with the consolidation of long-term synaptic plasticity (Engert and Bonhoeffer, 1999; Toni et al., 1999). Interestingly, MAP1B is enriched in areas of the vertebrate brain that show substantial activity-dependent synaptic plasticity (Caceres et al., 1986; Muller et al., 1994). Cytoskeletal rings have been observed in similar areas of the brain and in vertebrate hippocampal cell culture (Novotny, 1979; Shaw et al., 1985). We speculate that a MAP regulation of microtubule loops may participate in the process of synaptic morphological change within the vertebrate central nervous system during activity-dependent plasticity.

Conclusion

It has been hypothesized that the cellular mechanisms of growth cone motility and axon guidance are conserved during synapse elaboration and activity-dependent plasticity. However, morphological specializations that resemble the growth cone have not been observed at developing or plastic synapses (Zito et al., 1999). Data presented here and in Hummel et al. (2000) implicate a common mechanism in the control of growth cone motility and morphological synaptic plasticity. *Drosophila futsch* is essential for both axon elongation and synaptic growth. Futsch is implicated in the regulation of microtubule dynamics through the formation of microtubule loop structures at the synapse. Nearly identical microtubule structures have been previously demonstrated to regulate growth cone morphology and motility (Dent et al., 1999). The control of microtubule organization by MAPs may represent a common mechanism for regulated growth cone motility as well as synaptic growth and plasticity.

Experimental Procedures

Fly Stocks

Flies were raised on standard food at 25°C. The following strains were used for these studies: Canton S and w1118 (wild type), *futsch*^{N94}, *futsch*^{K68}, *UAS-Nterm-Futsch/Cyo*, ep(X)1419, *UAS-tau-GFP*, and *flexin*. *futsch*^{N94} and *futsch*^{K68} are EMS-induced alleles of the *futsch* gene (Hummel et al., 2000). ep(X)1419 is a P(EP) element insertion upstream of the *futsch* gene capable of driving expression of the predicted full-length *futsch* transcript (Hummel et al., 2000; stock provided by Berkeley Drosophila Genome Center). *UAS-Nterminal-Futsch* corresponds to the genomic DNA representing the N-terminal 571 amino acids of *futsch* cloned into the pUAST vector as described (Hummel et al., 2000). *elaV-GAL4* and *24B-GAL4* are GAL4 lines that drive expression in all neurons and all muscle, respectively (Davis et al., 1997).

Overexpression of full-length *futsch* in the motoneuron was achieved by crossing ep(X)1419 by *elaV-GAL4*. Overexpression of the N-terminal region of *futsch* was achieved by crossing *UAS-Nterminal-Futsch/Cyo-GFP* by *elaV-GAL4* and analyzing non-GFP-positive larvae. For rescue of *futsch*^{N94} and *futsch*^{K68}, *UAS-Nterminal-Futsch; elaV-GAL4/SM6-TM6b* males were crossed to either *futsch*^{N94}/*futsch*^{N94} or *futsch*^{N94}/*futsch*^{K68} females. *futsch*^{N94};*UAS-Nterminal-Futsch*/+; *elaV-GAL4*/+ or *futsch*^{K68}; *UAS-Nterminal-Futsch*/+; *elaV-GAL4*/+ third instar larval males were identified as non-Tubby larvae lacking the SM6-TM6b-fused second-third chromosome balancer. Overexpression of *flexin* in postsynaptic muscle in the *futsch* mutant background was achieved by crossing *futsch*^{N94}; P(EP)*flexin* by *futsch*^{N94}; *24B-GAL4*. All larvae were double stained with anti-syt to characterize synapse morphology and mAb 22C10 was used as an independent confirmation of the *futsch* genetic background.

Light Microscopy

Larval dissections and antibody staining were done as previously described (Schuster et al., 1996). Affinity-purified Dap160 polyclonal antibody (Roos and Kelly, 1999) was used at a concentration of 1:200; synaptotagmin antibody (Littleton et al., 1993) was used at a concentration of 1:1500; monoclonal antibody 22C10 (Developmental Studies Hybridoma Bank, University of Iowa) was used at a concentration of 1:50; α-tubulin monoclonal antibody (Sigma) was used at a concentration of 1:500. Fluorescent secondary antibodies (ICN/Cappel) were used at a concentration of 1:200. Direct conjugation of mAb 22C10 was achieved with 1 mg of antibody, diluted to 0.5 ml with PBS and conjugated with Alexa488 (Alexa488 Protein Labeling kit, Molecular Probes) as per the manufacturer's protocol. Images were acquired on a Delta-Vision workstation and processed with Delta-Vision deconvolution algorithms. For Figure 2, the deconvolved image was reconstructed in three dimensions using the volume viewer tool in the Delta-Vision software. Diameter of Futsch filaments were measured 0.5 μm before and after Futsch-positive loops. Control measurements were made on a 4 μm segment 2–3

μm upstream of the same loop. For each experimental genotype, between 30–50 segments in 10–20 animals were examined.

Acknowledgments

We would like to thank Regis Kelly for support and advice throughout this project. We also thank Pat O'Farrell for the use of the DeltaVision confocal microscope and Tony Shermoen for technical assistance with the confocal microscopy. We also thank Peter Clyne, Julia Kantor, Kurt Marek, and Suzanne Paradis for critical evaluation of a previous version of this manuscript. Finally, we thank Sarah Rice, Ron Vale, and Dyche Mullins for reagents, advice, and encouragement. Work was supported by a Burroughs Welcome Young Investigator Award, Merck Scholar Award, seed money, and a Young Investigator grant from the Sandler Foundation and NIH grant NS39313-01 (to G. W. D.). J. R. was supported by a NIH Postdoctoral Fellowship T32-CA 09270-23, and NIH grant NS15927 supported R. B. K.

Received January 27, 2000; revised April 18, 2000.

References

Aletta, J.M., Lewis, S.A., Cowan, N.J., and Greene, L.A. (1988). Nerve growth factor regulates both the phosphorylation and steady-state levels of microtubule-associated protein 1.2 (MAP1.2). J. Cell Biol. *106*, 1573–1581.

Bloom, G.S., Luca F.C., and Vallee, R.B. (1985). Microtubule-associated protein 1B: identification of a major component of the neuronal cytoskeleton. Proc. Natl. Acad. Sci. USA *82*, 5404–5408.

Brugg, B., and Matus, A. (1988). PC12 cells express juvenile microtubule-associated proteins during nerve growth factor-induced neurite outgrowth. J. Cell Biol. *107*, 643–650.

Caceres A., Banker, G.A., and Binder, L. (1986). Immunocytochemical localization of tubulin and microtubule-associated protein 2 during the development of hippocampal neurons in culture. J. Neurosci. *6*, 714–722.

Callahan, C.A., and Thomas, J.B. (1994). Tau-beta-galactosidase, an axon-targeted fusion protein. Proc. Natl. Acad. Sci. USA *91*, 5972–5976.

Casadio, A., Martin, K.C., Giustetto, M., Zhu, H., Chen, M., Bartsch, D., Bailey, C.H., and Kandel, E.R. (1999). A transient, neuron-wide form of CREB-mediated long-term facilitation can be stabilized at specific synapses by local protein synthesis. Cell *99*, 221–237.

Davis, G.W., Schuster, C.M., and Goodman, C.S. (1997). Genetic analysis of the mechanisms controlling target selection: target-derived Fasciclin II regulates the pattern of synapse formation. Neuron *19*, 561–573.

Dent, E.W., Callaway, J.L., Szebenyi, G., Baas, P.W., and Kalil, K. (1999). Reorganization and movement of microtubules in axonal growth cones and developing interstitial branches. J. Neurosci. *19*, 8894–8908.

Diaz-Nido, J., Serrano, L., Mendez, E., and Avila, J. (1988). A casein kinase II-related activity is involved in phosphorylation of microtubule-associated protein MAP1B during neuroblastoma cell differentiation. J. Cell Biol. *106*, 2057–2065.

Dogterom, M., and Yurke, B. (1997). Measurement of the force velocity relation for growing microtubules. Science *278*, 856–860.

Engert, F., and Bonhoeffer, T. (1999). Dendritic spine changes associated with hippocampal long-term synaptic plasticity. Nature *399*, 66–70.

Gallo, G., and Letourneau, P.C. (1999). Different contributions of microtubule dynamics and transport to the growth of axons and collateral sprouts. J. Neurosci. *15*, 3860–3873.

Gittes, F., Mickey, B., Nettleton, J., and Howard, J. (1993). Flexural rigidity of microtubules and actin filaments measured from thermal fluctuations in shape. J. Cell Biol. *120*, 923–934.

Goold, R.G., Owen, R., and Gordon-Weeks, P.R. (1999). Glycogen synthase kinase 3beta phosphorylation of microtubule-associated protein 1B regulates the stability of microtubules in growth cones. J. Cell Sci. *112*, 3373–3384.

Gordon-Weeks, P.R. (1997). MAPs in growth cones. In Brain Microtubule Proteins: Modifications in Alzheimer's Disease, J. Avila and K. Kosik, eds. (Harwood Academic Publishers), pp. 53–72.

Gordon-Weeks, P.R., Mansfield, S.G., Alberto, C., Johnstone, M., and Moya, F. (1993). A phosphorylation epitope on MAP 1B that is transiently expressed in growing axons in the developing rat nervous system. Eur. J. Neurosci. *5*, 1302–1311.

Grant, S.G., Karl, K.A., Kiebler, M.A., and Kandel, E.R. (1995). Focal adhesion kinase in the brain: novel subcellular localization and specific regulation by Fyn tyrosine kinase in mutant mice. Genes Dev. *9*, 1909–1921.

Halpain, S., Hipolito, A., and Saffer, L. (1998). Regulation of F-actin stability in dendritic spines by glutamate receptors and calcineurin. J. Neurosci. *18*, 9835–9844.

Hummel, T., Krukkert, K., and Klämbt, C. (2000). The *Drosophila* Futsch/22C10 protein is a MAP1B-like protein required for dendritic and axonal development. Neuron *26*, this issue, 357–370.

Ito, K., Sass, H., Urban, J., Hofbauer, A., and Schneuwly, S. (1997). GAL4 responsive UAS tau as a tool for studying the anatomy and development of the Drosophila central nervous system. Cell Tissue Res. *290*, 1–10.

Keshishian, H., Broadie, K., Chiba, A., and Bate, M. (1996). The drosophila neuromuscular junction: a model system for studying synaptic development and function. Annu. Rev. Neurosci. *19*, 545–575.

Littleton, J.T., Stern, M., Schulze, K., Perin, M., and Bellen, H.J. (1993). Mutational analysis of Drosophila synaptotagmin demonstrates its essential role in Ca(2+)-activated neurotransmitter release. Cell *74*, 1125–1134.

Luo, L., Jan, L.Y., and Jan, Y.N. (1997). Rho family GTP-binding proteins in growth cone signaling. Curr. Opin. Neurobiol. *7*, 81–86.

Mansfield, S.G., Diaz-Nido, J., Gordon-Weeks, P.R., and Avila, J. (1991). The distribution and phosphorylation of the microtubule-associated protein MAP 1B in growth cones. J. Neurocytol. *21*, 1007–1022.

Muller, R., Kindler, S., and Garner, C.C. (1994). The MAP1 family. In Microtubules, J.S. Hyams and C.W. Lloyd, eds. (New York: Wiley-Liss), pp. 141–151.

Novotny, G.E. (1979). Synaptic ring images after silver impregnation. Cell Tissue Res. *204*, 141–145.

Pedrotti, B., Francolini, M., Cotelli, F., and Islam, K. (1996). Modulation of microtubule shape in vitro by high molecular weight microtubule associated protein MAP1A, MAP1B, and MAP2. FEBS Lett. *384*, 147–150.

Rohatgi, R., Ma, L., Miki, H., Lopez, M., Kirchhausen, T., Takenawa, T., and Kirschner, M.W. (1999). The interaction between N-WASP and the Arp2/3 complex links Cdc42-dependent signals to actin assembly. Cell *97*, 221–231.

Roos, J., and Kelly, R.B. (1999). The endocytic machinery in nerve terminals surrounds sites of exocytosis. Curr. Biol. *9*, 1411–1414.

Schuster, C.M., Davis, G.W., Fetter, R.D., and Goodman, C.S. (1996). Genetic dissection of structural and functional components of synaptic plasticity. II. Fasciclin II controls presynaptic structural plasticity. Neuron *17*, 655–667.

Shaw, G., Banker, G.A., and Weber, K. (1985). An immunofluorescence study of neurofilament protein expression by developing hippocampal neurons in tissue culture. Eur. J. Cell Biol. *39*, 205–216.

Suter, D.M., and Forscher, P. (1998). An emerging link between cytoskeletal dynamics and cell adhesion molecules in growth cone guidance. Curr. Opin. Neurobiol. *8*, 106–116.

Tanaka, E.M., and Kirschner, M.W. (1991). Microtubule behavior in the growth cones of living neurons during axon elongation. J. Cell Biol. *115*, 345–363.

Tanaka, E., and Kirschner, M.W. (1995). The role of microtubules in growth cone turning at substrate boundaries. J. Cell Biol. *128*, 127–137.

Tanaka, E., and Sabry, J. (1995). Making the connection: cytoskeletal rearrangements during growth cone guidance. Cell *83*, 171–176.

Tanaka, E., Ho, T., and Kirschner, M.W. (1995). The role of microtubule dynamics in growth cone motility and axonal growth. J. Cell Biol. *128*, 139–155.

Togel, M., Wiche, G., and Propst, F. (1998). Novel features of the light chain of microtubule associated protein MAP1B: microtubule stabilization, self-interaction, actin filament binding and regulation by the heavy chain. J. Cell Biol. *143*, 695–707.

Toni, N., Buchs, P.A., Nikonenko, I., Bron, C.R., and Muller, D. (1999). LTP promotes formation of multiple spine synapses between a single axon terminal and a dendrite. Nature *402*, 421–425.

Tsui, H.T., Kankford, K.L., Ris, H., and Klein, W.L. (1984). Novel organization of microtubules in cultured central nervous system neurons: formation of hairpin loops at ends of maturing neurites. J. Neurosci. *4*, 3002–3013.

Wills, Z., Bateman, J., Korey, C.A., Comer, A., and Van Vactor, D. (1999a). The tyrosine kinase Abl and its substrate enabled collaborate with the receptor phosphatase Dlar to control motor axon guidance. Neuron *22*, 301–312.

Wills, Z., Marr, L., Zinn, K., Goodman, C.S., and Van Vactor, D. (1999b). Profilin and the Abl tyrosine kinase are required for motor axon outgrowth in the *Drosophila* embryo. Neuron *22*, 291–299.

Zito, K., Parnas, D., Fetter, R.D., Isacoff, E.Y., and Goodman, C.S. (1999). Watching a synapse grow: noninvasive confocal imaging of synaptic growth in *Drosophila*. Neuron *22*, 719–729.